People's Democratic Republic of Algeria
Ministry of Higher Education and Scientific Research
Mohamed Boudiaf University of M'sila
Faculty of Technology

الجمهورية الجزائرية الديمقراطية الشعبية
وزارة التعليم العالي والبحث العلمي
جامعة المسيلة
كلية التكنولوجيا

Department of Mechanical Engineering

THESIS

Presented with a view to obtaining the Grade of

Doctorate LMD

In Mechanical Engineering

Option: Mechanical Construction

By

ZERNADJI Sid Ali

Study of interfacial decohesion and damage mechanisms

Jury

ZERGANE Said	***President***	***Professor***	***M'sila University***
BENHAMIDA Mohamed	***Supervisor and rapporteur***	***Professor***	***M'sila University***
ROKBI Mansour	***Rapporteur***	***Professor***	***M'sila University***
DEBIH Ali	***Examiner***	***Professor***	***M'sila University***
Kheladi Mohamed Redha	***Examiner***	***Professor***	***Bordj Bou Arreridj University***
Khaldi Abd El Ghani	***Examiner***	***Associate Professor***	***Bordj Bou Arreridj University***

Academic year: 2024 / 2025
N° d'ordre: GM/……../2025

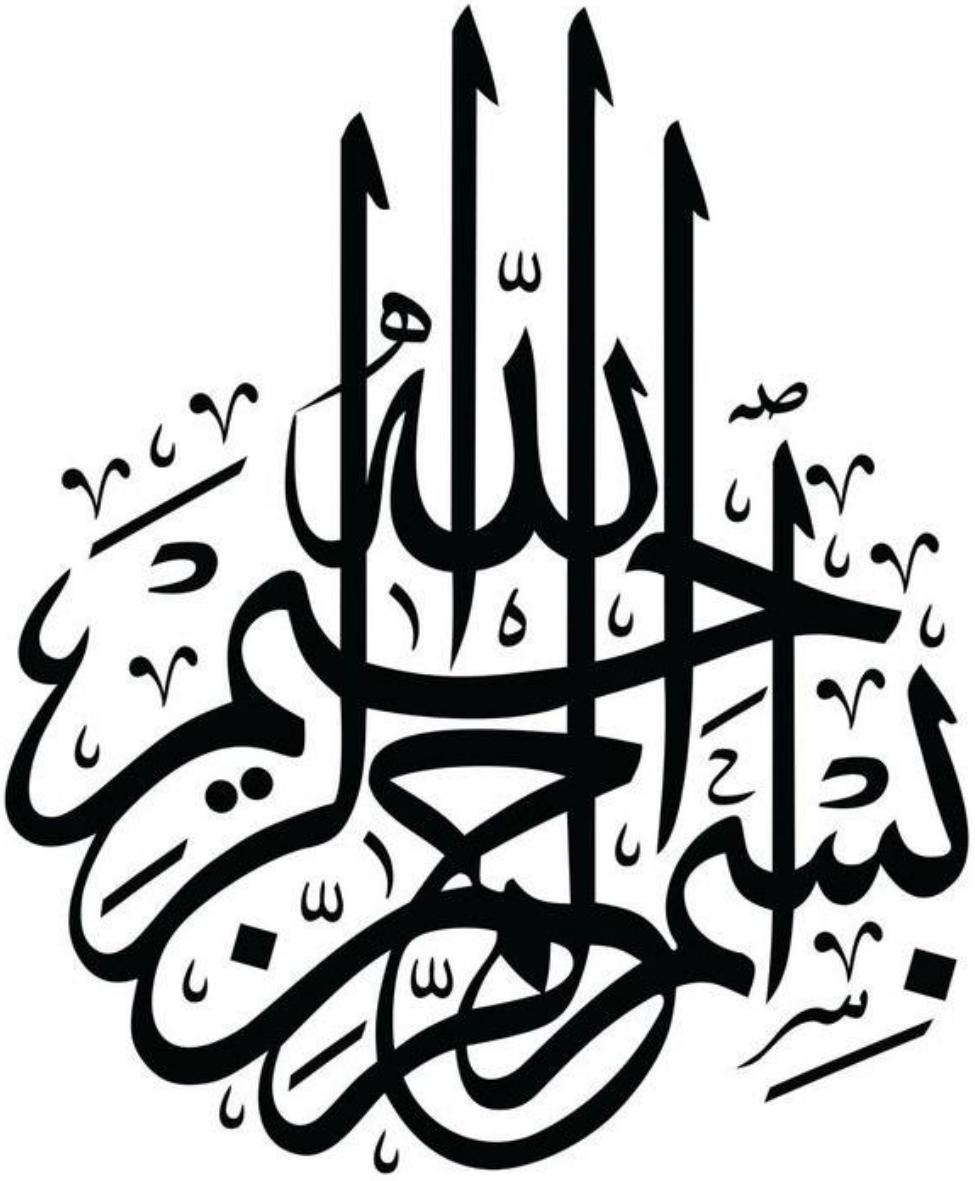
بسم الله الرحمن الرحيم

Dedication

To

My Family

Sid Ali

Acknowledgments

*I will first thank **Allah** for giving me the will, the courage and the patience to accomplish this modest work.*

*I would like to express my most sincere thanks to my thesis director, Professor **BENHAMIDA Mohamed**, for his availability at all times, for his judicious advice and our scientific debates that we were able to exchange during all these years of work that have sincerely and truly helped me. I also thank Professor **ROKBI Mansour**, thesis co-rapporteur for the help, the experience, the confidence he gave me and for allowing me to work on this theme.*

I would like to express my sincere gratitude to the members of the thesis jury:

*To Sir: **ZERGANE Said,** Professor from M'sila University*

*To Sir: **DEBIH Ali,** Professor from M'sila University*

*To Sir: **Kheladi Mohamed Redha,** Professor from Bordj Bou Arreridj University*

*To Sir: **Khaldi Abd El Ghani,** Associate Professor from Bordj Bou Arreridj University*

*I would also like to express my gratitude and thanks to Mr. **SEBASTIEN ALIX**, Professor at the University of Reims, France and Director of the **LASEM** laboratory. I dedicate to you the assurance of my high consideration for having received me in your laboratory, for your advice and guidance during my scientific stay and help during the realization of the tests.*

My thanks also go to all the staff of the University of M'sila who helped me directly or indirectly.

I also thank my dear friend and colleague ***KERMICHE Younes, SELMANE Tahar*** *and* ***LEBIAD Yacine*** *for your support, for your availability and your suggestions. I liked your scientific consistency but also your humor. You were fully committed to this thesis work and I am very grateful for your contribution to its good progress.*

Also, I would like to give a special thought to my dear parents for the encouragement and support they have given me. You have been an inspiration to my life. Thank you very much.

Finally, all my gratitude to my brother ***ZERNADJI Redha*** *who gave me some of his precious time and shared some of his knowledge in the accomplishment of this work.*

Résumé

L'industrie des matériaux composites connaît une évolution constante, marquée par l'émergence de nouveaux matériaux et technologies. Face à la substitution des matériaux d'origine fossile, les matériaux d'origine naturelle, et en particulier ceux d'origine végétale, commencent à prendre leur place parce que développement des matériaux composites a d'abord été étroitement lié à l'industrie aéronautique et aérospatiale. Plus récemment, leur champ d'application s'est considérablement élargi, touchant désormais divers secteurs tels que le sport de compétition, la construction mécanique, le stockage de fluides sous pression, les systèmes de freinage, ainsi que les domaines médicaux, notamment en chirurgie et en prothèses.

C'est dans ce cadre que s'inscrit notre travail de recherche. Celui-ci se concentre sur l'étude des mécanismes de décohésion et d'endommagement interfaciale présents dans une structure composite sous chargement statique, renforcée par des fibres de cellulose qui ont été étudiées pour la première fois, à partir d'une plante appelée Echinops spinosissimus qui pousse dans la région de M'Sila (Algérie) dans le cadre de la conception environnementale. Cette recherche vise à caractériser la force de déchaussement d'un renfort en résine époxy et en fibres de cellulose utilisé pour la première fois. Pour ce faire, plusieurs traitements sont effectués sur les fibres afin de les analyser de plusieurs façons. Parmi les traitements chimiques existants, le traitement alcalin et le traitement au permanganate de potassium ont été choisis. Trois séries de caractérisation sont réalisées. La première concerne les différentes analyses de nos fibres telles que : analyses FTIR, DRX, tests mécaniques. La deuxième série est l'étude de l'interface par analyse micromécanique utilisant des microgouttelettes. Enfin, la troisième série est la caractérisation mécanique de composites modèles fabriqués à partir de différentes fibres d'Echinops spinosissimus prétraitées. Le choix de ces fibres est tout à fait justifié compte tenu du fait qu'il n'existe quasiment pas de travaux sur ces fibres dans la littérature et d'autre part leur disponibilité en abondance en Algérie. Cette ressource naturelle renouvelable mérite d'être valorisée car elle est très utile pour développer des matériaux respectueux de l'environnement.

Cette approche nous a permis d'analyser la qualité et l'importance de l'interface fibre/matrice, un paramètre essentiel pour cette étude et pour l'élaboration de comportement du composite. Dont les diverses méthodes de caractérisation employées dans cette étude ont révélé que ces nouveaux matériaux possèdent des propriétés, notamment mécaniques, de très haut niveau, capables de rivaliser avec celles des composites classiques à base de fibres de verre et de carbone.

Mots clés : Echinops spinosissimus, composite, traitement chimique, pull-out, decohesion.

Abstract

The composite materials industry is undergoing constant evolution, marked by the emergence of new materials and technologies. Faced with the substitution of fossil-based materials, materials of natural origin, and in particular those of plant origin, are beginning to take their place because the development of composite materials was initially closely linked to the aeronautics and aerospace industry. More recently, their scope of application has expanded considerably, now affecting various sectors such as competitive sports, mechanical engineering, pressurized fluid storage, braking systems, as well as medical fields, particularly in surgery and prosthetics.

This is the framework of our research work. It focuses on the study of the mechanisms of decohesion and interfacial damage present in a composite structure under static loading, reinforced by cellulosic fibers that have been studied for the first time, extracted from a plant called Echinops spinosissimus that grows in the M'sila region (Algeria) as part of environmental design. This research aims to characterize the decohesion force of an epoxy resin and cellulose fiber reinforcement used for the first time. To do this, several treatments are carried out on the fibers in order to analyze them in several ways. Among the existing chemical treatments, alkaline treatment and permanganate treatment were chosen. Three series of characterization are carried out. The first concerns the different analyses of our fibers such as: Fourier Transform Infrared (FTIR) analyses, X-ray diffraction, mechanical tests. The second series is the study of the interface by micromechanical analysis using micro droplets. Finally, the third series is the mechanical characterization of model composites made from different pretreated Echinops spinosissimus fibers. Selecting these fibers is well justified considering that there is almost no work on these fibers in the literature and on the other hand their abundant availability in Algeria. This renewable natural resource deserves to be valued because it is very useful for developing environmentally friendly materials.

The various characterization methods used in this study revealed that these new materials have very high-level properties, particularly mechanical properties, capable of competing with those of conventional composites based on glass and carbon fibers.

Keywords: Echinops spinosissimus, composite, chemical treatment, interface, pull-out, decohesion.

ملخص

تشهد صناعة المواد المركبة تطورًا مستمرًا، يتميز بظهور مواد وتقنيات جديدة. في مواجهة استبدال المواد ذات الأصل الأحفوري، بدأت المواد ذات الأصل الطبيعي، وخاصة تلك ذات الأصل النباتي، تأخذ مكانها لأن تطوير المواد المركبة كان مرتبطًا في البداية ارتباطًا وثيقًا بصناعة الطيران والفضاء الجوي. وفي الآونة الأخيرة، توسع نطاق تطبيقها بشكل كبير، حيث أصبح يؤثر الآن على قطاعات مختلفة مثل الرياضة التنافسية، والهندسة الميكانيكية، وتخزين السوائل المضغوطة، وأنظمة الفرامل، فضلاً عن المجالات الطبية، وخاصة في الجراحة والأطراف الصناعية.

هذا هو الإطار الذي يتم من خلاله تنفيذ أعمالنا البحثية. حيث يركز هذا البحث على دراسة آليات فقدان التماسك والضرر السطحي الموجود في بنية مركبة تحت التحميل الساكن، معززة بألياف السليلوز التي تمت دراستها لأول مرة، من نبات يسمى Echinops spinosissimus والذي ينمو في منطقة المسيلة (الجزائر) في سياق التصميم البيئي. يهدف هذا البحث إلى تحديد قوة الانفصال بين راتنج الإيبوكسي وألياف السليلوز المستخدمة لأول مرة. وللقيام بذلك، يتم إجراء العديد من المعالجات على الألياف من أجل تحليلها بعدة طرق. ومن بين المعالجات الكيميائية الموجودة، تم اختيار المعالجة القلوية ومعالجة برمنجنات البوتاسيوم. يتم تنفيذ ثلاث سلاسل من التوصيف. يتعلق الأول بالتحليلات المختلفة لألياف مثل: تحليل تحويل فورييه للأشعة تحت الحمراء(FTIR) ، حيود الأشعة السينية، والاختبارات الميكانيكية. السلسلة الثانية هي دراسة الواجهة عن طريق التحليل الميكانيكي الدقيق باستخدام القطرات الدقيقة. وأخيرًا، السلسلة الثالثة هي التوصيف الميكانيكي للمركبات النموذجية المصنوعة من ألياف Echinops spinosissimus المختلفة المعالجة مسبقًا. إن اختيار هذه الألياف مبرر تمامًا نظرًا لحقيقة عدم وجود أي عمل تقريبًا حول هذه الألياف في الأدبيات ومن ناحية أخرى توفرها بكثرة في الجزائر. إن هذا المورد الطبيعي المتجدد يستحق التقدير لأنه مفيد جدًا لتطوير مواد صديقة للبيئة.

وقد كشفت طرق التوصيف المختلفة المستخدمة في هذه الدراسة أن هذه المواد الجديدة تمتلك خصائص عالية المستوى للغاية، وخاصة الخصائص الميكانيكية، القادرة على التنافس مع تلك الموجودة في المركبات التقليدية القائمة على الألياف الزجاجية والكربونية.

الكلمات المفتاحية : Echinops spinosissimus ، مركب، المعالجة الكيميائية، الانسحاب، إزالة التماسك.

CONTENTS TABLE

Chapter III Experimental part Materials and methods

Chapter IV Results and Discussions

General conclusion

Appendix

List of Figures

List of tables

List of abbreviations

HP: High performance
WPC: Wood/plastic composite
PP: Polypropylene
PLA: Polylactic acid
PVC: Polyvinyl chloride
PS: Polystyrene
LDPE: Low-density polyethylene
PE: Polyethylene
MUP: Polystyrene modified unsaturated polyester
MA: Maleic anhydride
TMA: Thermo mechanical analysis
TGA: Thermogravimetric analysis
DTG: Derivative of thermogravimetric mass variation
DSC: Differential scanning calorimetry
XPS: X-ray photoelectron spectroscopy
SEM: Scanning electron microscopy
EDX: Energy dispersive X-ray
FTIR: Fourier transform infrared
XRD: X-ray diffraction
IFSS: Interfacial shear strength
GC: Breakdown energy
ES: Echinops spinosissimus
ESF: Echinops spinosissimus Fibers
FB: Fiber bundles
VB: Vascular bundle
Cs: Crystallite size
R-ESF: Untreated Echinops spinosissimus fibers
NaOH-ESF: NaOH-treated Echinops spinosissimus fibers
$KMnO_4$-ESF: $KMnO_4$-treated Echinops spinosissimus fibers
ASTM: American Society for Testing Materials
LF: Loosening force

List of symbols

ρ_{ESF}: Density of ES fibers (g/cm3)
IC (%): Percentage of crystallinity
P (σ_r): Probability of failure at a threshold stress
Ɛ: Tensile strain at break (%)
σ: Tensile stress at break (MPa)
E: Tensile Young's modulus (MPa) or (GPa)
F: Maximum force (N)
V: Test speed (mm/min)
T: Thickness of specimens (mm)
L: Total length of specimens (mm)
l: Distance between specimen supports (mm).
CL: Critical length
W: Width of specimens (mm)
S: Section of specimens (mm2)
E_0: Characteristic Young's modulus

GENERAL INTRODUCTION

GENERAL INTRODUCTION

Technological development coupled with consumer expectations continues to increase at the expense of earth's resources, leading to significant issues related to material availability and environmental sustainability. Recently, general unanimity regarding the significant contribution of humans to global warming has been achieved. This awareness has also led to interest in sustainably sourced materials that require low energy for production, as well as recyclable materials, including those from which energy can be recovered, which found for example in composites with cellulosic fiber reinforcements, and assigned to non-structural applications such as in the context of automobile interior cladding. Although the use of these materials is not new (their use dates back civilizations), these more recent measures have encouraged the expansion of their use.

An important area of development over the last decade is the use of thermoplastic and thermopanels, made by compression molding and reinforced with natural fibers, which have been widely adopted in the aeronautics and aerospace sector, European automotive industry for parts such as door panels, automotive interiors, dashboards and car trunk linings.

At recent times, their applications have expanded to encompass various domains, including competitive sports, mechanical engineering, pressurized fluid storage, brake systems, and even the development of bone prostheses. Indeed, considerable effort has focused on improving the mechanical performance of thermoplastic and thermosetting composites with natural cellulosic fiber reinforcements, to allow the extension of their application, and replace traditional composites with synthetic reinforcement (mainly glass reinforcement). Much of this attention has been aimed at improving interfacial bonding strength, for which a range of fiber chemical treatments has been evaluated. The greatest success in terms of mechanical advantages and ease of use has been achieved with chemical treatments such as Alkaline and permanganate, giving significantly improved strength and stiffness compared to composites reinforced with untreated fiber.

Thus, gaining a deep insight into the interfacial properties and quantifying the interfacial shear strength becomes essential for evaluating the mechanical performance and capabilities of composite materials. Several analytical methods have been developed to comprehend interfacial decohesion in cellulose fiber-reinforced polymers. Common decohesion assessment approaches encompass pulling polymer drops from single fiber (pull-out test), single fiber fragmentation tests and longitudinal tensile tests. Among these techniques, the droplet pull-out test stands out as it allows for a comprehensive examination of the interfacial region and serves as a quick means for the materials industry to assess the behavior and mechanical properties of model composites.

The properties of composite materials are determined by various factors, including the manufacturing process, the origin of the matrix and fibers. However, the most significant influence is exerted by the interface between these components, as it plays a crucial role in transmitting forces and requires a strong affinity between the two elements. Numerous researchers have

investigated how the nature of this interface affects the properties of natural fiber composite materials, with this being closely linked to whether a chemical or physical treatment is employed.

My doctoral research, titled "Study of interfacial decohesion and damage mechanisms present in a composite structure under static loading", is in line with this overarching objective. Our primary aim is to conduct a quantitative assessment of the interface properties of composites reinforced with fiber specifically sourced from Echinops spinosissimus (also known as Chawki El Djabali) plants found in the M'sila region of Algeria, all within the context of eco-design.

In our pursuit of this goal, we have employed two chemical treatments to modify and make the fibers hydrophobic. However, we have encountered several challenges in this endeavor:

1- Harvesting Echinops spinosissimus plants and developing a procedure to extract fibers from this new plant, then assessing the impact of various treatments on these fibers by conducting a thorough examination of their physical, chemical, and mechanical properties.

2- Considering the current lack of comprehensive understanding regarding the influence of the surface properties of these novel fibers on the thermosetting resin polymerization process, encompassing factors such as the functions of activators and catalysts, the chemical reactions taking place at the interface, and the subsequent consequences on material properties arising from micromechanical interactions at the interface. Knowing that the primary obstacle revolves around finding ways to minimize the negative repercussions of the fiber surface within the process.

3- The crucial element in composite materials lies in the harmonious interaction between their two constituents: the matrix and the fibers. This interaction is significantly influenced by the surface properties and wettability of these components. Therefore, a compelling approach to improve the interface between the matrix and fibers is to introduce innovative functionalities on the surface of the fiber, requiring different chemical treatments to evaluate their effectiveness.

4- The primary site for effective stress transfer from the matrix to the fibers is the interface. To assess the efficiency of this property transfer, a thorough understanding and characterization of the individual properties of each component is essential. Currently, quantitatively estimating interface characteristics, including decohesion and stress transmission, or investigating the interface poses challenges. Although it is evident that the interface plays a role in influencing macroscopic characteristics, precisely measuring this influence remains a complex task. Therefore, the main objective is to uncover the debonding mechanisms occurring at the fiber-matrix interface in composite materials and they subsequently affect the performance traits of the resulting composite.

In response to this challenge, this thesis structured into three distinct sections.

Chapter 1 presents a thorough investigation into the use of plant-based fiber reinforcements in composites, aiming to establish a solid understanding of the research context. It encompasses the definitions of composite materials and their key components, such as matrices

and reinforcements. Furthermore, the chapter explores vital details regarding cellulose fibers, covering their classifications, chemical compositions, diverse extraction methods, and providing a nuanced discussion of their strengths and weaknesses

Chapter 2 focuses on the interface from its formation to its failure, encompassing all adhesion mechanisms and theories, as well as methods to enhance the quality of the fibre/matrix interface through various proposed treatments. It concludes with an analysis of adhesion, interface, and surface properties using a range of approaches chemical, physical, mechanical, and micromechanical. A specific device developed in the laboratory is used for testing: the 'droplet pull-out' technique, aimed at understanding the interfacial adhesion in natural fibre-reinforced polymers. The chapter also presents studies on the effects of chemical treatments on the natural fibre/matrix interface.

Subsequently, **Chapter 3** offers an extensive account of the various experimental methods utilized throughout the thesis research. These methods encompass everything from the materials and products used to the tools and devices employed for characterizing and analyzing the new cellulose fibers extracted from Echinops spinosissimus stems. Additionally, the chapter presents a detailed examination of the Echinops spinosissimus fibers, both in their natural state and after undergoing distinct chemical treatments, such as NaOH and KMnO4. It investigates the effects of the impact of these chemical treatments on the mechanical, physical, chemical, and thermal characteristics of Echinops spinosissimus fibers through utilizing a range of analytical techniques, including Fourier Transform Infrared Spectroscopic, X-ray diffraction, thermo gravimetry, scanning electron microscopy analysis, tensile tests. Moreover, it includes an assessment of the treatment's impact on the fiber-matrix interface using a micromechanical test known as micro-droplet, fragmentation tests and NFCs tensile tests.

Moving on to **Chapter 4**, this section is dedicated to a comprehensive discussion of the research findings.

Lastly, a broad-reaching conclusion serves to encapsulate the significant discoveries made throughout the course of this study

CHAPTER I

Composite materials reinforced by Plant fibers

I. 1. Introduction

Since time, materials have played a major role in human society. Humains used natural materials to make the initial tools they needed, such as hunting tools, small boats, clothing and the construction of huts to protect themselves from the heat of summer and the bitterness of winter. The continuous exploration and development of novel materials, notably composite materials, have been instrumental in driving progress in tools, constructions, lifestyles, and societal requirements.

Biomaterials extracted from nature (especially plant fibers) are witnessing an increasing demand due to the markets' need for these resources used in the production and development of composite materials, as we witness an increasing demand for these environmentally friendly materials year after year. To answer these urgent needs, work is being done in many research centers and laboratories around the world. These substances are generally called biocomposites.

This leaves us to say that the great economic interest of plant-reinforced composite materials will be constantly increasing in the years to come. Indeed, especially since plants constitute the only potentially inexhaustible source of exploitable carbon. A wide variety of materials is observed, from so-called "widespread" composite products to composites with high mechanical and thermo-mechanical performances.

Today, naturally reinforced composites are not only used in structural and semi-structural applications in the automotive industry, but also in other uses. To achieve a level of performance that can be matched with the application specifications, the characteristics and architecture of the reinforcement must be optimized.

Throughout this first chapter, a representation of polymer matrix/cellulosic fibrous reinforcement composite materials is given. Understanding the chemical composition and structure of the constituents individually is essential to better understand the reactions that will take place between the reinforcements and the matrices.

I. 2. Generalities on composite materials

Composite materials are solid and anisotropic substances [1] made up of at least two materials with different but complementary properties. Their combination makes it possible to obtain properties that would be impossible to obtain with a homogeneous material on the macroscopic scale. The general diagram of a composite material is given in Figure I. 1. The matrix ensures the cohesion and orientation of the fibers, it also allows the transmission of the stresses to which the parts are subjected. The reinforcement, generally fibrous in nature, makes it possible to support the load of the structure, reduces thermal stresses and ensures rigidity and macroscopic resistance. The matrix makes it possible to bind the reinforcement, provide protection against external agents [2] and transfer the loads to the reinforcement via the connection between the fiber and the matrix [3].

Composite materials have been used for decades. Their advantages over traditional materials lie in their performance and their lightness [4]. These assets have attracted many industries such as aerospace, automobiles, infrastructure, sport, etc. The development of composite materials has been evolutionary but also revolutionary.

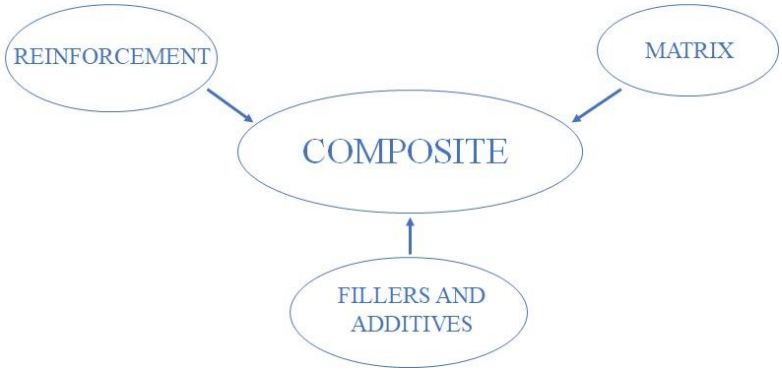

Figure I. 1. Structure of a composite material [5]

It is widely acknowledged that the matrix can consist of polymers, metals, or ceramics. The reinforcements may take the form of either fibrous or particulate elements (refer to Figure I. 2). The lengths of the fibers can be categorized as short, long, or continuous, typically falling within the ranges of (0.1 mm to 1.5 mm), (1.5 mm to 50 mm), and (greater than 50 mm), respectively [6].

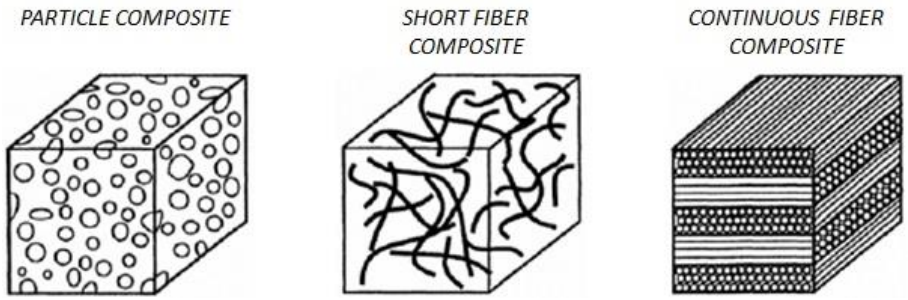

Figure I. 2. Particle, short fiber and continuous fiber composite materials

Composites can be classified according to several criteria. A classification into three families according to the type of matrix is often used. There we find composites with a polymer or organic matrix (CPM), with a metal matrix (CMM) and with a ceramic matrix (CCM). Composites with polymer matrices are the subject of this work and will therefore be discussed in more detail below.

The matrix is crucial to the overall performance of polymer matrix composites. The two main types of polymers, thermosets (TS) and thermoplastics (TP) each have advantages and disadvantages and can be adopted depending on the type of application. Thermosets are used by chemical reaction by crosslinking and formation of a three-dimensional network [7]. Once cured, a thermosets cannot be remelted. Among the TS, we find polyester resins, phenolics, melamines,

silicones, polyurethanes and epoxies. Thermoplastics are made of flexible linear chains and can be softened repeatedly allowing them to be recycled [8]. Among the TP we find: polyethylene (PE), polypropylene (PP), polyvinyl chloride (PVC), polyamide (PA) and others.

Fibers used for polymer matrix reinforcement are generally classified into two groups; continuous fibers and short fibers. Continuously reinforced composites are reserved for high performance applications [9]. High raw material costs, complex manufacturing processes, and limited production capacities contribute to the high cost of these composites and are limited to industries such as aeronautics and aerospace. Carbon fibers (high modulus or high strength) and Kevlar (very light) are most used in this type of composite.

Acting as a middle ground, short fiber composites balance the properties of long (continuous) fiber composites, for high performance, and unreinforced polymers used in low-stress applications [10]. Polymers reinforced with short fibers make it possible to couple the properties of its two extremes. If the fibers are long enough, the stiffness of the composites can approach that of a continuous fiber system. On the other hand, implementation similar to unreinforced polymers still remains possible, by injection, extrusion or compression, which allows large production capacities.

One of the most crucial parameters in optimizing the mechanical properties of composites lies in the interface where the load transfer between fiber and matrix occurs. Generally, the interface is not a separate phase, as it does not have a clear boundary. The interface can be composed of several layers as in the case of glass fiber sizing. For each composite, the interfacial zone is specific. Optimization of fiber/matrix load transfer involves characterizing its chemistry, morphology and mechanical properties [11].

Composite materials have several properties like those that they do not corrode [12], they do not plasticize (their elastic limit corresponds to the breaking limit) [13], they have better fire resistance than light alloys for the same (low) thickness [14] and they are very resistant to fatigue [15]. Composite materials are enjoying great success. Their main advantages (lightness and mechanical performances) are of interest to more and more applications [16].

I. 3. Plant fiber composites

Nowadays, the use of renewable resources in composite materials is becoming more and more frequent. These materials have the ability to renew themselves naturally (their use has become a necessity because, with the depletion of fossil resources, the emission of greenhouse gases and the problem of waste management, it is essential to find solutions for respecting the environment). At the same time, the plastic industry is expanding. It is in this context that new materials, resulting from the mixture of its constituents from biomass with plastic materials, are being developed that are increasingly efficient. These materials have the advantage of being biodegradable, renewable, etc. In other words, these fibers are an alternative to synthetic fibers

(glass, carbon, aramid, etc.) because of their recyclability. However, their properties must be further improved.

Natural fibers such as Inula Viscosa, hemp, sisal, jute and palm have certain technical, economic and ecological advantages over synthetic fibers (glass fibers, etc.). The interesting combination of their mechanical and physical properties as well as their environmental friendliness has attracted interest in a number of industrial sectors, including the automotive industry. The advantages and disadvantages of using natural fibers in composites are given in Table I. 1. Lignocellulosic fibers have an advantage over synthetic fibers in that they form loops instead of breaking during processing and manufacturing. In addition, cellulose has a flattened oval cross-section that increases load transfer by having an effectively higher aspect ratio.

Table I. 1. Main advantages and disadvantages of plant fibers [5]

Advantages	Disadvantages
Low cost	Water absorption
Biodegradability and renewable resource	Low dimensional stability
Neutral for the emission of co2	Poor aging resistance
No skin irritation when handling the fibers	Low thermal resistance (200 a 230 °C max)
No residue after incineration	Anisotropic fibers
Requires little energy to be produced	Discontinuous reinforcement
Important specific mechanical properties (strength and rigidity)	For industrial applications, requires stock management
Good thermal, acoustic insulation and non-abrasive for tools	Variation in quality depending on the place of growth, the weather...

I. 4. Plant Fibers

I. 4. 1. Description of plant fiber

Natural fibers are generally classified according to their origins: animal, plant and mineral. Fibers of plant origin are mainly made up of cellulose and have mechanical properties superior to those of animal origin. The latter, such as wool and silk, are widely used in the textile field. Fibers of plant origin can be classified into subfamilies depending on where they were extracted; seeds, fruits, bark, leaves, wood, stems or cane (Table. I. 2, Table. I. 3).

Table I. 2. Classification and examples of natural fibers [17]

Origin	**extraction part**	**Examples**
Vegetal	Seeds	Cotton, Kapok, Milkweed
	Fruits	Coconut
	Barks	Linen, Hemp, Jute, Amie, Kenaf
	Leaves	Sisal, Henequen, Abaca, Pineapple
	Bois	
	Stems	Wheat, Corn, Barley, Rye, Oats, Rice
	Cannes and Reeds	Bamboo, Bagasse, Esparto, Reed
Animal	Wool/Hair	Wool, Hair, Cashmere
	Silkworms	tussah silk, Mulberry silk
Mineral		Asbestos, Wollastonite

Table I. 3. World production of the most important vegetal fibers and their sources [18]

Fiber	World production (1000 t)	Source
Bamboo	10.000	Stems
Cotton	18.450	Fruits
Jute	2.300	Stems
Kenaf	970	Stems
Linen	830	Stems
Sisal	378	Leaves
Hemp	214	Stems
Coconut	100	Fruits
Abaca	70	Leaves

Vegetal fibers have managed to gain increasing interest as reinforcement in composites. This is due to their mechanical properties, their particularly low densities and low production costs. Plant fiber yields are quite high. The price of labor is relatively cheap in countries where source plants are grown, which can in some cases be harvested several times a year. The cost of producing plant fibers is one-third the price of glass fibers, one-quarter the cost of aramid fibers, and one-fifth the price of carbon fibers [19].

Compared to fibers conventionally used in the reinforcement of composites, such as glass fibers, natural fibers have weaker mechanical properties (Table. I. 4). However, these fibers have lower densities, and therefore specific property/density ratios comparable to glass fibers. Such properties can still be suitable for applications where stress levels are limited and where the concern for lightness combined with low costs is sought. In addition, the use of these fibers in composite materials, especially with thermoplastic matrices, presents an ecological advantage.

Table I. 4. Physical and mechanical properties of some vegetal fibers compared to glass fibers and carbon fibers

Fiber	Density (g/cm^3)	Diameter (µm)	Tensile limit (MPa)	Young's modulus (GPa)	Elongation (%)
Linen	1.5	40 - 600	345 - 1500	27.6	2.7 - 3.2
Hemp	1.47	10 - 100	650 - 900	30 - 70	1.6
Jute	1.3 - 1.49	25 - 200	393 - 800	13 - 26.5	1,16 - 1,5
Sisal	1.45	50 - 200	468 - 700	9.4 - 22	3 - 7
Glass fiber	2.55	17	3400	73	2.5
Carbon	1.78	5 - 7	3400 a - 4800 b	240 b - 425 a	1.4 - 1.8

I. 4. 2. Classification of plant fibers

The classification of cellulosic fibers is quite complicated. They can be classified into three categories, according to the literature [20]:

- The origin of the fibers: they are widely available and distributed, very abundant and very varied in terms of their origin. The fibers can come from stems (in this case, we speak of bast fibers: hemp, flax, jute, ramie, etc.), from the seminal hairs of seeds (cotton, kapok, etc.), from leaves or trunks (alfa, diss, sisal, abaca, etc.), from fruit envelopes (coir, etc.), or from canes, rushes, grasses (bamboo, bagasse, wheat, corn, rice, etc.), and from wood [21]. (Figure I. 3).

- The fibers length: is determined by the technological extraction method used. The majority of fibers from leaves and stems are observed as long fibers, and exhibit lengths greater than 120 mm. However, fibers with lengths recorded in the range of 25 to 60 mm, such as cotton, are observed as short-staple fibers [20].

- Functional tests: (i) fibers with low stiffness, usually originating from annual plants that are not rich in lignin (jute, cotton, flax, hemp), are defined by a smooth touch; (ii) fibers that are thick revealing a more considerable bending and torsional rigidity. They are solid and are determined by a heavier lignin percentage. Examples include sisal, wood, and abaca.

In return for these justifications, the classification of fibers remains somewhat random although they are often quite necessary.

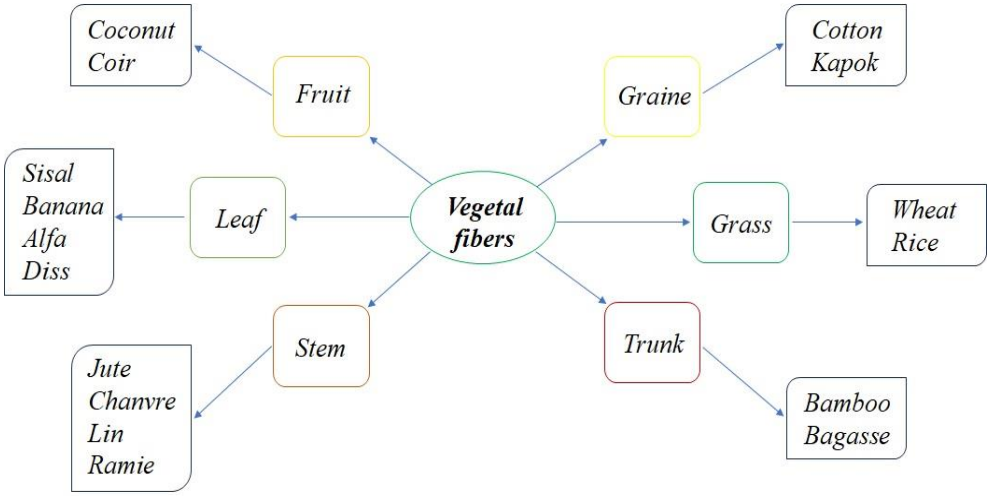

Figure I. 3. Classification of vegetal fibers according to origin [22]

We will present some plants that are the source of fibers used as filler in polymer matrix composite materials (Figure. I. 4).

Figure I. 4. The different sources of vegetal fibers

I. 4. 3. Fiber extraction methods

The extraction process consists of extracting bundles of fibers from the harvested plant. According to the literature Plant fibers can be extracted using four primary techniques: mechanical, chemical, biological, and physical methods [23]. The selection of the suitable method depends on the plant's type, age, and the specific organ being extracted. In certain instances, a combination of multiple processes is necessary.

I. 4. 3.1. Mechanical process

This process can be done by hand or with the assistance of a machine.

- Manual: The fibers are obtained by using a knife and a comb after being beaten [24].
- By machine: it is by crushing by rolling, under explosion or also by assembly of the two techniques, the fibers are detached from each other [23]. This is repeated many times consecutively until the fibers are separated. The advantage of this method is to carry out an extraction without destruction of the constituents [25].

I. 4. 3. 2. Chemical process

This method frequently uses basic or mild acid solutions for retting. The arrival of proteins (enzymes) activates the course of fiber extraction. Caustic soda is the most commonly used alkali. Mild acids, for example, oxalic acid and sulfuric acid in conjunction with a stain remover are also used to extract fibers. It is emphasized that the concentration of the substances in the treatment solution determines the nature of the fibers extracted [22, 26].

I. 4. 3. 3. Biological process

It is a natural, traditional and very old extraction process. Several biological processes are used such as field retting, enzymatic retting and pond retting (with water) [27]. The latter rely on the activity of microbial species in the environment to break down the extractables, these results in a longer extraction time compared to other extraction processes. Some fungi such as Pusillus and Fusariuslaterium are used during dew retting and certain bacteria, including Bacillus and Clostridium, are involved in the water retting process. The latter have been found to be very active in minimizing non-cellulosic substances in plants and releasing the fiber [28, 29].

I. 4. 3. 4. Physical process

The separation of fibers by steam pressure bursting is a very effective physical method. It is subsequently done in the most fragile cells [30]. This process is repeated many times, which results in the explosion of the middle lamellae which is an intercellular glue. Finally, the separation of the fibers will be completed by washing with running water [31]. There are also processes based on ultrasound, and others based on microwaves [32].

I. 4. 4. Structure and chemical composition of plant fiber

Plant fibers, such as cotton, linen, hemp, jute, sisal, kenaf, coconut, abaca, and wood, are primarily made up of biological materials like cellulose, hemicelluloses, and lignin. Cellulose, a polymer, stands out from the other fiber components because it has a predominantly crystalline structure, unlike the more amorphous structure of the others. This crystalline structure gives cellulose a much higher modulus of elasticity, around 136 GPa, in contrast to the 75 GPa of glass fiber. A plant fiber can be compared to a composite material, with cellulose fibrils acting as the reinforcing component. The surrounding matrix consists mainly of hemicellulose and lignin (**see** Table I.5). The cellulose fibrils are arranged in a helical pattern at a specific angle, known as the "microfibrillar angle." This angle, which is formed between the fibrils and the fiber's axis, plays a key role in determining the fiber's stiffness.

Table I. 5. Comparison of the chemical composition of different plant fibers [33]

Fiber	Pectins	Hemicelluloses	Cellulose
Zostera	10 ± 2	28 ± 5	57± 3
Linen	6 ± 3	7 ± 3	82 ± 5
Hemp	2.5	5.5	78.3
Jute	0.2	12	64.4
Ramie	1.9	13.1	68.6
Sisal	0.8	12	65.8

The properties of natural fibers are often contested due to the wide variety of methods involved in their cultivation, extraction, and separation, all of which significantly impact their characteristics. Many factors can influence the properties of natural fibers. Specifically, factors such as the fiber variety, growing conditions (including soil, climate, and treatment), maturity, preparation processes (like retting, scutching, and combing), moisture content, crystalline structure (such as crystallinity, polymerization degree, and cellulose type), and morphological aspects (including cell diameter, microfibrillar angle, and lumen size) all play a role [34].

In composite materials, the amount of fiber reinforcement and its alignment generally determine the elasticity and fracture behavior. Likewise, for plant fibers, their physical properties are primarily influenced by factors such as chemical and physical composition, structural features, cellulose content, microfibrillar angle, aspect ratio (L/d, which plays a crucial role in load transfer between the fibers and the matrix), cross-sectional shape, and degree of polymerization. In simple terms, for a given cellulose percentage, a lower microfibrillar angle results in greater fiber rigidity and strength; the greater microfibrillar angle, the greater elongation at break [11, 35].

The characterization of plant fibers is challenging due to the wide variability in the physical, mechanical, or thermal properties they exhibit [36]. This variability stems from the

structural differences within the fibers. For instance, cell size is influenced not only by the fiber's variety but also by factors such as its maturation stage, environmental conditions during growth, and its position within the plant.

Table. I. 6 presents the mechanical tensile characteristics of different fibers of natural origin as well as those of the reinforcing fibers commonly used for the reinforcement of common composite materials. Given the natural nature of these fibers, some dispersions are noted.

Table I. 6. Comparison of average tensile mechanical properties of different fibers [37]

Fibers	E (GPa)	ε_r (%)	σ_r (MPa)	Density
Synthetic fibers				
Glass E	72 - 73	4.6 - 3	2000 - 3400	2.54
Carbon	230 - 825	0.3 - 1.5	2350 - 3530	1.7 - 2
Aramid	124	2.9	3620	1.44
Plant fibers				
Linen	12 - 85	1 - 4	600 - 2000	1.54
Ramie	27 - 128	1.2 - 3.8	400 - 1000	1.56
Hemp	35	1.6	389	1.07
Jute	26.5	1.5 - 1.8	393 - 773	1.44
Sisal	9 - 21	3 - 7	350 - 700	1.45
Coconut	4 - 6	15 - 40	131 - 175	1.15
Cotton	5.5 - 12.6	7 - 8	287 - 597	1.5 - 1.6
Animal fibers				
Silkworm	5 - 16	18 - 15	200 - 650	-
Spider	7	30	600	-

The plant fiber derives its structure from the architecture and biochemical composition of its wall, which is composed of three layers superimposed in the radial direction, and they are aligned with the axis of the fiber. From the outside to the inside are located: the middle lamella, whose role is to glue the cells together to form the fibrillar bundle; followed by the primary wall and lastly the secondary wall. The latter being formed of 3 layers S1, S2 and S3 (Figure. I. 5). It borders a lumen, which has a diameter variable according to the plant nature. The arrangement of the cellulose microfibrils is not the same between these various cell layers. In the S1 and S3 layers, the microfibril angle is significant, that is to say that the fibrils have an orientation almost oblique to the axis of the fiber (Figure. I. 6). In contrast, the angle of the microfibrils in the S2 layer is

small, and these fibrils therefore have a parallel orientation with respect to the fiber axis. Cellulose obtains the maximum percentage in the S2 layer which composes the thickest portion of the cell wall in the fiber (taking 75% of the cell wall thickness) and controls the fiber characteristics [22, 38].

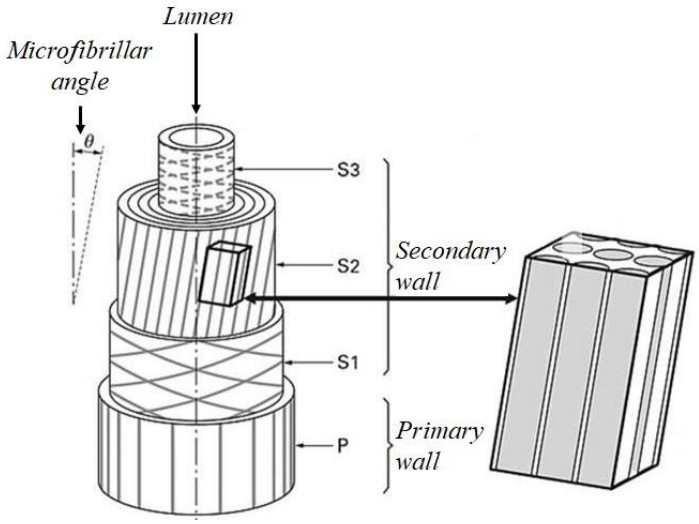

Figure I. 5. Structural of fiber cells [39]

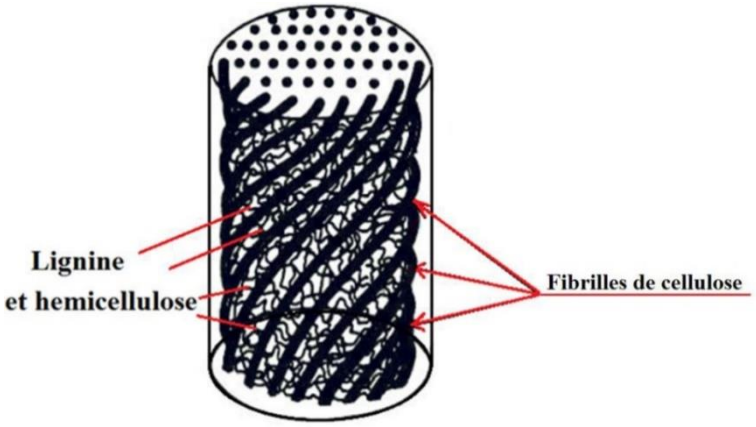

Figure I. 6. Structure diagram of a plant fiber [37]

Plant fibers consist of lignin, hemicellulose, cellulose, waxes and some water-melting components, where lignin, hemicellulose and cellulose are the major components. A good understanding of the chemical composition of these elements is essential to better understand their influences on the properties of plant fibers.

I. 4. 4. 1. Cellulose

Cellulose, with its distinctive chemical structure, is the primary component of plant fibers [40]. Its macromolecular nature was highlighted around the 1930s. Cellulose consists of D-anhydroglucose units linked together by β (1→4) bonds. It is considered a polymer of carbohydrate units. The fundamental building block of cellulose, however, is the "dimeric" cellobiose, which consists of two glucose units attached by the β (1→4) bond [41, 42]. Figure. I. 7 shows the cellulose molecule, with its hydrogen bonds.

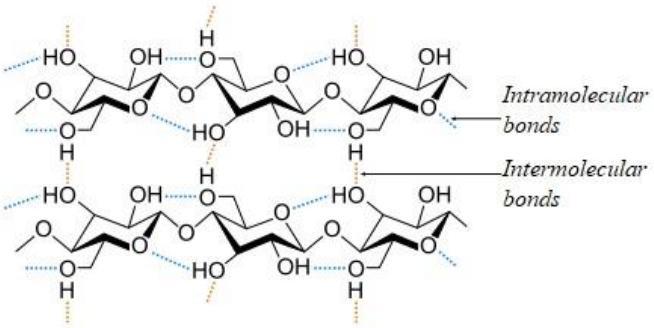

Figure I. 7**.** Diagram of cellulose molecules, with its hydrogen bonds [43]

The glucose units in cellulose can bond together to create crystalline structures through intramolecular hydrogen bonds, giving rise to a robust and rigid polymer. The arrangement of these glucose units within the linear polymer dictates the properties of cellulose [44]. The hydroxyl groups, along with their capacity to form hydrogen bonds, are crucial in determining the orientation of the crystal lattice and influencing the physical properties of cellulose [45]. Cellulose contains both highly organized crystalline regions and less structured, amorphous zones. These variations influence the fiber's properties and performance [44].

I. 4. 4. 2. Hemicellulose

Hemicellulose is a heterogeneous group of polysaccharides, Regarded as the most stable carbohydrate in plant cell walls whose composition varies between different types of plant fibers and includes a range of carbohydrates, such as arabinans $(C_5H_{10}O_5)n$, glucans $(C_6H_{12}O_6)n$, galactans $(C_6H_{12}O_6)n$, mannans $(C_6H_{12}O_6)n$, and xylans $(C_5H_{10}O_5)n$ represent hemicellulose (Figure. I. 8) [44]. It is in plant cell walls that hemicelluloses are linked to pectins, cellulose, and aromatic constituents [44]. Hemicellulose molecules are hydrogen bonded with cellulose microfibrils and form cementing materials for fiber structure. Unlike cellulose, hemicellulose is easily hydrolyzable in acids, soluble in alkaline media and very hydrophilic. Hemicellulose chains are subdivided and very short (50 - 300) compared to cellulose [45].

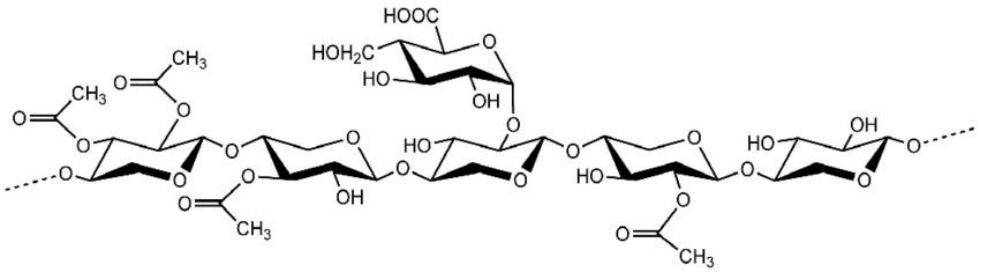

Figure I. 8**.** Example of Hemicellulose Structure [43]

I. 4. 4. 3. Lignin

Lignin is a non-crystalline material and hydrophobic in nature. It is a complicated three-dimensional copolymer composed of aliphatic and aromatic constituents with a considerable molecular mass. It is composed of three phenylpropane units: coniferyl, p-coumaryl alcohols and sinapyl (Figure. I. 9) [44]. Its chemistry has not yet been exactly confirmed, but the majority of the structural units of the macromolecule and its functional groups have been determined. A low proportion of hydrogen and a high proportion of carbon [45] characterize it.

Lignin provides cover against microbial pathogens and gives rigidity and strength to cell walls. In plants, the content of lignin is highly variable. Lignins are bound to cellulose and hemicellulose in plant cell walls [44]. It has a role as a sinking agent in the cellulose/hemicellulose matrix, which is why lignin is often called glue of the plant cell wall.

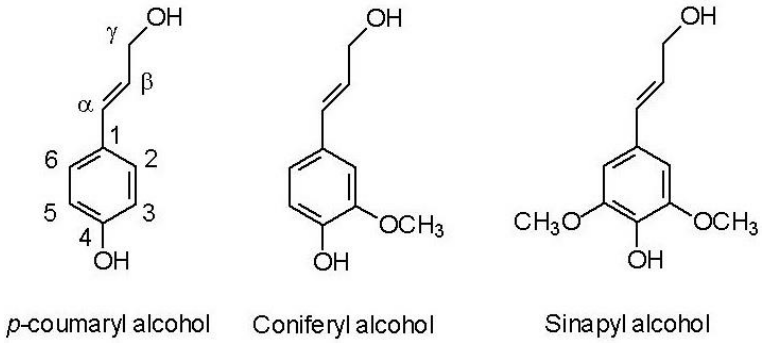

Figure I. 9**.** Lignin monomers [46]

I. 4. 4. 4. Extractable

These materials are considered as secondary and non-structural constituents. In other terms, they are not the primary components of the wall structure, unlike cellulose, hemicellulose, and lignin, although they are present within the cell wall. They have a remarkable influence on plant materials. These natural chemical compounds are extracted or removed from the plant substance by a proportionally mild chemical treatment, since they are usually soluble in water and/or organic solvents, hence their name. The percentage of extractables changes depending on the variety

examined and acts on the odor and color [47]. Table. I. 7 presents the percentage of chemical constituents of some plant fibers.

Table I. 7. Chemical composition (% by mass) of certain plant fibers [48-50]

Fibers	Cellulose	Hemicellulose	Lignin	Extractable
Bamboo	42.3 - 49.1	24.1 - 27.7	23.8	1.3 - 2
Hemp	70 - 78	17.9 - 22	3.7 - 5	2 - 5
Jute	51 - 72	12 - 20.4	5 - 13	0.8
Alfa	46.1 - 47.6	22.l - 22.2	17.7 - 22.3	3.1
Diss	44.1	27	16.8	3.9
Linen	60 - 81	14 - 18.6	2 - 3	0.8 - 2
cotton	82.7 - 92	2 - 5.7	0.5 - 1	0.5 - 2
Sisal	66 - 78	10 - 14	10 - 14	2
Kenaf	43 - 57	21	15 - 19	2 - 5
Spanish Broom	44.5	18.5	16.3	4
Ramie	53	13.1 - 15	0.6 - 1	-
Bagasse	40 - 46	24.5 - 29	12.5 - 20	1.5 - 2.4
Agave Americana	68.4 - 71.7	15.7 - 22.2	4.9 - 6.1	-

I. 4. 5. Properties of plant fibers

Cellulosic fibers or plant fibers are used in the presence of adhesive, alone, or in assembly with other materials. A group of parameters guides the characteristics of these plant fibers: chemical composition of the fibers, dimensions of the fiber, crystallinity of the cellulose, degree of polymerization of the cellulose, angle of orientation of cellulose chains and pre-existing defects.

- They are derived from the renewable parts of plants and they are highly available and easy to extract.
- They have a low environmental impact, moreover, cellulose fiber composites use, during their life cycle, 45% less energy than fiberglass composites, and lead to fewer atmospheric emissions [50].
- Compared to fiberglass, studies have found that plant fibers have interesting mechanical solutions (Table. I. 8). These performances usually depend on the plant and the organ from which the fibers are extracted [51].
- They also have a low cost: up to ten times cheaper than glass fibers and up to five hundred times cheaper than carbon fibers (Table. I. 9) [52].
- In addition to their low cost, they have a low density, which has made them highly sought after.

- Also, they are recyclable; their reintegration into the carbon cycle is ensured by microorganisms equipped with an enzymatic system capable of hydrolyzing polymers into digestible units.
- In addition, they are non-abrasive for equipment. On the health framework, they have no toxicity, non-irritating to the skin less and no risks for human health [52].
- Plant fibers can rival synthetic fibers when it comes to mechanical strength. This characteristic changes significantly in relation to the morphology of the fibers, the chemical composition, the method of extraction of the fibers, their crystallinity along with the cellulose's polymerization degree. Several researchers [53] have proposed an experimental relationship between the dimensions of the cells, the cellulose content and the angle of orientation of the microfibrils.
- Different properties exhibited by plant fibers vary according to plant type, fibers origin and growing conditions. The mechanical and physical properties of natural fibers are influenced by the fiber's cellulose content, the angle of the microfibrils, and the degree of cellulose polymerization [54, 55]. On the microscopic scale, structure, defects and chemical composition of the fibers, dimensions of the cells, are factors affecting the variability of the performances of plant fibers and which influence all the properties of the fibers. In general, as the cellulose content rises, both the tensile strength and Young's modulus of the fibers also increase.

Table I. 8. Physico-mechanical properties of natural fibers [48, 56]

Fiber	Density (g/cm3)	Length (mm)	Diameter (um)	Young's modulus (GPa)	Elongation at break (%)	Tensile strength (MPa)
Jute	1.5-1.6	2-5	40-350	27.6	1.5-1.8	393-773
Linen	1.4-1.5	9-70	12-177	45 - 100	2.7-3.2	345-1100
Hemp	1.5	5-55	5-51	70	1.6	690
Cotton	1.5-1.6	10-40	10-30	5.5 - 12.6	7-8	287-597
Ramie	1.5	60- 250	50	61.4-128	3.6-3.8	400-938
Sisal	1.33-1.5	1-8	100-300	9.4-22	2-2.5	511-635
Kenaf	1.45	2-6	-	53	1.6	930
Softwood	1.5	-	-	40	4.4	1000
Fiberglass	2.5-2.55	-	<17	70	2.5-3.4	2000- 3500
Carbon fiber	1.82	-	8.2	-	1.3	2550

Table I. 9. Comparison between natural fibers and glass fibers [57]

Properties	Natural fibers	Glass fibers
Density	Weak	Twice as much as natural fibers
Cost	Weak	superior to natural fibers
Renewal	Yes	No
Recyclability	Yes	Yes
Energy consumption	Weak	Raised
Distribution	Wide	Wide
CO_2 neutral	Yes	No
Machine abrasion	No	Yes
Health risk (inhalation)	No	Yes
Arrangement	Biodegradable	Non-biodegradable

Plant fibers also have a number of disadvantages that stem mainly from the natural nature of these fibers.

- Thus, the absorption of moisture and water causes swelling of the fiber which leads to a decrease in the physical, mechanical, thermal properties [58] and the dimensional stability of the composites [59]. This characteristic will reduce the life of materials designed for durable applications.
- They are also quite sensitive to temperature. Indeed, the chemical composition of plant fiber (lignin, hemicellulose and pectins) is thermally unstable and tends to degrade at relatively low temperatures (< 400 °C) [60].
- They also show a great variability of properties for the same species depending on many factors such as the age of the plant, the harvest season, the climate, etc. For example, the cellulose content of a plant fiber influences the characteristics of the fiber, which results in materials with variable quality. In addition, the density of plant fibers varies in relation to climatic conditions and harvest regions [61].
- The incompatibility of hydrophobic polymer matrices with hydrophilic natural fibers requires adequate treatments to improve the adhesion between fibers and matrix [62].

I. 4. 6. Applications of plant fibers

Cellulosic fibers have never been as widely used as they are today. In the past, the main areas of use were textiles, papermaking and, to a lesser extent, infrastructure (daub). At first, man used some plant parts in the form of fibers, initially allowing the manufacture of threads and ropes (Figure. I. 10. a, b). Then, thanks to increasingly developed technological means (knitting, hand weaving, machine weaving), the use of plant fibers expanded to the manufacture of fabrics (Figure. I. 10. c, d, e).

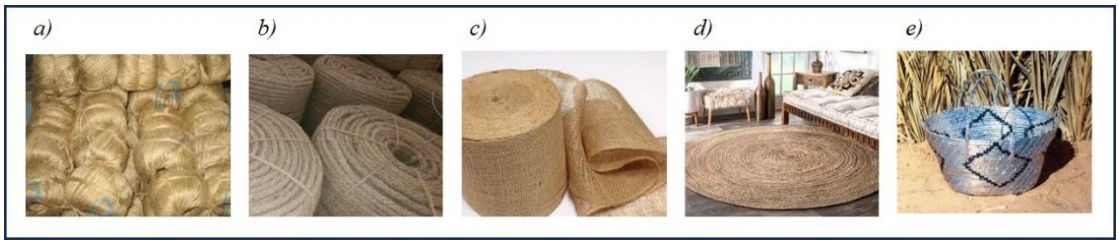

Figure I. 10. The different uses of plant fibers in the past; a) Thread, b) Rope, c) Jute fabric, d) Industrial carpet, e) handmade bassinet

Then their use began to grow, especially in the fields of insulation, where they are used alone, such as hemp wool or cellulose wadding. On the other hand, as composites, in association with a polymer material: new uses in all areas of life, such as plastics, automobiles, construction, the medical sector, sports, aerospace and aeronautics [41, 63] (Figure. I. 11. a, b, c).

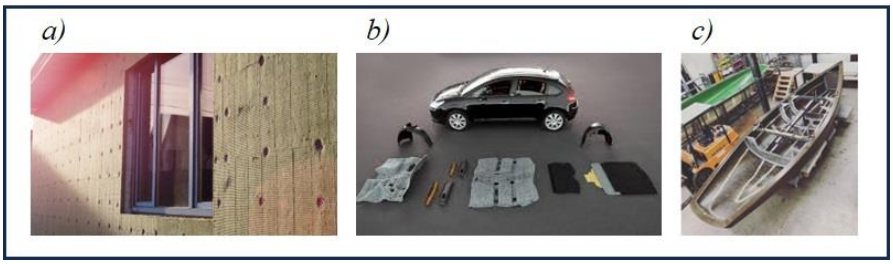

Figure I. 11**.** The different uses of plant fibers in the present; a) insulation in the building, b) Vehicle parts made of plant fibers, c) Boat made of plant fibers.

The optimization of the properties of composites with natural reinforcement and the search for new applications are of interest not only to the scientific world but also to the industrial world. Mainly several automobile manufacturers who find in these materials great economic and ecological interests (sustainable development) and partly a marketing aspect support the investments made in this vision. Compared to composite parts made of fiberglass and non-reinforced polymers, parts made of natural fibers in automobiles have better properties while being lighter: electrostatic, thermal and acoustic insulation and vibration absorption. The inclusion of natural fibers in composite components reduces their weight, which in turn lowers the overall weight of the vehicle. This contributes to environmental benefits by decreasing fuel consumption and, consequently, driving costs.

European car manufacturers use natural fiber-reinforced thermoplastics in mat form, that is to say a collection of non-woven staple fibers, oriented or not, for trim panels in doors, package trays, seat backs, engine protectors, and headrests. Daimler Chrysler, a key consumer of NFC, uses polypropylene reinforced with natural fibers for interior trim. Dashboards and door panels are manufactured for some of the brand's car models. The manufacturer asserts that car components made from natural fibers use 83% less energy and are 40% more cost-effective to produce than fiberglass parts. The BMW Group incorporates a significant amount of renewable materials in its

vehicles, with each BMW 7 Series featuring 24 kg of natural fibers. In 2000, Audi introduced the A2 model, where the door panels were constructed from polyurethane reinforced with a blend of flax and sisal mats. Table. I. 10 gives some examples of automobile parts made from natural fibers.

Table I. 10. Examples of naturally reinforced composite parts used by some car manufacturers[17]

Car manufacturer/model	Pieces	Plant fiber used
Brazilian trucks	Upholstery, seat cushions	Jute and coconut
Mercedes Benz (E-Class)	Interior door panels	Sisal and linen
Mercedes Benz (C-Class)	Rear window panels	Sisal and cotton
Mercedes Benz (S-Class)	Interior door panels	Hemp
Chevrolet Impala	Panel trim	Linen
Chrysler	Engine and transmission cover	Sisal, linen, coconut, hemp and cotton
Opel / Astra	Interior door panels, seat backs	Hemp, kenaf and flax
Toyota	Trunk shelf	Kenaf

The various challenges in the development and optimization of NFCs are being investigated under increased demand that is pushing the development of these composites. Much work remains to be done to be able to compete and overcome conventional composites such as those with glass fibers.

I. 5. Matrix

One way to classify composites is based on the type of matrix used.

We distinguish:

- Organic matrix composites that currently form most industrial composites (resins, fillers).
- Ceramic matrix composites that are used in high-tech applications for extreme conditions (high temperature): (nitride, carbide).
- Metal matrix composites: (light and ultra-light alloys of aluminum, magnesium).

The matrix can be made from any material, with organic matrices being the most commonly recognized because they represent more than 90% compared to others [5]. These polymers are mainly divided into two main categories: thermosetting and thermoplastic. The areas of use of polymer composites that prescribe the nature of the matrix. Indeed, thermosets find their use in the development of structural materials while thermoplastics are primarily employed in applications that don't require structural strength [64].

I. 5. 1. Thermoplastics

They are composed of a group of long macromolecules entangled with each other, and linear or branched. When exposed to heat, the intermolecular bonds can temporarily break, allowing the molecules to shift and adopt new positions. Upon cooling, the molecules lock into these new positions, forming secondary bonds that create a solid structure. The rigidity and strength of thermoplastics are associated with their high molecular weight and the inherent properties of their monomer units [65]. Their thermo reversibility and recyclability constitute very important advantages. The essential families of thermoplastics are plastics based on polyvinyl chloride, polyolefins (polyethylenes, polypropylenes), polystyrenes and acrylics. Some physicochemical properties of the most used matrices are grouped in Table. I. 11.

Table I. 11. Characteristics of some thermoplastics [66].

Polymers	Tg (°C)	Tf (°C)	Density	σ (MPa)	E (GPa)
PLA	60	175	1.25	40 - 60	3 - 4
PVC	80	160 - 220	1.38	58	2.9
PP	-	145 - 175	0.9	30	1.2
PS	90 - 100	-	1.05	55	3.2

I. 5. 2. Thermosetting

Unlike thermoplastics, thermosets harden irreversibly when heated. They cannot be reshaped or melted under heat and pressure. In thermosetting polymers, the molecules are chemically bonded through cross-linked linear chains, forming a rigid, three-dimensional, insoluble network. This structural transformation occurs during the composite's production process. Unlike thermoplastics, thermosets offer greater chemical resistance, enhanced thermal stability, and improved resistance to relaxation and creep. The mechanical and thermal characteristics of thermosets are based on molecular chains that create the network, density and length of crosslinks [65].

The matrices that are most frequently used are unsaturated polyester, venylester and epoxy. They are recognized for their very good resistance to chemicals (non-reactive materials), electrical, as well as mechanical, and heat. Table. I. 12 shows some properties of certain thermosetting agents.

Table I. 12. Characteristics of some thermosets [66]

Resin	Density	E (GPa)	σ (MPa)	T_{max} (°C)
Urethane	1.1	0.7 - 7	30	100
Urea formaldehyde	1.2	6 - 10	40 - 80	140
Epoxy	1.2	4.5	130	90 - 200
Unsaturated polyester	1.2	4	80	60 - 200
Vinyl ester	1.2	3.5 - 5	70 - 85	100 - 140

I. 6. Conclusion

Regarding what is in this bibliographic review, we note that plant fiber and its various components are widely presented and sometimes little valued. According to the different uses today, it seems that their use in the field of materials is interesting because it evokes on one hand the considerable use of biomass. This use in materials is still a method of transporting a more powerful added value towards applications used now (example: energy). As a result, the growth of this biomass employment sector contains some limits. To summarize the potential of this sector, this chapter highlights the weaknesses and strengths as well as the advantages and ultimatums of the evolution of bio sourced materials.

In this context, we have specifically highlighted plant fibers, a key source of biomass. We discuss their extraction methods, structure, properties, and applications. Our research extends beyond plant fibers to include composite materials, exploring their use as lightweight, biodegradable, recyclable, renewable, and cost-effective reinforcements. Plant-based reinforcements are diverse and available globally or some have mechanical characteristics that can compete with those of synthetic fibers while keeping a lower density.

References

[1] A. W. Ganczarski, S. Hernik, and J. J. Skrzypek, "Mechanics of anisotropic composite materials," *Mechanics of Anisotropic Materials,* pp. 87-131, 2015.

[2] H.-y. Cheung, M.-p. Ho, K.-t. Lau, F. Cardona, and D. Hui, "Natural fibre-reinforced composites for bioengineering and environmental engineering applications," *Composites Part B: Engineering,* vol. 40, pp. 655-663, 2009.

[3] L. McCartney, "New theoretical model of stress transfer between fibre and matrix in a uniaxially fibre-reinforced composite," *Proceedings of the royal society of London. A. Mathematical and physical sciences,* vol. 425, pp. 215-244, 1989.

[4] J. A. Sobrino and M. D. G. Pulido, "Towards advanced composite material footbridges," *Structural engineering international,* vol. 12, pp. 84-86, 2002.

[5] P.-E. Bourban, *Matériaux composites à matrice organique: constituants, procédés, propriétés* vol. 15: EPFL Press, 2004.

[6] Y. Akkaya, A. Peled, and S. Shah, "Parameters related to fiber length and processing in cementitious composites," *Materials and Structures,* vol. 33, pp. 515-524, 2000.

[7] B. Zhang, K. Kowsari, A. Serjouei, M. L. Dunn, and Q. Ge, "Reprocessable thermosets for sustainable three-dimensional printing," *Nature communications,* vol. 9, p. 1831, 2018.

[8] M. E. Grigore, "Methods of recycling, properties and applications of recycled thermoplastic polymers," *Recycling,* vol. 2, p. 24, 2017.

[9] P. J. Doorbar and S. Kyle-Henney, "4.19 development of continuously-reinforced metal matrix composites for aerospace applications," *Compr. Compos. Mater,* vol. 4, pp. 439-463, 2018.

[10] S. Mortazavian and A. Fatemi, "Fatigue behavior and modeling of short fiber reinforced polymer composites: A literature review," *International Journal of Fatigue,* vol. 70, pp. 297-321, 2015.

[11] S. Ali Zernadji, M. Rokbi, M. Benhamida, and D. Hammiche, "Estimation of fiber/polymer bond strength from maximum load values recorded in the micro-bond tests," *Materials Today: Proceedings,* vol. 53, pp. 247-252, 2022.

[12] V. Constantinescu, G. V. Bogus, R. G. Taran, and I. Carcea, "New composite materials that reduce the effect of reinforcement corrosion," *Advanced Materials Research,* vol. 837, pp. 265-270, 2014.

[13] R. Hsissou, R. Seghiri, Z. Benzekri, M. Hilali, M. Rafik, and A. Elharfi, "Polymer composite materials: A comprehensive review," *Composite structures,* vol. 262, p. 113640, 2021.

[14] J. Fan and J. Njuguna, "An introduction to lightweight composite materials and their use in transport structures," in *Lightweight Composite Structures in Transport*, ed: Elsevier, 2016, pp. 3-34.

[15] K. L. Reifsnider, *Fatigue of composite materials*: Elsevier, 2012.

[16] S. Bucuta and N. Ilie, "Light transmittance and micro-mechanical properties of bulk fill vs. conventional resin based composites," *Clinical oral investigations,* vol. 18, pp. 1991-2000, 2014.

[17] S. Bouzouita, "Optimisation des interfaces fibre-matrice de composites à renfort naturel," Ecole Centrale de Lyon; Ecole Nationale d'Ingénieurs de Monastir, 2011.

[18] S. Eichhorn, C. Baillie, N. Zafeiropoulos, L. Mwaikambo, M. Ansell, A. Dufresne, K. Entwistle, P. Herrera-Franco, G. Escamilla, and L. Groom, "Current international research into cellulosic fibres and composites," *Journal of materials Science,* vol. 36, pp. 2107-2131, 2001.

[19] A. Bledzki and J. Gassan, "Composites reinforced with cellulose based fibres," *Progress in polymer science,* vol. 24, pp. 221-274, 1999.

[20] S. K. Batra, "Other long vegetable fibres: abaca, banana, sisal, henequen, flax, ramie, hemp, sunn, and coir," 1985.

[21] O. Faruk, A. K. Bledzki, H.-P. Fink, and M. Sain, "Biocomposites reinforced with natural fibers: 2000–2010," *Progress in polymer science,* vol. 37, pp. 1552-1596, 2012.

[22] N. Moussaoui, M. Rokbi, H. Osmani, M. Jawaid, A. Atiqah, M. Asim, and L. Benhamadouche, "Extraction and characterization of fiber treatment Inula viscosa fibers as potential polymer composite reinforcement," *Journal of Polymers and the Environment,* vol. 29, pp. 3779-3793, 2021.

[23] Z. Belouadah, A. Ati, M. Rokbi, A. Bezazi, and A. Imad, "Optimisation Des méthodes D'extraction Et Caractérisation Mécanique De La Fibre Alfa En Vue De Son Application Comme Renfort Des Matériaux Composites," *Journal of Materials, Processes and Environment,* vol. 2, pp. 51-57, 2014.

[24] K. M. M. Rao and K. M. Rao, "Extraction and tensile properties of natural fibers: Vakka, date and bamboo," *Composite structures,* vol. 77, pp. 288-295, 2007.

[25] R. Tokoro, D. M. Vu, K. Okubo, T. Tanaka, T. Fujii, and T. Fujiura, "How to improve mechanical properties of polylactic acid with bamboo fibers," *Journal of materials science,* vol. 43, pp. 775-787, 2008.

[26] M. Rokbi, H. Osmani, A. Imad, and N. Benseddiq, "Effect of chemical treatment on flexure properties of natural fiber-reinforced polyester composite," *procedia Engineering,* vol. 10, pp. 2092-2097, 2011.

[27] S. A. Zernadji, M. Rokbi, M. Benhamida, and A. Kellai, "Extraction and characterization of novel natural cellulosic fiber from Echinops spinosissimus plant stem," *Journal of Composite Materials,* vol. 57, pp. 4503-4519, 2023.

[28] A. Ali, K. Shaker, Y. Nawab, M. Jabbar, T. Hussain, J. Militky, and V. Baheti, "Hydrophobic treatment of natural fibers and their composites—A review," *Journal of Industrial Textiles,* vol. 47, pp. 2153-2183, 2018.

[29] G. Henriksson, D. E. Akin, R. T. Hanlin, C. Rodriguez, D. D. Archibald, L. L. Rigsby, and K. Eriksson, "Identification and retting efficiencies of fungi isolated from dew-retted flax in the United States and Europe," *Applied and Environmental Microbiology,* vol. 63, pp. 3950-3956, 1997.

[30] M. Sotton and M. Ferrari, "Adjustment of the Steam Explosion Treatment to Extract Fibers From Plants, Usable for Textile and Related End-Uses," *Steam Explosion Techniques, Fundamentals and Industrial Applications, eds B. Focher, A. Marzetti, V. Crescenzi. Gordon and Breach Science Publisher, Philadelphia,* pp. 219-231, 1991.

[31] N. H. Tung, H. Yamamoto, T. Matsuoka, and T. Fujii, "Effect of surface treatment on interfacial strength between bamboo fiber and PP resin," *JSME International Journal Series A Solid Mechanics and Material Engineering,* vol. 47, pp. 561-565, 2004.

[32] G. R. Nair, J. Kurian, V. Yaylayan, D. Rho, D. Lyew, and G. Raghavan, "Microwave-assisted retting and optimization of the process through chemical composition analysis of the matrix," *Industrial Crops and Products,* vol. 52, pp. 85-94, 2014.

[33] A. Elouaer, "Contribution à la compréhension et à la modélisation du comportement mécanique de matériaux composites à renfort en fibres végétales," *Ecole doctorale Sciences, technologies, santé, Reims,* 2011.

[34] H. Makri, M. Rokbi, M. Meddah, N. Belayachi, and A. Khaldoune, "Extraction and characterization of novel lignocellulosic fibers from Centaurea hyalolepis plant as a potential reinforcement for composite materials," *Journal of Composite Materials,* p. 00219983231184020, 2023.

[35] M. Rokbi, A. Imad, C. Herbelot, and Z. Belouadah, "Fracture toughness of random short natural fibers polyester composites," in *Diffusion Foundations*, 2018, pp. 94-105.

[36] M. Meddah, M. Rokbi, and M. Zaoui, "Extraction and characterization of novel natural lignocellulosic fibers from Malva sylvestris L," *Journal of Composite Materials,* vol. 57, pp. 897-912, 2023.

[37] C. Baley, *Fibres naturelles de renfort pour matériaux composites*: Ed. Techniques Ingénieur, 2005.

[38] K. Persson, "Micromechanical modelling of wood and fibre properties," 2000.

[39] J. Page, "Formulation et caractérisation d'un composite cimentaire biofibré pour des procédés de construction préfabriquée," Normandie Université, 2017.

[40] R. Marchessault and P. Sundararajan, "Cellulose," in *The polysaccharides*, ed: Elsevier, 1983, pp. 11-95.

[41] A. Mohanty, M. a. Misra, and G. Hinrichsen, "Biofibres, biodegradable polymers and biocomposites: An overview," *Macromolecular materials and Engineering,* vol. 276, pp. 1-24, 2000.

[42] M. S. Doblin, I. Kurek, D. Jacob-Wilk, and D. P. Delmer, "Cellulose biosynthesis in plants: from genes to rosettes," *Plant and cell physiology,* vol. 43, pp. 1407-1420, 2002.

[43] R. Rowell, A. Raymond, and K. Judith, "Paper and composites from agro-based resources CRC Press Inc," *Madison, WI,* 1997.

[44] D. E. Akin, "Chemistry of plant fibres," *Industrial applications of natural fibres: structure, properties and technical applications,* vol. 10, p. 13, 2010.

[45] M. J. John and S. Thomas, "Biofibres and biocomposites," *Carbohydrate polymers,* vol. 71, pp. 343-364, 2008.

[46] Y. Ji, "Kinetics and mechanism of oxygen delignification," 2007.

[47] D. D. Stokke, Q. Wu, and G. Han, *Introduction to wood and natural fiber composites*: John Wiley & Sons, 2013.

[48] K. Mylsamy and I. Rajendran, "Influence of fibre length on the wear behaviour of chopped agave americana fibre reinforced epoxy composites," *Tribology Letters,* vol. 44, pp. 75-80, 2011.

[49] B. Bouiri and M. Amrani, "Production of dissolving grade pulp from alfa," *BioResources,* vol. 5, 2010.

[50] M. E. H. Bourahli and H. Osmani, "Chemical and mechanical properties of diss (Ampelodesmos mauritanicus) fibers," *Journal of Natural Fibers,* vol. 10, pp. 219-232, 2013.

[51] K. Charlet, J. Jernot, M. Gomina, J. Bréard, C. Morvan, and C. Baley, "Influence of an Agatha flax fibre location in a stem on its mechanical, chemical and morphological properties," *Composites Science and Technology,* vol. 69, pp. 1399-1403, 2009.

[52] X. Li, L. Tabil, S. Panigrahi, and W. Crerar, "The influence of fiber content on properties of injection molded flax fiber-HDPE biocomposites," in *2006 ASAE annual meeting*, 2006, p. 1.

[53] P. Mukherjee and K. Satyanarayana, "An empirical evaluation of structure-property relationships in natural fibres and their fracture behaviour," *Journal of materials science,* vol. 21, pp. 4162-4168, 1986.

[54] A. R. S. Neto, M. A. Araujo, F. V. Souza, L. H. Mattoso, and J. M. Marconcini, "Characterization and comparative evaluation of thermal, structural, chemical, mechanical and morphological properties of six pineapple leaf fiber varieties for use in composites," *Industrial Crops and Products,* vol. 43, pp. 529-537, 2013.

[55] A. Sanadi, "Natural fibers as fillers/reinforcements in thermoplastics," *Introduction to Low environmental impact polymers. UK: Rapra Tech. Ltd,* 2004.

[56] J. Summerscales, N. P. Dissanayake, A. S. Virk, and W. Hall, "A review of bast fibres and their composites. Part 1–Fibres as reinforcements," *Composites Part A: Applied Science and Manufacturing,* vol. 41, pp. 1329-1335, 2010.

[57] A. Valadez-Gonzalez, J. Cervantes-Uc, R. Olayo, and P. Herrera-Franco, "Chemical modification of henequen fibers with an organosilane coupling agent," *Composites Part B: Engineering,* vol. 30, pp. 321-331, 1999.

[58] M. M. Thwe and K. Liao, "Effects of environmental aging on the mechanical properties of bamboo–glass fiber reinforced polymer matrix hybrid composites," *Composites Part A: Applied Science and Manufacturing,* vol. 33, pp. 43-52, 2002.

[59] J. Rout, M. Misra, S. Tripathy, S. Nayak, and A. Mohanty, "The influence of fibre treatment on the performance of coir-polyester composites," *Composites Science and Technology,* vol. 61, pp. 1303-1310, 2001.

[60] A. Rachini, M. Le Troedec, C. Peyratout, and A. Smith, "Comparison of the thermal degradation of natural, alkali-treated and silane-treated hemp fibers under air and an inert atmosphere," *Journal of applied polymer science,* vol. 112, pp. 226-234, 2009.

[61] M. Malkamäki, "Engineering flax-protein composites," 2020.

[62] R. Malkapuram, V. Kumar, and Y. S. Negi, "Recent development in natural fiber reinforced polypropylene composites," *Journal of reinforced plastics and composites,* vol. 28, pp. 1169-1189, 2009.

[63] X. Huang and A. Netravali, "Characterization of flax fiber reinforced soy protein resin based green composites modified with nano-clay particles," *Composites Science and Technology,* vol. 67, pp. 2005-2014, 2007.

[64] F. T. Wallenberger and N. Weston, *Natural fibers, plastics and composites*: Springer Science & Business Media, 2003.
[65] K. Pickering, *Properties and performance of natural-fibre composites*: Elsevier, 2008.
[66] M. Ragoubi, "Contribution à l'amélioration de la compatiblilité interfaciale fibres naturelles/matrice thermoplastique via un traitement sous décharge couronne," Université Henri Poincaré-Nancy 1, 201

CHAPTER II

Improved fiber-matrix interface

II. 1. Introduction

The characteristics of a composite are strongly related to the properties of its components: fibers, matrix and their interfaces. Other factors are also important such as the elaboration techniques etc… [1] (Figure II. 1)

The use of lignocellulosic fibers has increased in recent years to meet the demand for cellulosic fibers as reinforcement for polymer matrix composites and are much more advantageous than inorganic fibers [2].

The main difficulty in using lignocellulosic fibers in polymer matrices is their highly hydrophilic character, which causes poor adhesion with matrices that are hydrophobic. In order to find a solution to this drawback, chemical modifications are used either of the fiber or the matrix. The appropriate chemical modification reduces the tendency of moisture absorption and facilitates the bonding between the matrix and the fiber, which results in obtaining better mechanical characteristics of the composites [3].

Throughout this bibliographic synthesis, the definition and the interest of highlighting the fiber/matrix interface in the composite material are presented, methods of improvement, as well as the characterization of adhesion.

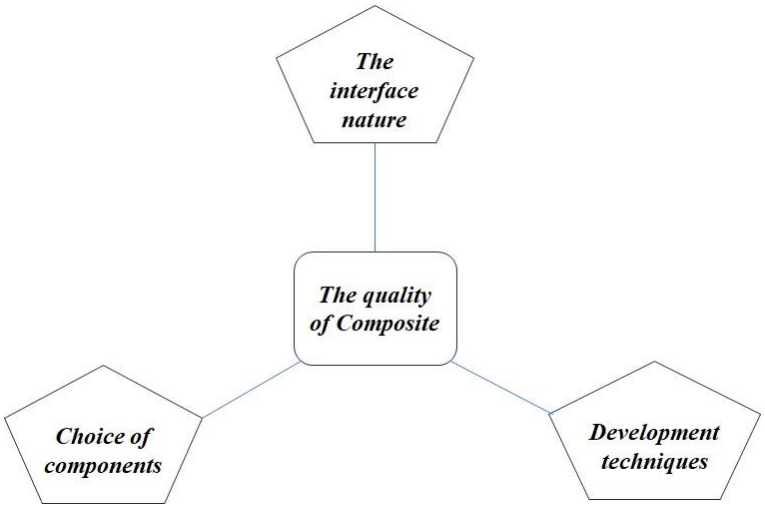

Figure II. 1**.** Factors related to the quality of a composite

II. 2. The interface in a composite

II. 2. 1. Definition

The association of the fibers with the matrix which are two distinct components induces a contact zone called interface (Figure II.2). This particular place of the material can be defined as a critical zone that has a significant effect on the mechanical characteristics of the composite. It guarantees the transmission of forces between the reinforcement and the matrix during a stress. [4]

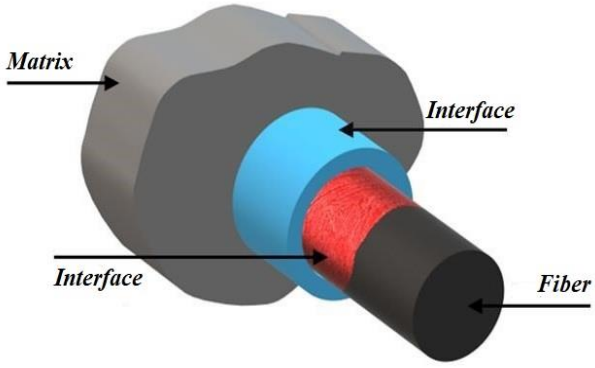

Figure II. 2. Fiber-matrix interface

The interface can have several forms and lead to the notion of interphase. The latter is a zone roughly extended between the two constituents of the composite, in which we find a rate of variation of characteristics of the two constituents. The rupture at the interface is one of the damage modes in composites (Figure II. 3). For this reason, several researches are conducted to understand the interfacial decohesion and damage mechanisms present in a composite structure under static loading. [5]

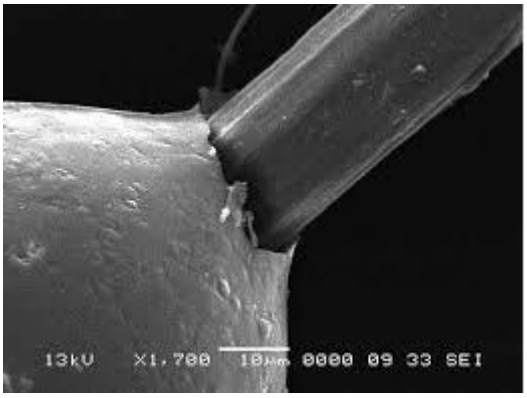

Figure II. 3. SEM micrograph of micro drop on the fiber after the IFSS test. [6]

Based on the main interactions of the fiber-matrix interface, some theories on decohesion are presented. These theories allow us to penetrate into the phenomena that are created at the interface.

II. 2. 2. Adhesion theories

The transfer of mechanical or thermochemical characteristics between the resin and the reinforcement in the composite material is a complicated concept because it will expose a large number of phenomena. In another way, cohesion is therefore composed of phenomena of diffusion, wettability, chemical interaction, adsorption, and it can be of mechanical origin [7]. Thus, the surface dictates the hypotheses of mechanical, physical or chemical bonds at the interface between materials. Different bonding theories are presented to develop the type of forces and interactions

highlighted during the bonding process. In the literature, [5-23] we find deductions from several works that show the difficulties of the phenomena exposed. According to this research, we can cite the different adhesion theories: the mechanical anchoring bond (mechanics), the thermodynamic bond (physical), as well as the chemical bond, of the importance that they will present when the treatment of a surface is considered.

II. 2. 2 .1. Mechanical bond

The mechanical interlocking model, proposed by Mc Bains as early as 1925 [5], considers that the mechanical anchoring of the adhesive in the cavities, pores and asperities of the solid surface is the major factor in determining the adhesion strength. One of the most consistent examples illustrating the contribution of interlocking was given many years ago by **Borroff and Wake** [6], who measured the adhesion between rubber and textile fabrics. These authors clearly showed that the penetration of the fiber ends into the rubber is the most important parameter in such bonding systems. However, the possibility of establishing good adhesion between smooth surfaces leads to the conclusion that the mechanical interlocking theory cannot be considered universal. To overcome this difficulty, following the approach suggested mainly by **Zhang and Schultz** [7, 8], **Wake** [9] proposed that the effects of both mechanical interlocking and thermodynamic interfacial interactions can be taken into account as multiplying factors for estimating the strength of G-joints.

Therefore, a high level of adhesion should be achieved by improving both the morphology and physicochemical characteristics of the substrate surface and cohesion. However, in most cases, the improvement of adhesion by mechanical keying can be attributed simply to the enlargement of the interfacial area caused by surface roughness, as long as the wetting conditions are met to allow the penetration of the adhesion into the pores and cavities. The total penetration of the adhesive into the cavities is, however, not always possible, due to the existence of back pressure coming from the air trapped in these cavities. The final depth and penetration rate strongly depend on the pore shape (cylindrical, conical) as shown schematically in Figure II. 4. In the case where the liquid (resin or prepolymer for example in fusion) is not able to penetrate into the interstices of the substrate, interfacial porosities are created which can constitute the beginnings of rupture [10].

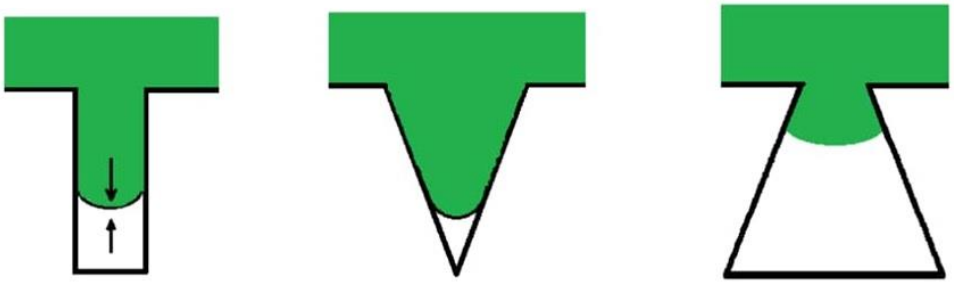

Figure II. 4. Representative diagram of a mechanical anchor formation at the interface [11]

II. 2. 2 .2. Physical or thermodynamic bond

The physical example of adhesion [12] concerns the study of the wettability of solids; it is currently the best-known theory in adhesion science. It is explained by the notion that cohesion is the consequence of covalent and electrovalence bonds that exist at the interface, generally van der Waals bonds and acid-base bonds in the Lewis sense. It is possible to quantify the wetting phenomenon: the wettability conditions as a result of the interface and surface free energies [13].

II. 2. 2. 2. 1. Concept of surface tension

A solid wetted by a fluid resembles that of a fiber with resin, and the interaction phenomena that are created will be evaluated using a well-known example: that of a droplet deposited on one face of a solid.

From a mechanical perspective, the system will reduce its energy conservation by minimizing its fluid/air contact surface. When the interface is stretched like an elastic layer, to generate a surface elevation dA, the energy expended is equal to γdA, where γ is called surface tension [10].

It refers to the energy required to expand the liquid/air interface by one square meter. At the scale of the triple line (contact line), γ represents the force per unit length exerted on the solid (N/m) **[14].**

When considering liquids in equilibrium with a gas, we have γ = σS [14]. Consequently:

- γ denotes the surface tension at the liquid/gas interface.
- The surface energies for the solid/liquid and solid/gas interfaces are expressed as γSL and γSG, respectively

II. 2. 2. 2. 2. Wetting and contact angle

We focus here on the position and behavior of a liquid at rest in contact with an ideal solid surface, assumed to be smooth and free of impurities. The dimensions of the liquid are considered small enough to neglect the effects of gravity. The critical size below which gravitational effects become negligible is defined by the capillary length, given by $\boldsymbol{lcap} = \sqrt{\frac{\gamma}{\rho_0 g}}$, where ρ_0 is the density of the pure liquid at rest and g is the acceleration due to gravity [14]. For water, this capillary length is 2.7 mm. Therefore, only droplets of a few millimeters in size, with small volumes, will be considered in our study

When the liquid is deposited onto the solid surface, an equilibrium is established between the liquid, solid, and gas phases. Under these conditions, the fluid adopts the shape of a droplet, where the tangent at the point of contact between the three phases (known as the triple line) forms an angle referred to as the contact angle or Young's angle, θ_Y (Figure II. 5).

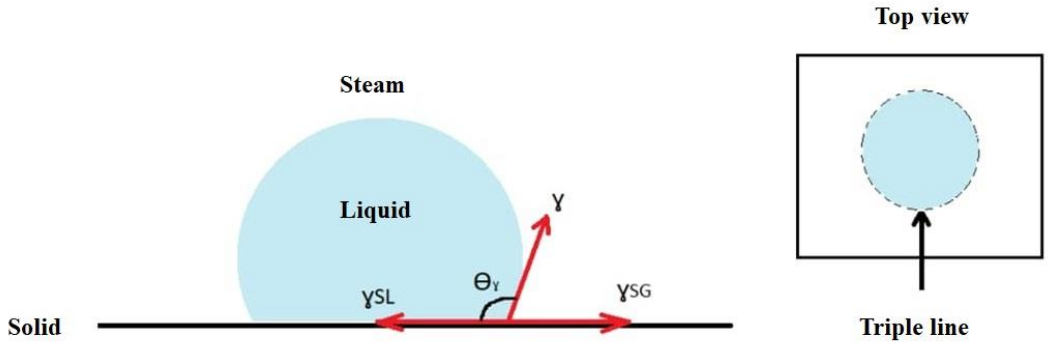

Figure II. 5. Diagram of the Young angle formed by a drop of fluid placed on a solid [14]

Thomas Young's equation [15] illustrates the equilibrium condition at the triple line. At equilibrium, for a contact angle θ_Y, the sum of the forces acting on the droplet is zero. By resolving the surface tensions along the x-axis, this condition can be expressed as (Eq. II.1):

$$\cos(\theta Y) = \frac{\gamma SG - \gamma SL}{\gamma} \qquad \text{II.1}$$

Several positions can then be operated depending on the values of the contact angle (Figure II.6):

When θY = 0°, the liquid spreads completely over the solid surface, forming a thin film, and the droplet shape disappears; this condition is referred to as perfect wetting.

For contact angles between 0° and 180°, spreading is incomplete: the surface is considered wetting when θY < 90°, and non-wetting when θY > 90°.

At θY = 180°, wetting is said to be absent.

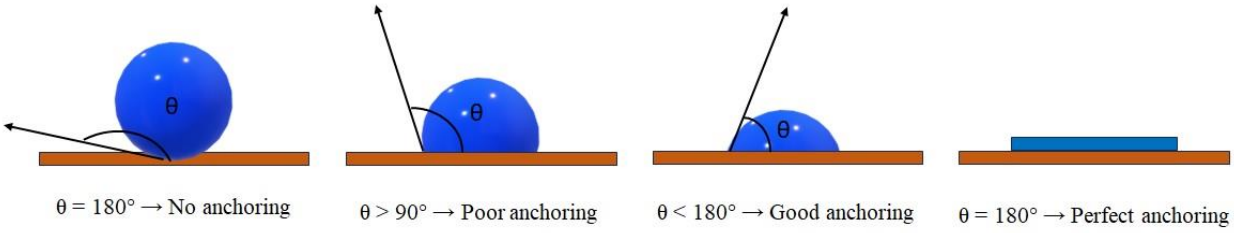

Figure II. 6. The different situations of the liquid drop on a solid surface [16]

The first approach was an empirical method developed by **Zisman** and his collaborators [17-19]. They demonstrated that there is often a linear relationship between the cosine of the contact angle, cosθ, of various liquids and their surface tension. Zisman introduced the concept of critical surface tension, defined as the surface energy value of a liquid that will just spread completely over the solid surface, resulting in a zero contact angle.

Guofeng Tian et al. [20] investigated the effect of alkali treatment on the surface free energy of polyimide (PI) fibers and their interfacial adhesion behavior with epoxy resins. Their findings revealed that the alkali treatment significantly enhances both the surface free energy and the wettability of PI fibers. Untreated PI fibers exhibited contact angles of 78.7° in water and 54.2° in ethylene glycol, with a surface free energy of 32.3 mJ/m². Following alkali treatment, the contact angles decreased to minimum values of 59.6° in water and 40.9° in ethylene glycol, while the surface free energy increased to a maximum of 44.0 mJ/m².

II. 2. 2 .3. The chemical bond

The chemical bonding model proposes the formation of covalent or ionic bonds also referred to as primary bonds (Figure II. 7) between the reinforcement and the matrix. These bonds arise from chemical groups that are typically scarce on the native surface of the material, and therefore must be introduced through chemical treatment [21]. This model is commonly used to explain the mechanism of action of coupling agents such as titanates and silanes. For instance, the work of **Ahagon and Gent** [22] focused on chemical bonds formed between glass and polybutadiene, demonstrating a correlation between the intrinsic fracture energy and the initial bond density facilitated by silane-type coupling agents.

However, it is important to note that despite the high bond energy associated with chemical bonds, they do not necessarily result in a better interface compared to weaker interactions. Therefore, a critical factor to consider is the interfacial bond density. The primary function of chemical bonds is to establish a stable interface.

On another note, at sufficiently high temperatures (around 1500°C), most mineral fibers chemically react with the metallic matrix, compromising their reinforcing capability. This behavior reflects a thermodynamic incompatibility.

In certain composites, particularly those with metallic matrices, adhesion is primarily attributed to the diffusion layer formed at the reinforcement/matrix interface. During processing, interdiffusion occurs between atoms and molecules at the surface layers, resulting in the formation of a strong transitional zone between the two materials. To control or enhance this interfacial interaction, fibers can be modified through coating, cladding, or grafting techniques (either to promote desirable reactions or to limit detrimental ones). For example, boron fibers embedded in a molten metal matrix are typically pre-coated with boron carbide (B_4C) or silicon carbide (SiC) to ensure chemical compatibility at high temperatures and to prevent reactions that would otherwise degrade the fiber's properties.

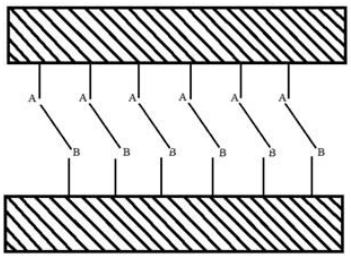

Figure II. 7**.** Diagram of the principle of plant fiber-matrix interfaces [23, 24].

II. 3. Methods for improving the fiber/matrix interface

Matrix composites, whether thermoset or thermoplastic, reinforced with natural fibers, have a certain incompatibility at the fiber-matrix interface. The interfacial bond is weak. Improving the interface first requires adequate treatment of the fibers. Modifications (morphological or microstructural) of the fiber surface can improve the interface properties [8].

On this subject, many studies have presented several treatments that can be classified into:

- Physical treatment methods [8-11, 25-31] [32, 33].
- Chemical treatment methods [2, 10, 11, 25-31, 34-52].

II. 3. 1. Physical methods

These types of treatments modify the properties and structure of fiber surface and therefore, will influence the mechanical engagement with the matrices [8, 11, 53-56]. There are many methods of fiber modification such as: laser, UV or gamma (treatments by exposure to radiation) [57, 58] and by Corona and cold plasma (dielectric discharges). The majority of these treatments are also coating and copolymerization routes.

Gassan. J, et al [59] used corona discharge to create active sites in jute fibers and immersed them in an epoxy matrix. This study highlights the progression of the content of carboxyl and hydroxyl groups (the increase in functional groups) on the surface of the fiber and therefore its polarity.

Martin. A.R, et al [60] studied the effectiveness of cold plasma on the properties of polyethylene/sisal fiber composites. The matrix was functionalized with dichlorosilane in a plasma reactor. While the plant fibers were treated by plasma which seems to produce degradation processes of the surface layers and does not participate in a clear increase in the mechanical behavior of the composites.

Takacs. E, et al [9] conducted a study on the effect of γ irradiation with high energy on the cellulose/cotton structure. γ irradiation causes a decrease in the degree of polymerization with a degradation of cellulose and an increase in carbonyl groups. Also, a modification of the crystalline part of type I cellulose to type II cellulose was noted. The same authors have done research by pre-γ irradiation on the grafting of monomers on cellulose/cotton.

These types of physical treatments have not found a wide diffusion in the field of plant fibers since they require specific materials. We will not dwell on this method, since none of them intercede in our project.

On the other hand, the methods of chemical treatments find a great application in the scientific and industrial field. These treatments have been able to achieve varying levels of success, not only in reducing water absorption but also in increasing the wettability between the fibers and the matrix which induces an improvement in interfacial bond strengths.

In this section, we are more interested in chemical treatments that aim to separate the fibers and clean their surfaces, increase their adhesion with a polymer matrix and reduce constraints related to the properties of plant fibers. Their limited thermal stability and their incompatibility with synthetic polymer matrices constitute a major challenge to their introduction to industrial uses [53].

II. 3. 2. Chemical treatment methods

Various chemical methods used to modify the surface of fibers facilitate the adhesion between hydrophilic plant fibers and hydrophobic polymers [10]. These surface treatments promote the formation of chemical bonds between bio-based fibers and polymer matrices. Appropriate treatment of fibers has been shown to improve their compatibility with the polymer matrix and enhance interfacial bonding quality. High-performance composite materials require good fiber dispersion and strong interfacial cohesion within the polymer matrix to ensure efficient stress transfer throughout the structure. Consequently, numerous studies have explored chemical modification techniques such as mercerization, acylation, permanganate treatment, coupling agents (grafting), silanes, and isocyanates to overcome these interfacial challenges. As a result, the resulting composites exhibit improved mechanical properties [53, 54].

II. 3. 2. 1. Alkaline treatment

Alkaline treatment using sodium hydroxide (NaOH) is the most widely employed method for modifying the structure of plant fibers. Natural fibers are prone to moisture absorption due to the presence of hydroxyl groups within the amorphous regions of cellulose, hemicellulose, and lignin. During alkaline treatment, the alkali ions (NaO-H) react with these hydroxyl groups (-OH) in the fiber, forming water molecules (H-OH) that are subsequently removed from the fiber structure. The remaining alkali ions (Na-O-) then interact with the fiber's cell wall, resulting in the formation of Fiber-cellulose-O-Na groups [61]. The chemical reaction between the fiber cell and NaOH is illustrated in Equation II.2.

$$\text{Cellulose - OH} + \text{NaOH} \rightarrow (\text{Cellulose - O -}) + \text{Na}^{+} + \text{H}_2\text{O impurities} \qquad \text{II.2}$$

These chemical interactions reduce the number of moisture-attracting (hydrophilic) hydroxyl groups, thereby increasing the hydrophobicity of the fibers. The treatment also removes a portion of hemicellulose, lignin, pectin, waxes, and oily coatings (which act as weak boundary

layers) from the cellulose surface [25]. As a result, the cellulose fibrils become more exposed at the fiber surface. This treatment alters the tightly packed crystalline structure of cellulose, leading to the formation of an amorphous region [2]. This amorphous region can more readily interact with matrix materials, facilitating strong interfacial bonding and enhancing the load transfer capability within the composite structure.

Alkaline treatment also separates the elementary fibers from their fiber bundles by removing surface coatings. This increases the effective surface area available for matrix adhesion and improves fiber dispersion within the composite. The treated fiber surfaces become rougher, which can further enhance fiber–matrix adhesion by providing additional sites for mechanical interlocking [26]. As a result, the mechanical and thermal properties of the composite are significantly improved. However, an excessively high alkali concentration can lead to the over-removal of surface materials, potentially weakening or damaging the fiber structure.

L. Boopathi et al. [27] investigated the effect of alkaline treatment on Borassus fruit fibers. The fibers were treated with sodium hydroxide (NaOH) at three different concentrations: 5%, 10%, and 15% by weight. The results indicated that the 5% NaOH treatment yielded better mechanical properties compared to untreated fibers and those treated at higher concentrations. Therefore, Borassus fibers treated with 5% NaOH show potential as reinforcement materials in structural composite applications.

M. K. Joshy et al. [28] studied the impact of alkaline treatment on Isora fibers by varying both treatment duration and NaOH concentration. Mechanical testing of Isora/polyester composites revealed that tensile and flexural properties were maximized with a treatment duration of 4 hours, while impact strength was minimized under the same condition. Additionally, the composite's optimal tensile and flexural performance was observed at an alkali concentration of 1%.

E. T. N. Bisanda [29] investigated the impact of alkaline treatment on the wettability and interfacial integrity of sisal-epoxy composites. Treating the sisal fibers with a 0.5 N sodium hydroxide solution resulted in stiffer composites with reduced porosity and consequently higher density. The treatment was found to enhance adhesion properties by increasing surface energy and surface roughness, leading to improved interfacial bonding. The treated composites exhibited enhanced compressive strength and improved water resistance.

M. Rokbi and H. Osmani [62] treated alfa fibers using sodium hydroxide (NaOH) solutions at concentrations of 1%, 5%, and 10%, with immersion times of 0, 24, and 48 hours. Their results demonstrated that both the concentration and duration of the alkaline treatment significantly affected the behavior of the polyester/alfa fiber composites. The optimal treatment yielding improved interfacial adhesion without damaging the fibrils was found to be a 10% NaOH solution with a 24-hour immersion period.

V. Fiore et al. [31] investigated the effect of a 6% NaOH treatment on kenaf fibers over two immersion durations: 48 and 144 hours. They observed that a 48-hour alkaline treatment effectively cleaned the fiber surfaces by removing impurities, whereas a 144-hour treatment had a detrimental impact on the fiber surface and, consequently, on their mechanical properties. The alkaline treatment enhanced the mechanical performance of Kenaf/Epoxy composites, attributed to improved fiber–matrix compatibility.

S. Sugiman et al. [34] examined the effect of alkaline treatment using NaOH at concentrations of 4%, 8%, and 12% on the tensile and flexural properties of bamboo fiber composites reinforced with polystyrene-modified unsaturated polyester (MUP). The treatment durations were 0.5, 1, and 2 hours, conducted at both room temperature and elevated temperature (50 °C). Under room temperature conditions, the tensile and flexural properties of the bamboo fiber/MUP composites improved with increasing alkali concentration. However, a high concentration (12%) combined with a prolonged treatment time (2 hours) led to a decline in both tensile and flexural properties.

II. 3. 2. 2. Permanganate treatment

Permanganate treatment of natural fibers is carried out using potassium permanganate ($KMnO_4$) dissolved in acetone, with immersion times ranging from 1 to 3 minutes at various concentrations, following an initial alkaline pre-treatment [35]. This process generates highly reactive permanganate ions (Mn^{3+}), which interact with the hydroxyl groups of cellulose to form cellulose manganate and initiate graft copolymerization. The treatment enhances chemical interlocking at the fiber-matrix interface, thereby improving interfacial adhesion [44]. Additionally, it reacts with hydroxyl groups in lignin, removing them from the fiber and thus reducing its hydrophilicity. The reaction between the fiber - OH groups and potassium permanganate is represented in Equation II.3.

$$\text{Fibre - OH} + KMnO_4 \rightarrow \text{Fibre} - \text{H - O - } \underset{\underset{\|}{O}}{\overset{\overset{\|}{O}}{Mn}} \text{ - } OK^+ \qquad \text{II. 3}$$

Paul et al. [35] reported that during the oxidation reaction, $KMnO_4$ interacts with the fiber surface, increasing its physical roughness and thereby enhancing mechanical interlocking with the matrix. As a result, the flexural strength and modulus of banana fiber-reinforced polypropylene composites improved by 5% and 10%, respectively.

Li et al. [35] treated alkali-pretreated flax fibers (2% NaOH for one hour) with a 0.2% $KMnO_4$ solution in 2% acetone, and reported that the resulting LLDPE and HDPE fiber-reinforced composites exhibited higher tensile strength compared to untreated samples.

Dhanalakshmi et al. [37] investigated surface modifications and spectral characterization of areca fibers. In this study, the fibers underwent various chemical treatments, including alkali treatment, permanganate treatment, benzoylation, acrylation, and acetylation. The FTIR spectra of untreated areca fibers were dominated by peaks at 3419.18 cm^{-1} and 1040-1060 cm^{-1}, corresponding to O-H and C-O stretching vibrations, respectively. Peaks observed in the 1100-1600 cm^{-1} range indicated the presence of hemicellulose, while the peak at 1377.86 cm^{-1} was attributed to the alcoholic groups in cellulose. Following permanganate and alkali treatments, hydrolysis occurred, breaking ester or ether linkages, which resulted in the disappearance of the 1727.65 cm^{-1} peak. The reduced intensity of the peaks in the 1100-1600 cm^{-1} region after both treatments suggests partial removal of hemicellulose.

Muhammad Arsyad [38] investigated the interfacial shear strength and tensile strength of coconut fibers treated with sodium hydroxide and potassium permanganate. The highest tensile and interfacial shear strengths 289.94 N/mm^2 and 3.09 N/mm^2, respectively were achieved with a 20% NaOH alkaline treatment. Based on these results, Muhammad Arsyad concluded that:

a) The tensile strength of coconut fiber increases with alkali treatment but decreases following potassium permanganate treatment.

b) Both NaOH and potassium permanganate treatments enhance the interfacial compatibility between coconut fiber and the polyester matrix.

II. 3. 2. 3. Acetylation treatment

Acetylation is a technique used to modify the surface of plant fibers in order to render them more hydrophobic [39]. This process is based on the reaction between the hydroxyl groups (-OH) present in the fibers and acetyl groups (CH_3CO-). The substitution alters the surface characteristics of the fibers, resulting in reduced hydrophilicity. During the reaction, hydroxyl groups from both amorphous cellulose and the fiber's minor constituents (hemicelluloses and lignin) are involved. In contrast, the hydroxyl groups in the crystalline regions of cellulose are tightly packed due to strong intermolecular hydrogen bonding and are thus inaccessible to chemical reagents. The acetylation reactions, both with (Eq. II.4) and without an acid catalyst (Eq. II.5), are presented below [25].

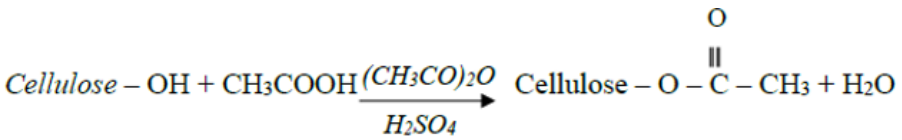

II.4

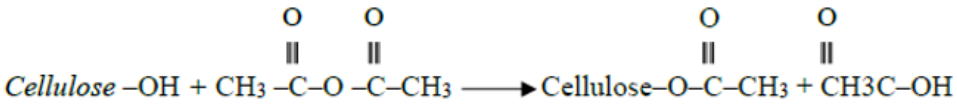

II. 5

A. Bessadok et al. [40] investigated the effect of esterification using acetic anhydride, acrylic acid, and maleic anhydride on Alfa fibers (Stipa tenacissima). FTIR analysis confirmed the

presence of ester groups on the fiber surface and a reduction in hydroxyl groups, indicating a decrease in the water absorption capacity of the Alfa fibers. As a result, the interfacial adhesion between the modified fibers and the polymer matrix was improved.

E. Tronc et al. [41] conducted a study on the esterification of agave fibers using a mixture of acetic anhydride and octanoic acid, and evaluated their use in composite materials. Mechanical property characterization confirmed that the chemical modification was successfully achieved. This treatment enhanced both the impact resistance and the elastic modulus of the composites. Scanning Electron Microscopy (SEM) images revealed improved adhesion between the chemically modified fibers and the matrix, indicating enhanced interfacial interactions with the HDPE matrix. This improvement is attributed to the reduced polarity of the fibers resulting from the esterification process.

Behbood Mohebby et al. [42] investigated the effect of thickness irregularities in acetylated wood fibers used as reinforcement in composites on their overall properties. The characterization of the resulting composites revealed the following findings:

- Moisture content and dimensional swelling of the composites were reduced.
- An increase in thickness defects and a decrease in the elastic modulus were correlated with a higher degree of acetylation.

A.K. Bledzki et al. [43] studied the effect of varying acetylation levels on flax fibers. The results showed that increasing the degree of acetylation enhanced the tensile strength of PP/flax fiber composites. However, beyond an acetylation level of 18%, the tensile strength began to decline.

II. 3. 2. 4. Silane treatment

Silane is a multifunctional molecule commonly used as a coupling agent to modify fiber surfaces. It establishes chemical bonds between the fiber surface and the polymer matrix via siloxane bridges. During fiber treatment, silane undergoes a sequence of hydrolysis, condensation, and bond formation steps. In the presence of moisture from the fiber, silane is hydrolyzed to form silanol groups (see Eq. II.6) [25]. During the condensation process, one end of the silanol reacts with hydroxyl groups on the cellulose surface to form Si-O-cellulose bonds (see Eq. II.7) [25], while the other end reacts with the functional groups of the polymer matrix. This co-reactivity creates a molecular bridge across the fiber-matrix interface, enhancing interfacial continuity. Additionally, the hydrocarbon chain of silane helps reduce fiber swelling within the matrix. As a result, fiber-matrix adhesion improves, contributing to the stability and performance of the composite. Natural fibers possess surface micro pores, and silane coupling agents act as surface coatings that can penetrate these pores. In such cases, the silane coating functions as a mechanical interlocking material, further enhancing the fiber-matrix interface.

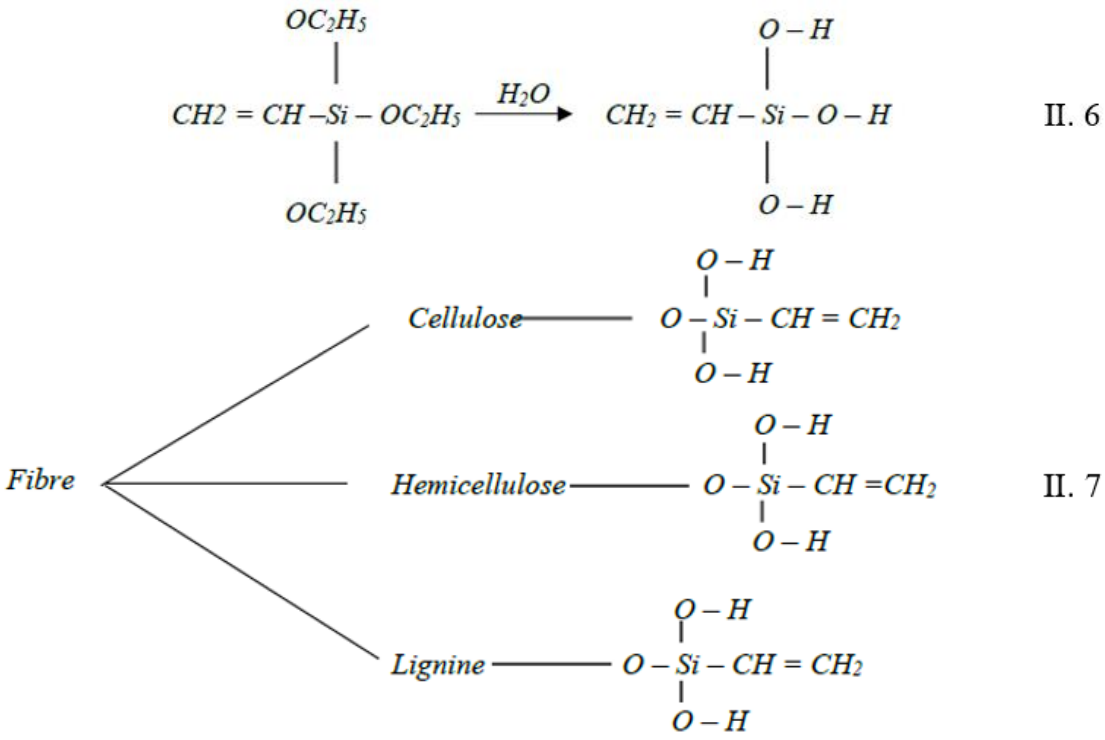

During silane treatment, the hydroxyl groups on the fiber surface become coated with silane molecules. As a result, the hydroxyl groups present in hemicellulose and lignin components are no longer able to absorb atmospheric moisture, leading to a reduced moisture absorption capacity in the treated fibers.

R. Agrawal et al. [44] investigated the effects of silane chemical treatment on palm fibers. Their findings demonstrated that silane treatment enhances the compatibility between the resin and the fibers, resulting in improved tensile strength and thermal stability of the composites.

Y. Seki [32] examined the effects of alkali treatment (5% NaOH for 2 hours) and silane treatment (1% siloxane oligomer in 96% alcohol solution for 1 hour) on the flexural properties of jute-epoxy and jute-polyester composites. For the jute-epoxy composites, silane treatment following alkali pretreatment resulted in approximately 12% higher flexural strength and 7% higher modulus compared to alkali treatment alone. Similar treatments led to improvements of about 20% in strength and 8% in modulus for the jute-polyester composites.

K. Sever et al. [33] applied different concentrations (0.1%, 0.3%, and 0.5%) of silane treatment (γ-methacryloxy-propyl-trimethoxy-silane) to polyester/jute fabric composites. The flexural, tensile, and interlaminar shear properties were evaluated and compared with untreated samples. The composite treated with 0.3% silane showed significant improvements of approximately 30%, 40%, and 55% in flexural strength, tensile strength, and interlaminar shear strength, respectively. Additionally, the silane-treated fiber composites exhibited superior tensile performance compared to those treated with alkali.

Alix, S., et al. [45] investigated the effect of silane treatment using γ-methacryloxy-propyl -trimethoxy-silane (MAPS) on flax fibers, applied for 24 hours in a 20/80 ethanol/water solution by volume. The treatment resulted in a significant reduction in the fiber's polarity. Additionally, MAPS treatment enhanced the mechanical properties of flax cellulose and contributed to moisture resistance, as the grafted silane molecules were able to form intermolecular bonds, creating a barrier effect.

S. Nekkaa [46] investigated the effects of stearic acid and silane treatment specifically N-[3-(trimethoxysilyl) propyl] ethylenediamine (Z-6020) on Spanish Broom (Genêt d'Espagne, GE) fibers to evaluate the performance of PP/GE composites at varying fiber contents. The study found that treatment with either stearic acid or Z-6020 improved the mechanical properties of the PP/GE composites. This enhancement was attributed to the formation of bonds between the coupling agents and the polymer matrix.

II. 4. Characterization of adhesion, interface and surfaces

Adhesion occurs at the interface between the composite constituents. To evaluate this bonding either prior to or following modification, various methods are available that provide relatively direct insights into its effectiveness. Due to its critical role, the relationship between interfacial properties and overall composite performance is a key focus of studies aimed at interface analysis. Characterizing the fiber-matrix interface reveals the nature of their interactions and the strength of adhesion between them.

II. 4. 1. Physicochemical characterization

Various techniques are commonly used in composite research to analyze interfacial properties. Among these are X-ray Photoelectron Spectroscopy (XPS), Fourier Transform Infrared Spectroscopy (FTIR), Secondary Ion Mass Spectrometry (SIMS), and Auger Electron Spectroscopy (AES), which is particularly effective for characterizing fiber surfaces and near-surface regions. These methods provide valuable information that can be used to optimize composite manufacturing.

Figure II. 8 illustrates an example of physicochemical characterization conducted by Sreekumar et al. [52] on sisal fibers following chemical treatment. Using FTIR analysis, the authors demonstrated the effects of different chemical treatments: benzoylation, mercerization, permanganate, and silane on the fiber structure. The spectrum of untreated sisal fiber served as a reference for identifying the structural modifications induced by each treatment.

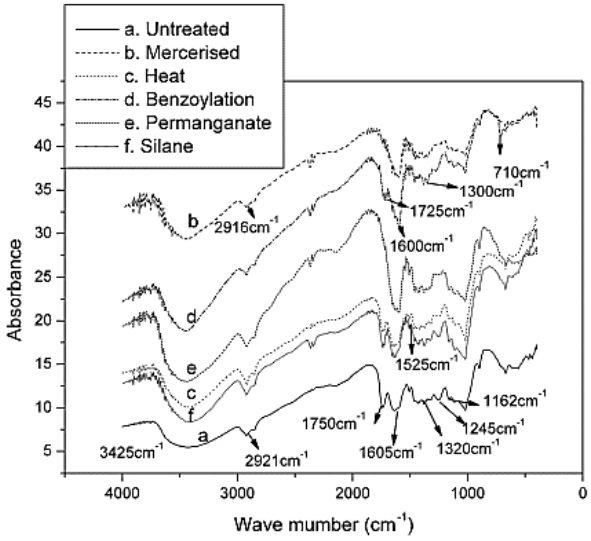

Figure II. 8. IRTF analysis of raw and treated fibers (Sreekumar et al.) [52].

Indirect analytical techniques such as Thermomechanical Analysis (TMA), Nuclear Magnetic Resonance (NMR) spectroscopy, and Differential Scanning Calorimetry (DSC) are also employed to characterize fiber-matrix interfaces. These methods primarily assess changes in the matrix near the interface, particularly in terms of crystallinity and plasticity [52, 61, 63].

ViVi Do Thi [63] utilized DSC analysis to obtain heat flow (W/g) versus temperature (°C) curves (Figure II. 9), providing insights into the melting temperature (Tm) and degree of crystallinity of bamboo fiber-reinforced composites. According to the data, the melting temperature ranges from 164.8°C to 169.1°C. The crystallinity percentage of composites reinforced with bamboo fibers treated with acetic acid or silane is higher than that of the other composite samples.

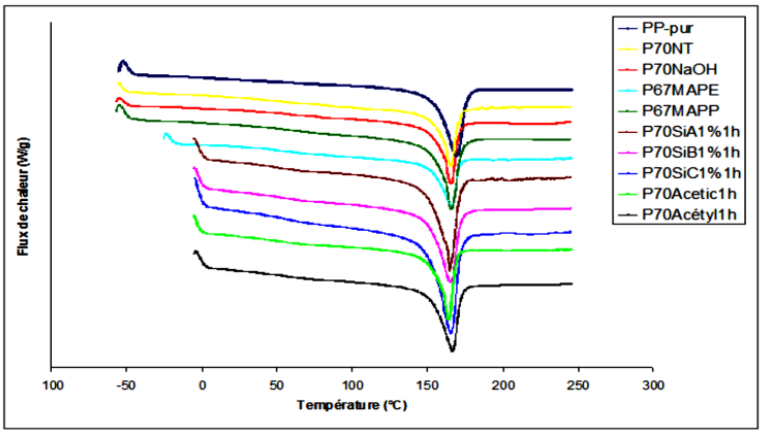

Figure II. 9. DSC thermograms of composites with 30% bamboo fibers and addition of coupling agents **(**ViVi Do Thi.) [63].

II. 4. 2. Microscopic characterization

These are known as direct analysis techniques, which provide insight into the physical mechanisms of interfacial bonding. Among them are interface imaging methods such as Scanning Electron Microscopy (SEM), fluorescence microscopy, optical microscopy, and stereomicroscopy. These techniques are powerful tools for high-resolution analysis of cell walls, surfaces, fiber morphology, and fiber-matrix interfaces. They are, unsurprisingly, the most frequently employed methods in the investigation of natural fiber-reinforced composites.

Figure II. 10 presents the fracture surfaces of epoxy composites reinforced with both untreated and alkali-treated (NaOH) Ziziphus mauritiana (ZM) fibers following a flexural test [64]. Based on the SEM images, Vinod et al. [64] observed that the improved flexural strength in composites with treated fibers is due to enhanced fiber-matrix adhesion. This improvement is attributed to increased surface roughness of the fibers, which promotes mechanical interlocking with the matrix during processing (Figure II. 10 b). In contrast, the untreated fiber composite (Figure II. 10 a) shows signs of fiber pull-out and tearing, indicative of poor interfacial adhesion.

Among various imaging techniques, X-ray tomography is used to detect internal defects within composite materials. However, its application remains limited due to its high cost.

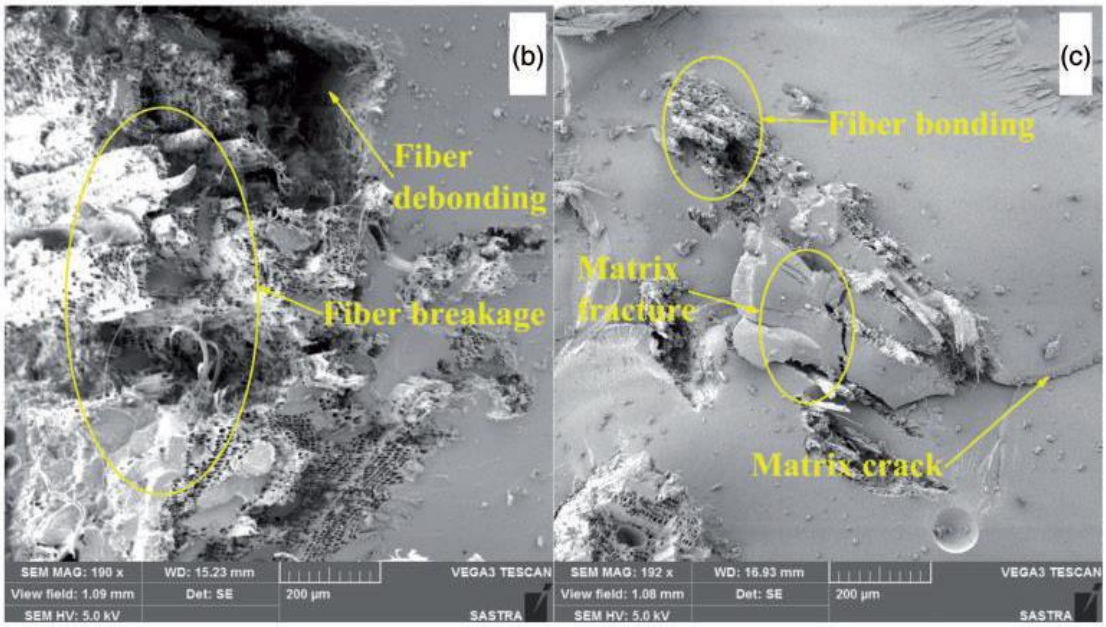

Figure II. 10. SEM images of the composites after bending test a) Raw ZM fibers/Epoxy b) NaOH/Epoxy treated ZM fibers (Vinod et al) [64].

II. 4. 3. Mechanical characterization

Mechanical analysis methods that primarily engage the interface in composites are among the most commonly used by industry. However, some of these methods can be quite challenging to implement.

The most well-known tests include three-point bending, compression, and tensile tests. These typically require the fabrication of composite specimens in the form of plates, which are then cut into samples for testing. Achieving consistent and reliable results demands uniformity and precision in specimen preparation. Figure II. 11 shows the outcome of a tensile test, which provides insight into the interfacial behavior of LDPE/sisal composites [48].

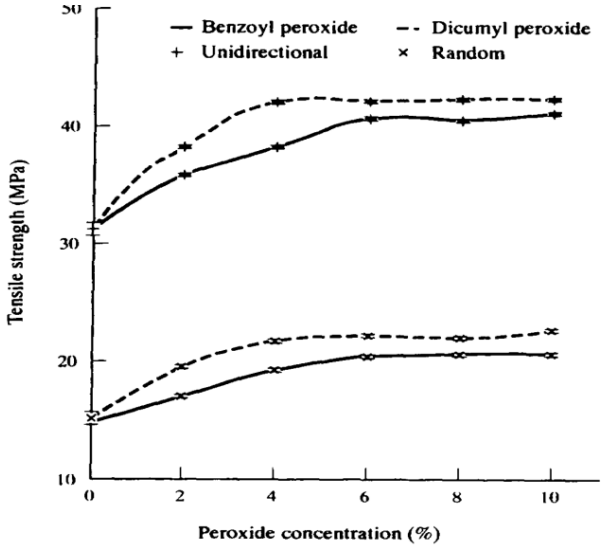

Figure II. 11. Effect of peroxide concentration on tensile strength of LDPE/sisal composite at 30% filler (K. Joseph et al) [48].

As reported by K. Joseph et al., the data in Figure II. 11 clearly show that the tensile strength of the composites increases with increasing peroxide concentration, up to a certain point (4% for dicumyl peroxide and 6% for benzoyl peroxide), after which it plateaus. This concentration can be considered the critical peroxide concentration at which maximum tensile strength is achieved for a given fiber content of 19%. An excess of peroxide leads to some degree of crosslinking in the polyethylene (PE), but this has only a minor impact on the overall mechanical properties of the composites.

II. 4. 4. Micromechanical characterization techniques

To accurately interpret the mechanical properties of a composite material, it is essential to analyze the interfacial behavior and assess the fiber/matrix adhesion. The load transfer between the matrix and the fiber can be evaluated through the interfacial shear strength (IFSS). This property can be measured using micromechanical testing methods such as:

II. 4. 4. 1. The “Pull-out” test

Originally developed by **Broutman** [65], this test was designed to evaluate fibers embedded in polymer matrices. The procedure involves applying a uniaxial tensile force (Figure II. 12) to a single fiber partially embedded in a matrix sheath. The force increases until it reaches a maximum value, corresponding to interfacial debonding, followed by complete fiber extraction.

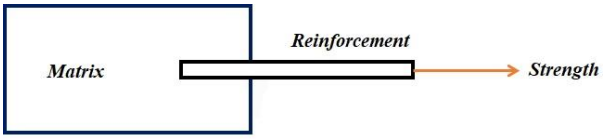

Figure II. 12. Representative diagram of the single fiber pull-out test [66].

II. 4. 4. 2. The microdroplet test

The microdroplet-debonding test is an evolution of the traditional pullout test, developed to facilitate data acquisition for finer fibers. Introduced by **Miller et al**. [67], this method simplifies the testing process by depositing a small ellipsoidal droplet of resin coaxially around a single fiber.

During the test, a longitudinal force is applied to the fiber while the droplet is held in place between two small blades (Figure II. 13). The applied tensile force is transferred to the interface as a shear stress, which is assumed to be uniformly distributed along the fiber-resin contact length. When the interfacial shear stress reaches its critical value, debonding occurs, and the droplet slides along the fiber.

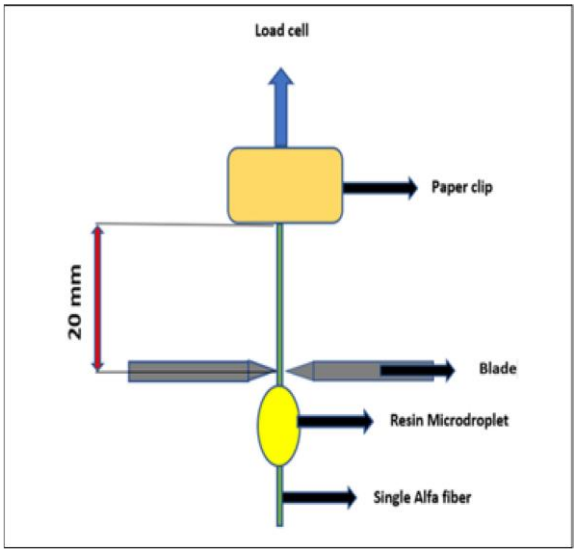

Figure II. 13. Representative diagram of the principle of the microdroplet test [6].

During the test, the applied force–displacement curve is recorded (Figure II. 14). As reported by several researchers, including **S. Zhandarov et al**. [66], this curve typically consists of two distinct regions. The first region (A) corresponds to the elastic deformation of the free portion of the fiber, which eventually leads to interfacial debonding. The maximum force (F_d) represents the point of complete debonding. Following this, the force decreases, and fiber extraction begins at a force level denoted as F_0, which may involve frictional effects. The second region (B) reflects the progressive withdrawal of the fiber from the matrix. These region characterized by a continuous decline in applied force due to the decreasing contact area between the fiber and the matrix.

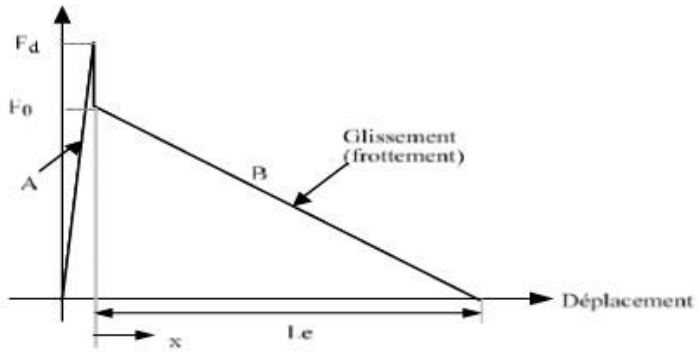

Figure II. 14. Pull-out force-displacement curve [66].

To assess the quality of the interface, the interfacial shear strength (IFSS) is used. It is calculated based on the maximum debonding force (F_d) and the geometry of the microdroplet specimen (see Eq. II.8).

$$\tau = \text{IFSS} = \frac{F_d}{\pi dL} \qquad \text{II.8}$$

Where d: the fiber diameter

L: the included length (fiber/matrix contact)

It is important to note that this technique is challenging to perform, particularly with fibers of small diameters. Although the results often exhibit significant variability, the method still provides valuable insights into several interfacial parameters, such as debonding and frictional stresses, the coefficient of friction, and the evolution of interfacial strength (i.e., interfacial wear).

II. 4. 4. 3. The fragmentation test

The single fiber fragmentation test (SSFT) is used to determine the interfacial shear strength (IFSS). In this method, a single fiber is embedded in a dog-bone-shaped tensile specimen, which is then subjected to uniaxial tensile loading. The tensile forces are transferred from the matrix to the fiber, leading to an accumulation of tensile stress within the fiber. When the stress reaches a critical level, the fiber fractures. This loading process continues until the resulting fiber fragments become so short that the induced tensile stress is no longer sufficient to cause further breakage, thus halting the fragmentation process [68]. The final fiber fragment length is referred to as the critical fiber length (L_c). The ratio between the critical length and the fiber diameter serves as a reliable indicator of the fiber–matrix interfacial adhesion strength. The single fiber fragmentation test is illustrated in Figure II. 15.

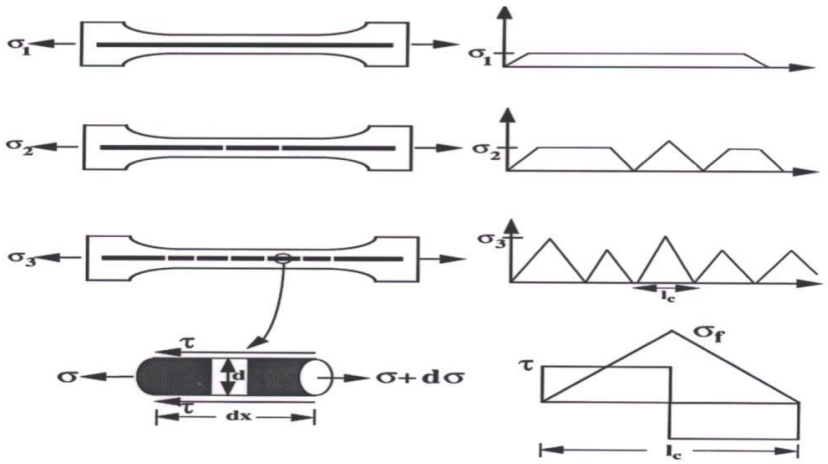

Figure II. 15. Diagram of the fragmentation test principle [68].

$\frac{l_c}{2} < l < l_c$ Critical length distribution

$\tau = \frac{\sigma_f}{2\beta}\Gamma(1-\frac{1}{\alpha})$ Weibull distribution

The load transfer efficiency in the fiber/matrix sample can be evaluated in terms of the interfacial shear strength (τ) (see Eq. II.9):

$$\tau = \text{IFSS} = \frac{\sigma_f}{2dlc} \qquad \text{II.9}$$

Where d: the fiber diameter

σf: the ultimate tensile stress for a fiber of critical length lc

II. 5. Conclusion

The use of natural fibers as reinforcement in polymer composites has attracted significant interest due to their potential mechanical properties, ease of processing, and environmental benefits. However, the hydrophilic nature of these fibers limits their compatibility with hydrophobic polymer matrices, often resulting in poor mechanical performance of the composites. Chemical treatment of the fibers is therefore essential to reduce their hydrophilicity and enhance interfacial adhesion with the matrix. Numerous studies have reported notable improvements in the mechanical properties of composites through the application of various chemical treatment methods to the reinforcing fibers.

This theoretical section provided a comprehensive overview of the key techniques used to investigate the mechanical behavior of plant fiber-reinforced composites subjected to various chemical treatments. Particular emphasis was placed on analyzing the fiber-matrix interface and understanding how interfacial strength influences the macroscopic properties of the composites. This study also guided the selection of appropriate experimental methods employed to characterize our materials. Among the most suitable micromechanical tests for evaluating the fiber/matrix interface in composites are the fiber pull-out test and the single fiber fragmentation test. In the following section, the microdroplet pull-out method will be discussed in detail.

All the analytical techniques can be combined to evaluate the collected data, as they are complementary and may at times provide overlapping information. Due to the complexity of the bonding mechanisms involved, employing a variety of methods is often necessary, even though this approach may not always yield entirely consistent or conclusive results.

References

[1] Z. Belouadah, A. Ati, M. Rokbi, A. Bezazi, and A. Imad, "Optimisation Des méthodes D'extraction Et Caractérisation Mécanique De La Fibre Alfa En Vue De Son Application Comme Renfort Des Matériaux Composites," *Journal of Materials, Processes and Environment,* vol. 2, pp. 51-57, 2014.

[2] G. Beckermann and K. L. Pickering, "Engineering and evaluation of hemp fibre reinforced polypropylene composites: fibre treatment and matrix modification," *Composites Part A: Applied Science and Manufacturing,* vol. 39, pp. 979-988, 2008.

[3] J. Rout, M. Misra, S. Tripathy, S. Nayak, and A. Mohanty, "The influence of fibre treatment on the performance of coir-polyester composites," *Composites Science and Technology,* vol. 61, pp. 1303-1310, 2001.

[4] S. Pinho, R. Darvizeh, P. Robinson, C. Schuecker, and P. Camanho, "Material and structural response of polymer-matrix fibre-reinforced composites," *Journal of Composite Materials,* vol. 46, pp. 2313-2341, 2012.

[5] S. Koloor, M. Abdullah, M. Tamin, and M. Ayatollahi, "Fatigue damage of cohesive interfaces in fiber-reinforced polymer composite laminates," *Composites Science and Technology,* vol. 183, p. 107779, 2019.

[6] S. Ali Zernadji, M. Rokbi, M. Benhamida, and D. Hammiche, "Estimation of fiber/polymer bond strength from maximum load values recorded in the micro-bond tests," *Materials Today: Proceedings,* vol. 53, pp. 247-252, 2022.

[7] M. Rokbi, Z. E. A. Rahmouni, and B. Baali, "Flexural characterization of polymer concrete comprising waste marble and date palm fibers," *Technical Sciences/University of Warmia and Mazury in Olsztyn,* 2019.

[8] A. Bledzki and J. Gassan, "Composites reinforced with cellulose based fibres," *Progress in polymer science,* vol. 24, pp. 221-274, 1999.

[9] E. Takacs, L. Wojnarovits, C. Földváry, P. Hargittai, J. Borsa, and I. Sajo, "Effect of combined gamma-irradiation and alkali treatment on cotton–cellulose," *Radiation Physics and Chemistry,* vol. 57, pp. 399-403, 2000.

[10] D. Gulati and M. Sain, "Fungal-modification of natural fibers: a novel method of treating natural fibers for composite reinforcement," *Journal of Polymers and the Environment,* vol. 14, pp. 347-352, 2006.

[11] M. J. John and R. D. Anandjiwala, "Recent developments in chemical modification and characterization of natural fiber-reinforced composites," *Polymer composites,* vol. 29, pp. 187-207, 2008.

[12] A. Kinloch, "The science of adhesion," *Journal of Materials Science,* vol. 17, pp. 617-651, 1982.

[13] S.-J. Park and M.-K. Seo, *Interface science and composites* vol. 18: Academic Press, 2011.

[14] C. Virgilio, "Caractérisation du mouillage de surfaces micro/nanostructurées par méthode acoustique haute fréquence: application aux traitements humides dans l'industrie de la microélectronique," Université de Valenciennes et du Hainaut-Cambresis, 2017.

[15] T. Young, "III. An essay on the cohesion of fluids," *Philosophical transactions of the royal society of London,* pp. 65-87, 1805.

[16] P.-F. Thomas, *Précis de Physique-chimie: cours et exercices*: Editions Bréal, 2006.
[17] H. Fox and W. Zisman, "The spreading of liquids on low-energy surfaces. III. Hydrocarbon surfaces," *Journal of Colloid Science,* vol. 7, pp. 428-442, 1952.
[18] E. G. SHAFRIN and W. Zisman, "Effect of Adsorbed Water on the Spreading of Organic Liquids on Soda-Lime Glass," *Journal of the American Ceramic Society,* vol. 50, pp. 478-484, 1967.
[19] W. A. Zisman, "Contact angle, wettability, and adhesion," *Advances in chemistry series,* vol. 43, p. 1, 1964.
[20] G. Tian, B. Chen, S. Qi, H. Niu, E. Han, and D. Wu, "Enhanced surface free energy of polyimide fibers by alkali treatment and its interfacial adhesion behavior to epoxy resins," *Composite Interfaces,* vol. 23, pp. 145-155, 2016.
[21] M. Slamani, J.-F. Chatelain, and H. Hamedanianpour, "Comparison of two models for predicting tool wear and cutting force components during high speed trimming of CFRP," *International Journal of Material Forming,* vol. 8, pp. 305-316, 2015.
[22] A. Ahagon and A. Gent, "Effect of interfacial bonding on the strength of adhesion," *Journal of Polymer Science: Polymer Physics Edition,* vol. 13, pp. 1285-1300, 1975.
[23] J.-K. Kim and Y.-W. Mai, *Engineered interfaces in fiber reinforced composites*: Elsevier, 1998.
[24] N. Moussaoui, M. Rokbi, H. Osmani, M. Jawaid, A. Atiqah, M. Asim, and L. Benhamadouche, "Extraction and characterization of fiber treatment Inula viscosa fibers as potential polymer composite reinforcement," *Journal of Polymers and the Environment,* vol. 29, pp. 3779-3793, 2021.
[25] X. Li, L. G. Tabil, and S. Panigrahi, "Chemical treatments of natural fiber for use in natural fiber-reinforced composites: a review," *Journal of Polymers and the Environment,* vol. 15, pp. 25-33, 2007.
[26] P. Joseph, G. Mathew, K. Joseph, G. Groeninckx, and S. Thomas, "Dynamic mechanical properties of short sisal fibre reinforced polypropylene composites," *Composites Part A: applied science and manufacturing,* vol. 34, pp. 275-290, 2003.
[27] L. Boopathi, P. Sampath, and K. Mylsamy, "Investigation of physical, chemical and mechanical properties of raw and alkali treated Borassus fruit fiber," *Composites Part B: Engineering,* vol. 43, pp. 3044-3052, 2012.
[28] M. Joshy, L. Mathew, and R. Joseph, "Effect of alkali treatment on the mechanical properties of short randomly oriented isora fibre-polyester composites," *Progress in rubber, plastics and recycling technology,* vol. 24, pp. 255-272, 2008.
[29] E. Bisanda, "The effect of alkali treatment on the adhesion characteristics of sisal fibres," *Applied Composite Materials,* vol. 7, pp. 331-339, 2000.
[30] M. Rokbi, H. Osmani, A. Imad, and N. Benseddiq, "Effect of chemical treatment on flexure properties of natural fiber-reinforced polyester composite," *procedia Engineering,* vol. 10, pp. 2092-2097, 2011.
[31] V. Fiore, G. Di Bella, and A. Valenza, "The effect of alkaline treatment on mechanical properties of kenaf fibers and their epoxy composites," *Composites Part B: Engineering,* vol. 68, pp. 14-21, 2015.

[32] Y. Seki, "Innovative multifunctional siloxane treatment of jute fiber surface and its effect on the mechanical properties of jute/thermoset composites," *Materials Science and Engineering: A,* vol. 508, pp. 247-252, 2009.

[33] K. Sever, M. Sarikanat, Y. Seki, G. Erkan, and Ü. H. Erdoğan, "The mechanical properties of γ-methacryloxypropyltrimethoxy silane-treated jute/polyester composites," *Journal of composite Materials,* vol. 44, pp. 1913-1924, 2010.

[34] S. Sugiman, P. D. Setyawan, and B. Anshari, "Effects of alkali treatment of bamboo fibre under various conditions on the tensile and flexural properties of bamboo fibre/polystyrene-modified unsaturated polyester composites," *Journal of Engineering Science and Technology,* vol. 14, pp. 27-47, 2019.

[35] M. M. Rahman, A. K. Mallik, and M. A. Khan, "Influences of various surface pretreatments on the mechanical and degradable properties of photografted oil palm fibers," *Journal of applied polymer science,* vol. 105, pp. 3077-3086, 2007.

[36] S. A. Paul, C. Oommen, K. Joseph, G. Mathew, and S. Thomas, "The role of interface modification on thermal degradation and crystallization behavior of composites from commingled polypropylene fiber and banana fiber," *Polymer Composites,* vol. 31, pp. 1113-1123, 2010.

[37] S. Dhanalakshmi, P. Ramadevi, and B. Basavaraju, "Areca fiber reinforced epoxy composites: Effect of chemical treatments on impact strength," *Oriental Journal of Chemistry,* vol. 31, pp. 763-769, 2015.

[38] M. Arsyad, "Sodium hydroxide and potassium permanganate treatment on mechanical properties of coconut fibers," in *IOP Conference Series: Materials Science and Engineering*, 2019, p. 012011.

[39] A. Haseena, G. Unnikrishnan, and G. Kalaprasad, "Dielectric properties of short sisal/coir hybrid fibre reinforced natural rubber composites," *Composite Interfaces,* vol. 14, pp. 763-786, 2007.

[40] A. Bessadok, S. Roudesli, S. Marais, N. Follain, and L. Lebrun, "Alfa fibres for unsaturated polyester composites reinforcement: Effects of chemical treatments on mechanical and permeation properties," *Composites Part A: Applied Science and Manufacturing,* vol. 40, pp. 184-195, 2009.

[41] E. Tronc, C. Hernández-Escobar, R. Ibarra-Gómez, A. Estrada-Monje, J. Navarrete-Bolaños, and E. Zaragoza-Contreras, "Blue agave fiber esterification for the reinforcement of thermoplastic composites," *Carbohydrate Polymers,* vol. 67, pp. 245-255, 2007.

[42] B. Mohebby, M. Gorbani-Kokandeh, and M. Soltani, "Springback in acetylated wood based composites," *Construction and Building Materials,* vol. 23, pp. 3103-3106, 2009.

[43] A. Bledzki, A. Mamun, M. Lucka-Gabor, and V. Gutowski, "The effects of acetylation on properties of flax fibre and its polypropylene composites," *Express polymer letters,* vol. 2, pp. 413-422, 2008.

[44] R. Agrawal, N. Saxena, K. Sharma, S. Thomas, and M. Sreekala, "Activation energy and crystallization kinetics of untreated and treated oil palm fibre reinforced phenol formaldehyde composites," *Materials Science and Engineering: A,* vol. 277, pp. 77-82, 2000.

[45] S. Alix, L. Lebrun, C. Morvan, and S. Marais, "Study of water behaviour of chemically treated flax fibres-based composites: A way to approach the hydric interface," *Composites Science and Technology,* vol. 71, pp. 893-899, 2011.

[46] S. Nekkaa, M. Guessoum, A. Grillet, and N. Haddaoui, "Mechanical properties of biodegradable composites reinforced with short spartium junceum fibers before and after treatments," *International Journal of Polymeric Materials,* vol. 61, pp. 1021-1034, 2012.

[47] M. Sreekala, M. Kumaran, S. Joseph, M. Jacob, and S. Thomas, "Oil palm fibre reinforced phenol formaldehyde composites: influence of fibre surface modifications on the mechanical performance," *Applied composite materials,* vol. 7, pp. 295-329, 2000.

[48] K. Joseph, S. Thomas, and C. Pavithran, "Effect of chemical treatment on the tensile properties of short sisal fibre-reinforced polyethylene composites," *Polymer,* vol. 37, pp. 5139-5149, 1996.

[49] Y.-T. Zheng, D.-R. Cao, D.-S. Wang, and J.-J. Chen, "Study on the interface modification of bagasse fibre and the mechanical properties of its composite with PVC," *Composites part A: applied science and manufacturing,* vol. 38, pp. 20-25, 2007.

[50] S. Sapieha, P. Allard, and Y. Zang, "Dicumyl peroxide-modified cellulose/LLDPE composites," *Journal of Applied Polymer Science,* vol. 41, pp. 2039-2048, 1990.

[51] J. George and J. I. Verpoest, I, "Mechanical properties of flax fibre reinforced epoxy composites," *Die Angewandte Makromolekulare Chemie,* vol. 272, pp. 41-45, 1999.

[52] P. Sreekumar, R. Saiah, J. M. Saiter, N. Leblanc, K. Joseph, G. Unnikrishnan, and S. Thomas, "Effect of chemical treatment on dynamic mechanical properties of sisal fiber-reinforced polyester composites fabricated by resin transfer molding," *Composite Interfaces,* vol. 15, pp. 263-279, 2008.

[53] A. Mohanty, M. Misra, and L. T. Drzal, "Surface modifications of natural fibers and performance of the resulting biocomposites: An overview," *Composite interfaces,* vol. 8, pp. 313-343, 2001.

[54] S. Kalia, K. Thakur, A. Celli, M. A. Kiechel, and C. L. Schauer, "Surface modification of plant fibers using environment friendly methods for their application in polymer composites, textile industry and antimicrobial activities: A review," *Journal of Environmental Chemical Engineering,* vol. 1, pp. 97-112, 2013.

[55] Priyanka and S. Palsule, "Banana fiber/chemically functionalized polypropylene composites with in-situ fiber/matrix interfacial adhesion by Palsule process," *Composite Interfaces,* vol. 20, pp. 309-329, 2013.

[56] A. Ali, K. Shaker, Y. Nawab, M. Jabbar, T. Hussain, J. Militky, and V. Baheti, "Hydrophobic treatment of natural fibers and their composites—A review," *Journal of Industrial Textiles,* vol. 47, pp. 2153-2183, 2018.

[57] B. Koohestani, A. Darban, P. Mokhtari, E. Yilmaz, and E. Darezereshki, "Comparison of different natural fiber treatments: a literature review," *International Journal of Environmental Science and Technology,* vol. 16, pp. 629-642, 2019.

[58] N. Le Moigne, B. Otazaghine, S. Corn, H. Angellier-Coussy, A. Bergeret, and H. Angellier-Coussy, "Modification of the interface/interphase in natural fibre reinforced composites:

Treatments and processes," *Surfaces and Interfaces in Natural Fibre Reinforced Composites: Fundamentals, Modifications and Characterization,* pp. 35-70, 2018.

[59] J. Gassan, V. S. Gutowski, and A. K. Bledzki, "About the surface characteristics of natural fibres," *Macromolecular materials and engineering,* vol. 283, pp. 132-139, 2000.

[60] A. R. Martin, F. S. Denes, R. M. Rowell, and L. H. Mattoso, "Mechanical behavior of cold plasma–treated sisal and high-density polyethylene composites," *Polymer composites,* vol. 24, pp. 464-474, 2003.

[61] M. Jiao, S. Cao, L. Ren, and R. Li, "Analysis of composite microplastics in sediment using 3D Raman spectroscopy and imaging method," *Journal of Hazardous Materials Advances,* vol. 3, p. 100016, 2021.

[62] M. Rokbi and H. Osmani, "L'effet des traitements de surface des fibres sur les propriétés mécaniques de composites Polyester-fibres Alfa," in *CFM 2011-20ème Congrès Français de Mécanique*, 2011.

[63] V. V. D. T. Do Thi, "Matériaux composites à fibres naturelles/polymère biodégradables ou non," Université de Grenoble; Université des Sciences Naturelles d'Ho Chi Minh Ville, 2011.

[64] A. Vinod, R. Vijay, D. Lenin Singaravelu, A. Khan, M. Sanjay, S. Siengchin, F. Verpoort, K. A. Alamry, and A. M. Asiri, "Effect of alkali treatment on performance characterization of Ziziphus mauritiana fiber and its epoxy composites," *Journal of Industrial Textiles,* vol. 51, pp. 2444S-2466S, 2022.

[65] L. Broutmari, "Measurement of the fiber-polymer matrix interfacial strength," *Interfaces in composites,* vol. 452, p. 27, 1969.

[66] S. Zhandarov and E. Mäder, "An alternative method of determining the local interfacial shear strength from force–displacement curves in the pull-out and microbond tests," *International Journal of Adhesion and Adhesives,* vol. 55, pp. 37-42, 2014.

[67] B. Miller, P. Muri, and L. Rebenfeld, "A microbond method for determination of the shear strength of a fiber/resin interface," *Composites Science and Technology,* vol. 28, pp. 17-32, 1987.

[68] M. Rich, L. Drzal, D. Hunston, G. Holmes, and W. McDonough, "Round robin assessment of the single fiber fragmentation test," in *Procedings of the American Society for Composites 17th Technical Conference*, 2002.

CHAPTER III

Experimental part

Materials and methods

III. 1. Introduction

To achieve the effective use of plant fibers as reinforcement, it is essential to subject them to pretreatment to get the desired physical, thermal and mechanical properties for the composites. Before incorporating this material into engineering applications, a thorough understanding of fiber and composite characteristics, as well as their failure mechanisms is imperative. For this reason a micromechanical characterizations were done to study the interfacial decohesion and damage mechanisms present in a composite structure under static loading.

The experimental methods outlined in this chapter encompass: (1) chemical treatments applied to Echinops spinosissimus fibers; (2) physico-chemical and mechanical characterization of the fibers; (3) micromechanical characterization using micro-drops. (4) creation of a model composite using Echinops spinosissimus fibers and resin and (5) mechanical characterization through tensile testing on the developed model composites

III. 2. Presentation of the materials used

III. 2. 1. The fibers of Echinops spinosissimus (ES)

III. 2. 1. 1. Botanical description of the Echinops spinosissimus plant

Echinops spinosissimus is a spiny plant made up of stems and is identifiable by its long, deeply cut, toothed, and pointed leaves. The leaves are characterized by a prominent central vein and lateral veins that end in long white spines. The plant reaches a height of 0.6 to 1 meter and develops a robust root system extending up to 20 cm in length. It is classified within the order Asterales, family Asteraceae, genus Echinops, and species ES [1]. The inflorescences form spherical clusters measuring 6 to 8 cm in diameter, covered with long, stiff, sharp spines (actually bracts), which is why they are commonly known in English as 'Thistle-ball.' These spines enclose the flowers, each consisting of five white petals fused at the base into a tube and slightly curved at the tip [2]. These flowers bloom in late summer and early autumn. (Figure III. 1).

Echinops spinosissimus (ES) has a very large distribution area. It is widely distributed in the Mediterranean basin in some Eurasian countries (Italy, Greece and Turkey) and in Africa (Morocco, Algeria, Tunisia, Libya and Egypt) [3].

Echinops (E): Greek word, meaning hedgehog or sea urchin [sea hedgehog] and spinosissimus is the Latin superlative of spina (thorn), therefore means very spiny sea urchin.

In Algeria, ES plant is known as Chawki El Djabali. It is a widely spread plant in the Algerian hill. It is found in places unsuitable for plants: roadsides, abandoned lands, wastelands. It grows in dry soil.

Its therapeutic history is very diverse and healers have known about it for a long time. Our ancestors used it as a diuretic, hypoglycemic, for stomach upsets, liver disorders, and for postpartum care [1].

Figure III.1. Echinops spinosissimus plant

III. 2. 1. 2. From the plant to the fiber of Echinops spinosissimus

This part is primarily intended to present the growth evolution of an Echinops spinosissimus plant. After that, the essential phases for fiber extraction will be explained.

III. 2. 1. 2. 1. Plant growth

It is a plant resistant to heat and drought, and its growth begins in late January, lasting for about 5 months (fast growing), and then developing from February to May after different periods represents the completion of growth and flowering on September. The rate of plant growth is directly related to the accumulation of temperatures that the plant maintains during its growth.

III. 2. 1. 2. 2 Extraction of Echinops spinosissimus fibers

In our work, this is the first time that the Echinops spinosissimus plant is studied as reinforcement fibers in composite materials. The primary goal of the extraction process aims to obtain stronger and more intact fibers by removing non-cellulosic components such as pectin, lignin, and wax. In this study, following the harvest of the plant stems in the Hodna region, Msila, Algeria (35° 44' 30" N, 4° 32' 30" E), as shown in Figure III.2 during the month of May, the extraction procedure was carried out. For further details, please refer to the following source: Initially, leaves, dust, and other foreign matter were removed from the stems of the ES plant. The stems, measuring between 8 and 15 mm in diameter, were then cut into sections approximately 50 to 70 cm in length. These ES stems were repeatedly washed with distilled water to eliminate impurities and dirt, ensuring their cleanliness.

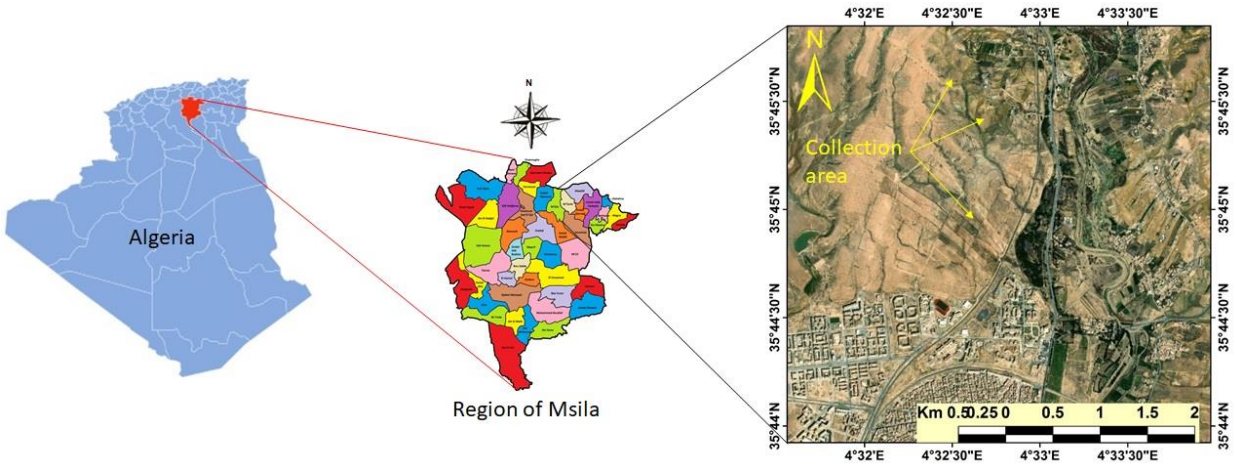

Figure III. 2. Echinops spinosissimus (ES) plant collection area

Based on the bibliographic study presented in the fiber extraction methods paragraph of Chapter I, A green biological method involving microbial degradation has been applied. This simple and inexpensive technique provided an excellent quality of long fibers. Figure III.3 illustrate the main followed steps. The stems of ES are left to soak for 28 days at room temperature in a barrel with water and 0.060% sodium bicarbonate to speed up bacterial decomposition. Once the retting period is complete, each stem is crushed using a scraper [4], then a manual process is carried out in order to completely separate the fibers [5], either short or long, from the stem, As a result, only the ES fibers were retained. These fibers were thoroughly washed with distilled water to remove any surface deposits, left to drain for 24 hours, and then dried in an oven at 70 °C for 6 hours to eliminate moisture [6, 7].

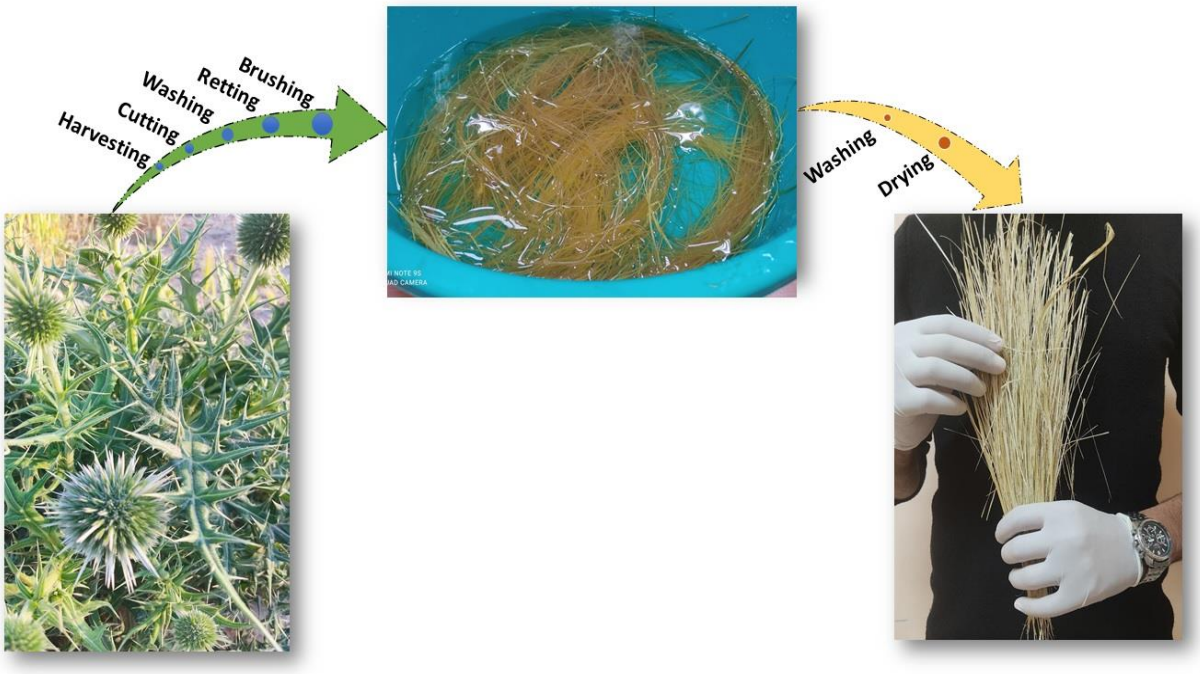

Figure III. 3. Extraction process of ESFs from the plant

III. 2. 2. Polymeric matrix

In this study, epoxy resin was used is provided by the company HUNTSMAN-Switzerland. The trade name of this epoxy resin (ER) is ARALDITE LY 564. As shown in Figure III.4a. Regarding the hardener, HUNTSMAN-Germany Company provided it. The trade name of this hardener is ARADUR 3486 BD. As shown in Figure III.4b.

Figure III. 4. Polymeric matrix: (a) Epoxy resin and (b) Hardener

III. 3. Chemical fiber treatments

Two different chemical treatments were used in this investigation. They are carried out with the aim of change the morphological properties of ES fibers to became have rough surfaces to improve fiber/matrix interfacial cohesion [8], also to improve the mechanical properties of the composite materials reinforced with these fibers chemically treated. **Table III.1 summarize these two kinds of** treatments**.**

Table III.1. Summary of chemical treatment techniques

Fibers	Treatment		Designation
	NaOH	$KMnO_4$	
Raw Echinops Spinosissimus Fibers	/	/	R_{ESFs}
Alkali Echinops Spinosissimus Fibers	3%	/	A_{ESFs}
Permanganate Echinops Spinosissimus Fibers	3%	0.033%	P_{ESFs}

III. 3. 1. Alkaline treatment

Before the treatment carried out, ES fibers must undergo steaming at 70° C to eliminate the absorbed humidity. Thus, alkali treatment was applied by immersing ES fibers in a solution of a 3% sodium hydroxide (NaOH) solution prepared with distilled water, for a duration of 3 hours [9]. The fibers were repeatedly washed with distilled water, with the addition of two drops of acetic acid (CH_3COOH) to adjust the pH to neutral. After rinsing and draining, the ES fibers were dried for 8 hours prior to characterization (Figure III. 5).

Figure III. 5. Echinops spinosissimus (ES) fibers treated with NaOH (3%)

The structure of fibers is typically modified using alkali treatment. These chemical interactions reduce moisture-bound hydroxyl groups (hydrophilic) and thus improve the hydrophobicity of fibers. The treatment also removes some hemicellulose, lignin, pectin, wax and oil coatings from the surface [10]. As a result, cellulose fibrils are exposed on the surface of the fiber. This amorphous region of cellulose can easily mix with matrix materials and form a strong interface bond that results in greater load transfer capacity of the composites.

Alkaline treatment also separates elementary fibers from their fiber bundles by removing coating materials. Thus, increasing the effective surface area of the fiber for matrix adhesion and improving fiber dispersion in the composite. The surfaces of treated fibers become rougher, which can further improve fiber-matrix adhesion by providing additional fiber sites for mechanical interlocking [11]. The mechanical and thermal properties of the composite are significantly increased by this treatment. However, too high a concentration of alkalis can cause excessive removal of coating materials from the cellulosic surface, resulting in weakening or damage to the fiber structure

III. 3. 2. Permanganate treatment

For the KMnO4 treatment, ES fibers pretreated with an alkaline solution were immersed in a Solution in a 0.033% solution of potassium permanganate ($KMnO_4$) for a duration of 3 minutes [9]. Before making various characterization, ES fibers must be washing, then neutralize and finally dried at ambient conditions for 48 h (Figure III. 6).

Figure III. 6. Echinops spinosissimus (ES) fibers treated with $KMnO_4$ (0.033%)

The permanganate treatment on natural fibers forms highly reactive permanganate ions (Mn_3^+) which react with cellulose (hydroxyl groups) and form cellulose manganate and initiate graft copolymerization. This treatment improves the chemical interlocking at the interface and provides better adhesion of the fibers with the matrix [12]. The treatment also reacts with the OH groups of the lignin and removes them from the fiber, thereby reducing the hydrophilic nature of the fiber.

III. 4. Structural and physico-chemical analyzes of ES fibers

Following chemical treatments, extensive research was conducted on the physico-chemical and structural characteristics of Echinops Spinosissimus fibers. The investigation employed a variety of analysis methods, as outlined in the subsequent paragraphs.

III. 4. 1. Morphological characterization

There are several ways to conduct morphological analysis, and the methods used vary according to the information to be obtained, the characteristics of the sample, the extent of accuracy required, as well as the nature of the tested compounds.

III. 4. 1. 1. Analysis by optical microscope

This method allowed us to make observations on the cross sections of the ES fibers. At first, thin cross-sections (0.3–0.8 mm) of the ES plant stem were cut using a cutter. These sections were stained with methylene blue, rinsed with distilled water, then mounted on microscope slides, covered with coverslips, and observed under an OPTIKA optical microscope, which was connected to a camera for capturing images. (Figure III. 7). This microscope performs ocular observations with magnification varying from (10 x to 100 x).

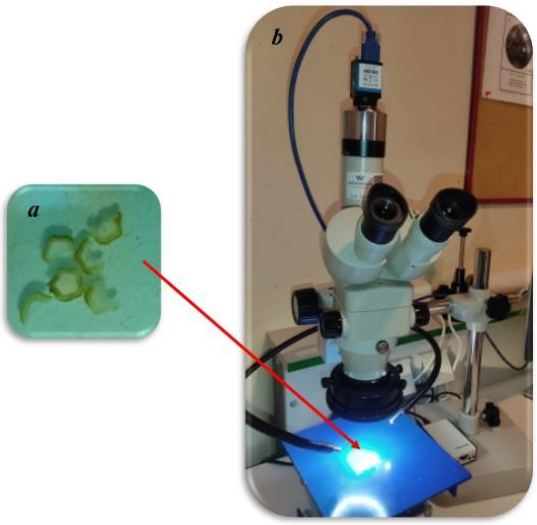

Figure III. 7: (*a*) Thin cross-sectional slices of ES fibers and (*b*) OPTIKA optical microscope

III. 4. 1. 2. Analysis by scanning electron microscopy (SEM)

In this work, the SEM (scanning electron microscope) is used to see the influence of chemical treatments on the morphology of plant fibers. The surface and morphology of ES fibers were analyzed employing a Thermo Scientific Quattro field emission scanning electron microscope (FEG-SEM) USA, which offers comprehensive imaging and analytical capabilities, Featuring a specialized environmental mode (ESEM) that allows analysis of samples in their

natural condition. The samples were prepared are small pieces of fibers that are placed on the sample holder and then placed in the designated places in the SEM. The working distance was set between 3.1 and 13.4 mm, with an accelerating voltage of 2.0 kV. Images were captured using an infrared camera equipped with two external signal inputs and an image processor (Figure III. 8). Images are recorded at different magnifications (x350, x600 and x1000).

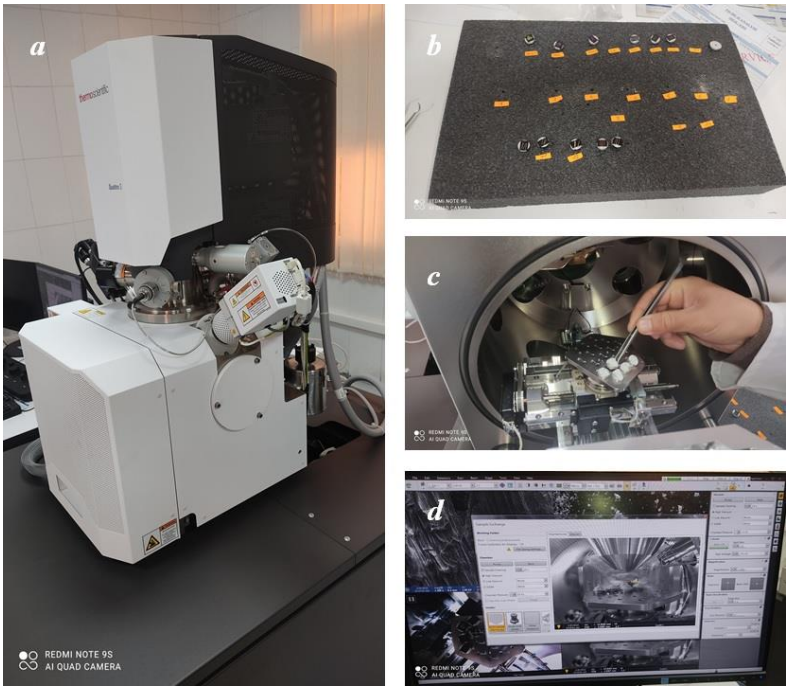

Figure III. 8**:** (*a*) Scanning Electron Microscopy ESEM and (*b*, *c* and *d*) Steps to use it

III. 4. 2. Spectroscopic characterization of energy dispersive X-rays (EDX)

EDX uses an analytical method for analysing the elements of a sample attached to SEM images. To analyze the elemental composition of the ESF specimens to assess the weight and atomic proportions, Energy Dispersive X-ray Spectroscopy (EDX) was utilized [13]. This approach makes it possible to detect elements from all of the chemical elements of the periodic table with the exception of H, He, and Li. Consequently, hydrogen, which represents one of the main constituents of the natural fiber, cannot be observed by this technique [14].

III. 4. 3. Attenuated Total Reflectance-Fourier Transform Infrared Spectroscopic Characterization (ATR-FTIR)

The chemical and structural composition, as well as the alterations in functional groups on the surfaces of treated and untreated ES fibers, were analyzed using Fourier Transform Infrared Spectroscopy (FTIR). ATR-FTIR analysis was performed on three types of ES fibers using an Agilent Cary 630 FTIR spectrometer (Malaysia), with a spectral resolution of 2 cm^{-1} and a wavenumber range from 4000 to 500 cm^{-1}

III. 4. 4. Characterization by X-ray diffraction (XRD)

The degree of crystallinity of the cellulosic ESFs was assessed using X-ray diffraction (XRD) analysis was performed using an X'Pert Pro EMPYREAN diffractometer (P Analytical, Netherlands) at the Physics Laboratory of the University of Msila. XRD is a rapid and non-destructive technique. Tests were carried out on raw fibers, fibers treated with 3% alkali, and fibers treated with 0.033% potassium permanganate. For analysis, ESF samples were prepared in powder form and mounted on the sample holder. The XRD instrument operated at a wavelength of 0.154 nm, with a current of 30 mA and a voltage of 40 kV. Continuous scanning mode was employed over a 2θ range of 10° to 60°, with a scan speed of 4.67°/min and a step size of 0.02°, at room temperature (28°C). Phase identification was conducted by comparing the XRD patterns of the samples with the Joint Committee on Powder Diffraction Standards (JCPDS) database. The degree of crystallinity of the cellulosic ESF samples was calculated from the XRD data, and the crystallinity index (CI) of the three types of ESF was determined using the empirical method proposed by Segal [15] displayed in the equation (III.1) [16]:

$$CI\% = \left[\frac{I_{002}-I_{am}}{I_{002}}\right] \times 100 \qquad \text{III.1}$$

where I_{200} denotes the maximum intensity of the crystalline phase peak, and I_{am} represents the intensity of the amorphous phase in the cellulose present in the fiber [17].

III. 4. 5. Thermogravimetric analysis characterization (TGA)

The thermal stability and thermal decomposition behavior of the fibers was analyzed using a thermogravimetric analyzer (TGA), model NETZSCH STA 409 PC/PG, at the Analytical Physico-Chemical Research Center (C.R.A.P.C) in Laghouat. The temperature range was set from 20 to 700°C with a heating rate of 10°C/min under a nitrogen (N_2) atmosphere at a flow rate of 25 ml/min. Sample masses of 30.613 mg for RESF, 31.072 mg for AESF, and 32.971 mg for PESF were used for the tests.

III. 4. 6. Density measurement

The density of each concentration of the three types of ES fibers was measured using a 50 ml solid pycnometer with ethanol (ρEth = 0.789 g/cm³) as the immersion liquid. Measurements were conducted using a balance with a sensitivity of 0.00001 g at 28°C. Initially, approximately 1 g of ES fibers was cut into pieces ranging from 1 to 5 mm in length. The fibers were then dried at 80°C until their weight was reduced to less than 95% of the initial value, in order to minimize moisture content. The density of the ESFs (ρ_{ESFs}) was calculated using the following parameters:[18, 19]. ρEth (density of ethanol, g/cm³); m1 (mass of the empty pycnometer, g); m2 (mass of the pycnometer with fibers, g); m3 (mass of the pycnometer filled with ethanol, g); and

m4 (mass of the pycnometer with fibers and ethanol, g)[5]. The apparent density of ESFs is given by the formula (III.2) [18]:

$$\rho_{ESFs} = \left(\frac{m_2 - m_1}{(m_3 - m_1) - (m_4 - m_2)}\right)\rho_{Eth} \quad \text{III.2}$$

III. 4. 7. Diameter measurement

To determine the average diameter of each type of ESF, with the fibers considered to be cylindrical in shape, a weighing process was carried out on more than 30 separate fibers, each 200 mm in length, in order to obtain the average mass of the ESFs using an analytical balance with a resolution of 0.00001 g. Subsequently, the cross-sectional area of the fibers was calculated using the following formula. (III.3):

$$S_f = \frac{M}{\rho_{ESFs} \times L} \quad \text{III.3}$$

Where Sf is the cross-sectional area of the fiber; M is its mass; L is its length; and ρESFs is its density. Finally, the diameters of the ESFs are given by the formula (III.4):

$$D_{ESFs} = \sqrt{4M / (\rho_{ESFs} \times \pi \times L)} \quad \text{III.4}$$

III. 5. Micromechanical and mechanical characterization

III. 5. 1. Tensile test on monofilament fibers

The tensile properties of the electrostatic glass fibers were evaluated in accordance with ASTM D3322-01 using a Zwick/Roell universal testing machine equipped with a 2.5 kN load cell. Single-fiber tensile tests were performed on fibers 40 mm in length, at a crosshead speed of 2 mm/min. A total of 30 specimens for each fiber type were prepared and tested to determine the average tensile strength values (Figure III. 9). Tests are conducted at an ambient temperature 28°C with a relative humidity of about 68 % ± 2%. The tensile strength of fibers was calculated from the following Equation. (III.5) [20]:

$$T = F / A \quad \text{III.5}$$

Where, T tensile strength in Pa, *F* the breaking force in N, and *A* the average cross-sectional area of the fibers in mm^2.

The mechanical properties determined from the stress-strain curves are: elastic modulus E, stress at break σ_r and strain at break ε_r.

- The modulus of elasticity is expressed as follows in Equation. (III.6):

$$E = {}^{\sigma}/_{\varepsilon} \qquad \text{III.6}$$

E: Modulus of elasticity (N/mm^2);
σ: Stress (N/mm^2);
ε: Elongation.

❖ The breaking stress is given by the following expression in Equation. (III.7):

$$\sigma_R = \frac{F}{S_0} \qquad \text{III.7}$$

F: Tensile load supported by the specimen (N);

S_0: Initial section (mm^2).

Under the assumption of fiber cylindricity: $S_0 = \frac{\pi d^2}{4}$

With d: fiber diameter.

❖ The elongation at break is indicated as a percentage in the following form (Equation. III.8):

$$\varepsilon_R = \frac{\Delta l}{l_0} = \frac{(l - l_0)}{l_0} \qquad \text{III.8}$$

$\Delta l = l - l_0$: Deformation at break;

l_0: Initial length of the sample;

l: Final length of the sample.

Figure III. 9: (*a*) Tensile samples of single ES fiber test according to ASTM D3322-01 Standard [21] and (*b*) Zwick/Roell tensile testing machine

III. 5. 2. Micro-droplet test (Pull-out test)

To study the interfacial decohesion between single fiber of Echinops spinosissimus and the matrix (**epoxy resin)**, a micro-droplet decohesion test (pull-out) was performed. This is the

technique developed by Miller et al. [22]. The procedure involves stick ES fibers into wood frames. With the use of thin plastic tool to put small droplets give an elliptical shape around the fibers and retain them after hardening. After that, we selected the fibers with the ideal drops, and then we glued paper clips at the tip of each fiber to finally get the microbond specimens ready for testing. The length of the micro-droplets and the diameter of the fibers are measured using an optical microscope. All this is shown in Figure III. 10.

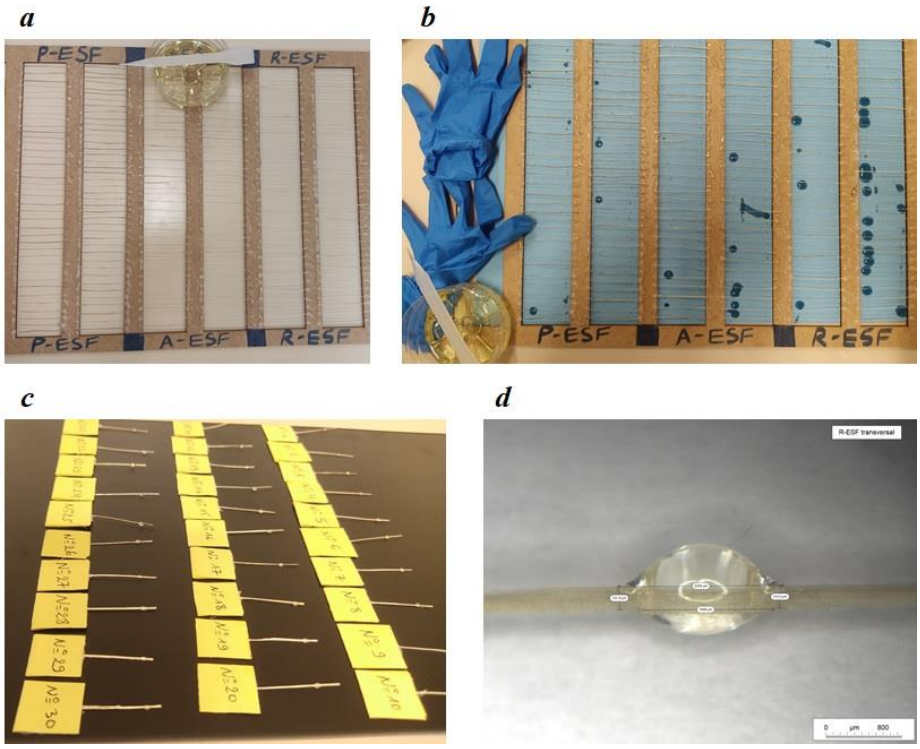

Figure III. 10. Microbond specimens: (a), (b) and (c) Preparation and (d) Measurement

The value of the interfacial shear strength (IFSS) is calculated from equation (III. 9):

$$IFSS = \frac{F_d}{\pi d l} \qquad \text{III.9}$$

With F_d: the decohesion force.
d: the diameter of the fiber.
l: the embedded length.

For the tests, we selected samples whose micro-droplet shape was symmetrical with respect to the fiber axis. On the universal traction machine (INSTRON UTM), equipped with a 5 kN load cell, specimens are placed in the down mandrel of the machine. The fine droplet is then carefully adjusted between the edges of the two blades that adapts to the fiber diameter as shown in Figure III. 11. Crossing speed 2 mm/min. This makes it possible to apply force to the interface and

measure shear stress during fiber extraction. The shear force at the interface is transferred to the fiber through the interfacial bond to the fiber matrix. The rupture occurs when the shear force exceeds the bond strength between the two faces.

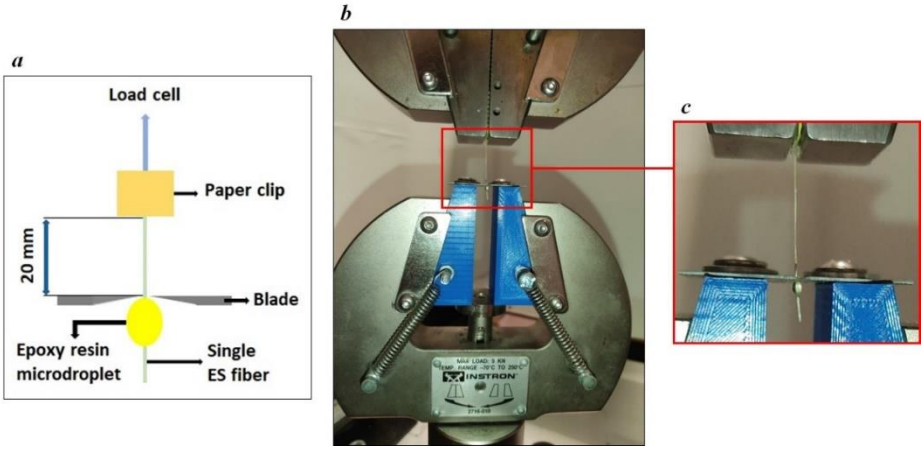

Figure III. 11. Microbond test.: (a) Schematic view (b) micro-drop test system and (c) zoom on micro-drop test system

During the tests, several phenomena were observed: the micro-droplet sliding between the edges (not retained), the fiber broke because the length of the embedded droplet was too large.

Finally, the small droplet is released. Only about ten samples of each fiber matrix combination was successful. There were a large number of samples broken during testing or placing the specimen on the tensile machine.

III. 5. 3. Tensile test on composite

III. 5. 3. 1. Tensile test on a single fiber fragmentation

The mechanical properties of composites made from natural fibers are influenced by the stability of the interfacial region. Consequently, understanding and characterizing this interface plays a vital role in studying the influence of treatments on the interface's micromechanical behavior, we have developed a model composite material using monofilaments from natural fibers. Tensile test on a single fiber fragmentation, in accordance with the ASTM standard (D 638-03 type V) [8] and illustrated in Figure III. 12 with specimen dimensions mentioned in Table III. 2. The monofilament-based model composites were tested using the universal testing machine (INSTRON UTM).

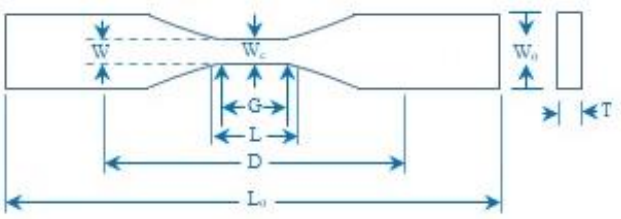

Figure III. 12. Fragmentation test specimen with the ASTM standard (D 638-03 type V)
With:

Table III. 2. Single fiber fragmentation specimen Dimensions

Dimensions of the specimen (mm)	W_o	W_c	L	D	L_o	R	T
Values	9,53	3,18	9,53	25,4	63,5	12,7	3,2
Tolerances	± 6,4	± 0,5	± 3,18	± 5	± 0,5	± 1	± 0,2

The fragmentation test specimens are produced by molding. First, their appearance is carried out by means of laser cutting on a wooden mold (Figure III.13. a). The test specimen has the same thickness as the mold. Then, perforations are made on both ends of each wood impression to be able to insert the ES fibers. Once the fibers are positioned (Figure III.13. b), they are embedded in the resin (Figure III.13. c). Following polymerization, the fragmentation test specimens are moved away from the mold (Figure III.13. d).

Figure III. 13. Fragmentation specimens preparation: (*a*) Wooden mold, (*b*) Positioning of ESFs in mold, (*c*) Embedding fibers in epoxy resin and (*d*) Test specimens obtained

III. 5. 3. 2. Tensile test on a composite reinforced by ES fibers (NFCs)

The stability of the interfacial zone plays a major role in shaping the mechanical properties of composites reinforced by natural fibers (NFCs). Therefore, it is necessary to gain insight and characterize this interface. To examine how chemical treatments of fibers affect the micromechanical properties at the interface, we created a prototype composite material that uses textile layers of natural fibers as the reinforcement material. By following these steps: First, an anti-adhesion agent was applied to the inner sides of both the upper and lower molds (Figure III. 14. a), then the layers of long fibers were placed in an organized manner in the cavity of the lower mold measuring: 400 x 400 x 30 mm^3. Height, width and depth respectively. Great care was taken to obtain a uniform orientation of the fibers (Figure III. 14. b). Then, the mold was closed tightly for the epoxy to be injected, and after 24 hours, the shape of a plate was obtained as shown in Figure III. 14.c. Three plates of NFCs are manufactured (see Table III. 3).

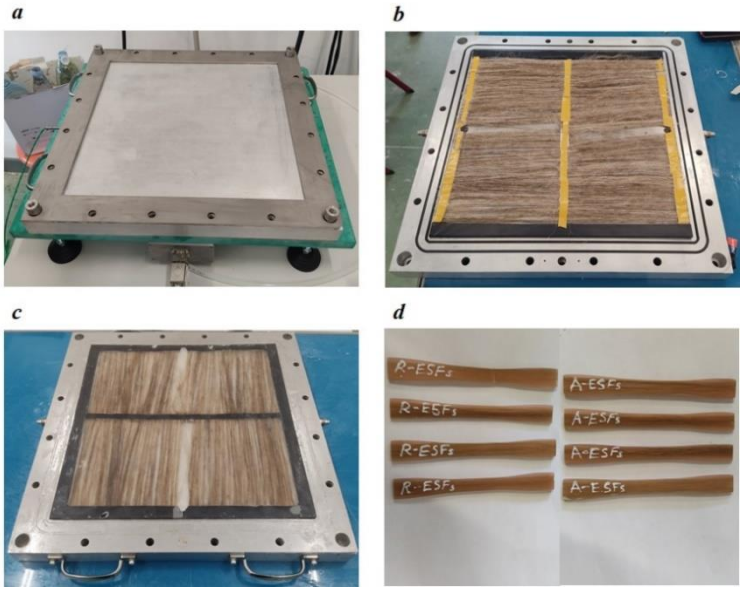

Figure III. 14. NFCs specimens' preparation: (*a*) Lower mold, (*b*) Positioning of ES fibers in mold, (*c*) Plaque of NFCs and (*d*) NFCs test specimens obtained

Table III. 3. Different manufacturing composites

Composites	Fibers treatment	Designation
1	Untreated ES	NFC 1
2	3% NaOH	NFC 2
3	0.033% $KMnO_4$	NFC 3

Tensile tests, according to ASTM standard (D 638-03 Type Ⅰ) [21] and illustrated in Figure III. 15 with specimen dimensions mentioned in Table III. 4. Were carried out on these model composites (NFCs) shown in Figure III. 14 (d). The assessments were conducted using the INSTRON UTM (universal traction machine).

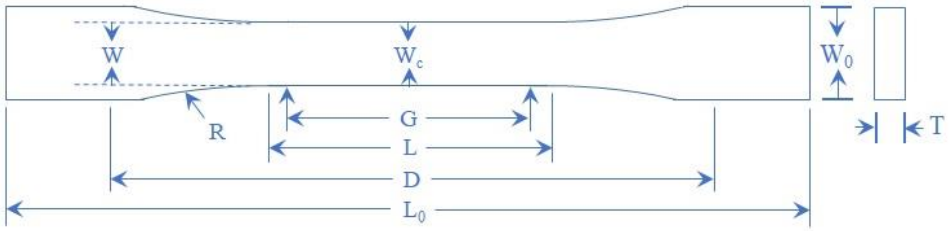

Figure III. 15. NFCs test specimen with the ASTM standard (D 638-03 type I)

Table III. 4. NFCs specimen dimensions

specimen Dimensions (mm)	W_o	W_c	L	D	L_o	R	T
Values	19	13	57	115	165	76	3,2
Tolerances	± 6,4	± 0,5	± 3,18	± 5	± 0,5	± 1	± 0,2

References

[1] S. H. Zitouni-Nourine, N. Belyagoubi-Benhammou, F. El-Houaria Zitouni-Haouar, O. Douahi, F. Chenafi, H. Fetati, S. Chabane Sari, A. Benmahieddine, C. Zaoui, and F. Z. N. Mekaouche, "Echinops spinosissimus Turra Root Methanolic Extract: Characterization of the Bioactive Components and Relative Wound Healing, Antimicrobial and Antioxidant Properties," *Plants,* vol. 11, p. 3440, 2022.

[2] L. M. Al Masoudi and A. M. Hashim, "Morphological Features and Biological Activity of Different Extracts of Echinops spinosissimus Grown in Saudi Arabia," *Agronomy,* vol. 13, p. 573, 2023.

[3] I. Sánchez-jiménez, O. Hidalgo, and T. Garnatje, "Echinops spinosissimusTurra subsp.neumayeri(Vis.) Kožuharov (Asteraceae, Cardueae): a new record for the flora of Greece," *Adansonia,* vol. 34, pp. 129-132, 2012.

[4] Z. Belouadah, A. Ati, M. Rokbi, A. Bezazi, and A. Imad, "Optimisation Des méthodes D'extraction Et Caractérisation Mécanique De La Fibre Alfa En Vue De Son Application Comme Renfort Des Matériaux Composites," *Journal of Materials, Processes and Environment,* vol. 2, pp. 51-57, 2014.

[5] R. Mansour, A. Abdelaziz, and A. F. Zohra, "Characterization of long lignocellulosic fibers extracted from Hyphaene thebaica L. leaves," *Research Journal of Textile and Apparel,* 2018.

[6] P. Manimaran, K. Solai Senthil Kumar, and M. Prithiviraj, "Investigation of physico chemical, mechanical and thermal properties of the albizia lebbeck bark fibers," *Journal of Natural Fibers,* vol. 18, pp. 1151-1162, 2021.

[7] D. Atalie and R. K. Gideon, "Extraction and characterization of Ethiopian palm leaf fibers," *Research Journal of Textile and Apparel,* 2018.

[8] N. Moussaoui, M. Rokbi, H. Osmani, M. Jawaid, A. Atiqah, M. Asim, and L. Benhamadouche, "Extraction and characterization of fiber treatment Inula viscosa fibers as potential polymer composite reinforcement," *Journal of Polymers and the Environment,* vol. 29, pp. 3779-3793, 2021.

[9] M. Rokbi, H. Osmani, A. Imad, and N. Benseddiq, "Effect of chemical treatment on flexure properties of natural fiber-reinforced polyester composite," *procedia Engineering,* vol. 10, pp. 2092-2097, 2011.

[10] X. Li, L. G. Tabil, and S. Panigrahi, "Chemical treatments of natural fiber for use in natural fiber-reinforced composites: a review," *Journal of Polymers and the Environment,* vol. 15, pp. 25-33, 2007.

[11] P. Joseph, G. Mathew, K. Joseph, G. Groeninckx, and S. Thomas, "Dynamic mechanical properties of short sisal fibre reinforced polypropylene composites," *Composites Part A: applied science and manufacturing,* vol. 34, pp. 275-290, 2003.

[12] S. A. Paul, C. Oommen, K. Joseph, G. Mathew, and S. Thomas, "The role of interface modification on thermal degradation and crystallization behavior of composites from commingled polypropylene fiber and banana fiber," *Polymer Composites,* vol. 31, pp. 1113-1123, 2010.

[13] A. W. Burton, K. Ong, T. Rea, and I. Y. Chan, "On the estimation of average crystallite size of zeolites from the Scherrer equation: A critical evaluation of its application to zeolites with one-dimensional pore systems," *Microporous and Mesoporous Materials,* vol. 117, pp. 75-90, 2009.

[14] P. Manimaran, P. Senthamaraikannan, M. Sanjay, M. Marichelvam, and M. Jawaid, "Study on characterization of Furcraea foetida new natural fiber as composite reinforcement for lightweight applications," *Carbohydrate polymers,* vol. 181, pp. 650-658, 2018.

[15] L. Segal, J. J. Creely, A. Martin Jr, and C. Conrad, "An empirical method for estimating the degree of crystallinity of native cellulose using the X-ray diffractometer," *Textile research journal,* vol. 29, pp. 786-794, 1959.

[16] A. D. French and M. Santiago Cintrón, "Cellulose polymorphy, crystallite size, and the Segal Crystallinity Index," *Cellulose,* vol. 20, pp. 583-588, 2013.

[17] R. Vijay, S. Manoharan, S. Arjun, A. Vinod, and D. Singaravelu, "Characterization of silane-treated and untreated natural fibers from stem of Leucas aspera. J Nat Fibers," ed, 2020.

[18] K. M. M. Rao and K. M. Rao, "Extraction and tensile properties of natural fibers: Vakka, date and bamboo," *Composite structures,* vol. 77, pp. 288-295, 2007.

[19] M. Truong, W. Zhong, S. Boyko, and M. Alcock, "A comparative study on natural fibre density measurement," *The journal of the Textile Institute,* vol. 100, pp. 525-529, 2009.

[20] M. Kabir, H. Wang, K. Lau, and F. Cardona, "Tensile properties of chemically treated hemp fibres as reinforcement for composites," *Composites Part B: Engineering,* vol. 53, pp. 362-368, 2013.

[21] D. ASTM, "3379: Standard test method for tensile strength and Young's modulus for high modulus single filament fibers," *ASTM Standards,* 1975.

[22] B. Miller, P. Muri, and L. Rebenfeld, "A microbond method for determination of the shear strength of a fiber/resin interface," *Composites Science and Technology,* vol. 28, pp. 17-32, 1987.

CHAPTER IV

Results and Discussions

IV. 1. Introduction

The experimental results obtained from the different tests carried out on the ES fiber and the different model composites will be presented and interpreted in this chapter.

First, we will present the effect of chemical modification by different treatments on the characteristics of the fibers, namely, alkaline, permanganate treatments, in terms of spectral, physical, morphological and mechanical analysis. Then the study of interfacial decohesion and damage mechanisms present in a composite structure under static loading will be analyzed by micromechanical characterization.

The results and discussions outlined in this chapter encompass: (1) Anatomical analysis applied to Echinops spinosissimus stem; (2) physical and chemical characterization of the ES fibers; (3) mechanical characterization on monofilament fibers; (4) micromechanical characterization using micro-drops and (5) mechanical characterization through tensile testing on two different developed model composites.

IV. 2. Anatomical analysis of the Echinops spinosissimus stem

The stem of the Echinops spinosissimus plant can reach a height of 0.6 to 1 m and a diameter of 8 to 15 mm. The fibers in our work are extracted from the stems of this plant [1].

Figure IV. 1 below shows a thin cross section of a still green ES rod taken by optical microscope. The sample is soaked in a methylene blue solution [2], It is then rinsed with distilled water, to bring out the lignified parts and those particularly cellulosic [3]. It clearly exposes the different elements that compose it.

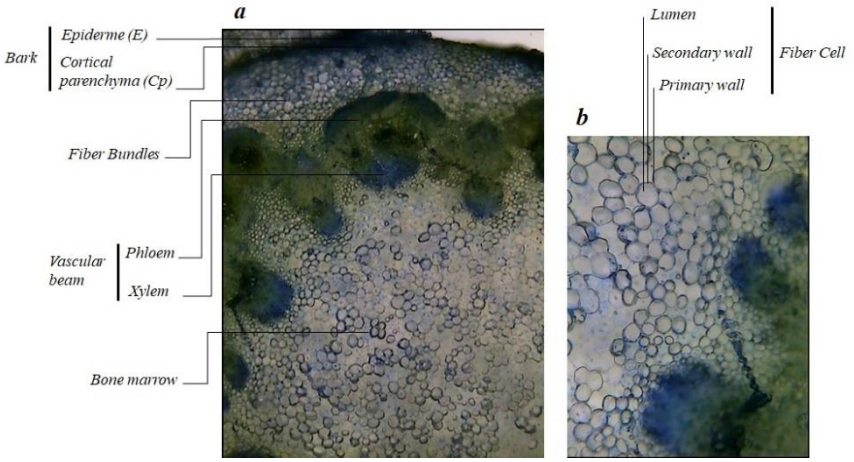

Figure IV. 1: Schematization of the Echinops spinosissimus (ES) stem section:
(a) General appearance of the transverse cut (b) Fiber bundles

Starting from the outer edge towards the center of the cross-section of the ES rod, we observe the following in succession:

1- Bark (B): structured from the outer layer, known as the epidermis (E), to the inner cortical parenchyma (CP). The epidermis contains numerous glandular hairs filled with aromatic essences, emitting a potent fragrance upon touch [4]. The bark serves to enhance the plant's respiratory capabilities and provides protection against external threats.

2- Fiber bundles (FB): These bundles are located around the periphery of the stem, adjacent to the phloem (see Figure IV. 1. a). Their primary function is to enhance the overall toughness of the plant, providing resilience against natural elements such as thunderstorms, rain, and sandstorms [5].

Within a stem, there are typically more than 40 to 60 fiber bundles arranged along its length. Each bundle consists of multiple individual fiber cells are connected to each other by substances known as lignin and hemicellulose, which is rich in amorphous polysaccharides.

3- Vascular bundles (VB) are regularly arranged beneath the bark, though their size and quantity vary. These differences are influenced by various internal and external factors, with the most significant being the plant's age (maturity), as well as soil conditions and climate. Primarily composed of phloem (PH) and xylem (X), these bundles are situated next to the fiber bundles [6]. The phloem functions as a conduit for transporting sap, which includes water and sucrose. It also serves as a reservoir for parenchyma cells and provides support to the fibers. On the other hand, the xylem facilitates the movement of raw sap, Composed of water and mineral salts absorbed from the soil by the roots, as previously reported in studies on the anatomical structure of natural fibers by various researchers, such as those on Centaurea melitensis. [7], Malva sylvestris L [8] and Centaurea hyalolepis [9].

4- Pith (P): The supportive portion housing the wood that forms the clusters (abundant in lignin) [10].

5- Fiber cell (FC): Comprising a central cavity known as the lumen (L) and concentric layers referred to as cell walls (**primary** P and **secondary** S walls) (Figure IV. 1. b), the lumen helps in the transport of nutrients and other compounds to different tissues through water-based transport systems with its size intricately linked to maturity [11]. Fiber elongation occurs in two phases:

Initial elongation, guiding the fiber to its ultimate length [12].

Secondary elongation, contributing to an increase in fiber thickness [13]. The cellulose composition peaks during the flowering period [14].

In the literature, the fiber section is typically assumed to be circular [15]. Nevertheless, the actual shape of the section is polygonal and exhibits non-uniformity across the entire fiber [1]. This assumption results in an overestimation of the section and consequently leads to an underestimation of the mechanical characteristics.

Moreover, upon examining the fibers, it becomes apparent that they are not oriented in a uniform alignment; instead, they intersect to optimize the connection within the bundle [16]. The presence of fibers in the central part of the bundle gives rise to concentrated compressive stress points and, consequently, disparities in the size and shape of the section.

IV. 3. Characterization of Echinops spinosissimus fiber

IV. 3. 1. Density measurement

One of the key factors considered is the density of natural cellulosic fibers. A lower fiber density results in lighter composite materials when used as reinforcement. [17]. This is the objective researchers strive to achieve. In contrast to composites reinforced with synthetic fibers like glass or carbon, which are generally heavier.

In our research paper, the effect of chemical treatments appears in increasing the density compared to that of the untreated fiber [18], the values of Echinops spinosissimus (ES) fiber density are shown in Table IV.1. These values are comparable to the fiber densities reported in previous studies, where an increase in the density of electrolytic cellulose fibers (ECF) was observed. This increase is attributed to the filling of pores and voids on the fiber surface as a result of chemical treatment. The reported values range between 0.70 and 1.20 g/cm³, which is typical for certain natural cellulosic fibers, such as Albizia lebbeck., [19], Sansevieria cylindrica [20], and Rhectophyllum camerunense [21]. The variations in the density of natural cellulosic fibers can be attributed to several factors, including climatic conditions [22], soil type, [23], maturity rate [24] and the extraction process [25].

Therefore, ESFs may be considered as a potential fiber for reinforcing lightweight materials.

Table IV. 1. Density of ESFs

Echinops spinosissimus fibers	Density ($g.cm^{-3}$)
Untreated	0.80 ± 0.06
Treated with NaOH	0.93 ± 0.03
Treated with $KMnO_4$	0.97 ± 0.01

IV. 3. 2. Diameter measurement

Speaking about ESF diameter measurement, the information that the diameter gives is very considerable for the various measurements and calculations, especially for mechanical tests.

The untreated, alkali-treated and permanganate-treated fibers had an average diameter of 336.52 ± 2.84 µm, 305.34 ± 1.28 µm, and 280.76 ± 1.56 µm, respectively. This demonstrates a

reduction in the diameters of ESF after chemical treatment with alkaline and permanganate solutions, resulting in the effective removal of lignin, pectin, wax, and other impurities from the fiber surface, thereby enhancing fiber purity [18, 26].

Chemical treatment of cellulosic fibers was found to improve their properties, reduce the diameter of the fiber and enhanced their performance, aligning with the findings of earlier studies

IV. 3. 3. Scanning electron microscopy (SEM) analysis of ESFs

The microscopic characterization of untreated and treated Echinops spinosissimus (ES) fibers allowed us to understand their morphology and their framework on a microscopic scale, as well as to observe the influence of each treatment.

IV. 3. 3. 1. Scanning electron microscopy analysis of R_{ESFs}

Longitudinal and cross-sectional views of the R_{ESF} are shown in Figure IV.2 (a–d). The longitudinal image in Figure IV.2 (a) reveals an intact fiber with a relatively rough surface, where the fiber bundles are clearly composed of numerous fiber cells exhibiting diameter irregularities [15] are aligned parallel to a single axis and are interconnected by lignin, wax, and hemicellulose. A higher magnification in Figure IV.2 (b) reveals the presence of impurities and several spherical protrusions that promote strong adhesion with the polymer matrix [27, 28] as mentioned in previous work on natural fibers such as Lygeum Spartum L [2] and Vachellia farnesiana [29].

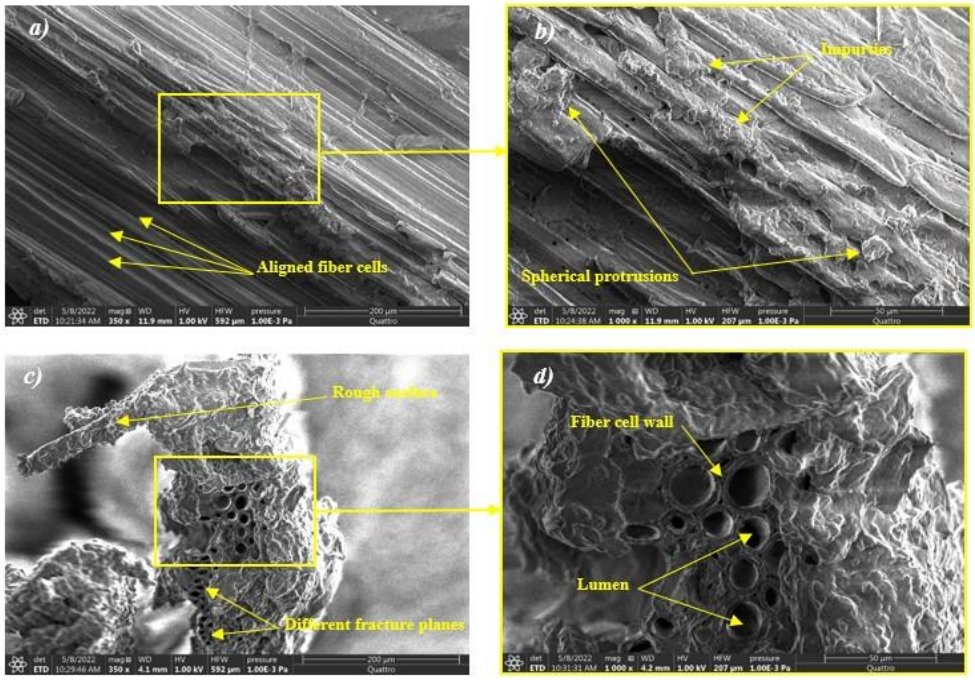

Figure IV. 2: SEM micrographs of R_{ESFs}: (a) & (b) longitudinal section and (c) & (d) cross-section

The cross-sectional view in Figure IV.2 (c) displays bundles of microfibrils interconnected by non-cellulosic compounds. As shown in the figure, these microfibrils exhibit a rough surface, with nearly all fibrils displaying minimal deviation from the fiber axis [30], which supports the angle of the microfibers and causes a different fracture plane as shown in this figure [31]. Figure IV.2 (d), at higher magnification, shows a cluster of porous cells along with numerous cavities of varying shapes and sizes, including circular, triangular, and irregular forms [32]. These cavities, known as lumens, influence the cell diameter of the fibers, which in turn directly impacts their mechanical properties [33].

IV. 3. 3. 2. Scanning electron microscopy analysis of A_{ESFs}

The SEM micrographs in Figure IV.3 (a–d) illustrate the morphology of alkali-treated ES fibers. Figure IV.3 (a) provides an overall longitudinal view, revealing numerous aligned fiber cells interconnected by lignin and hemicellulose. It is evident that the surface of the alkali-treated glass fibers becomes significantly roughened, which enhances adhesion to the polymer matrix compared to the untreated fibers [27]. Figure IV.3 (b) provides a magnified view of Figure IV.3 (a), where it can be observed that impurities such as waxes and oils are absent due to the 3% alkali treatment [34].

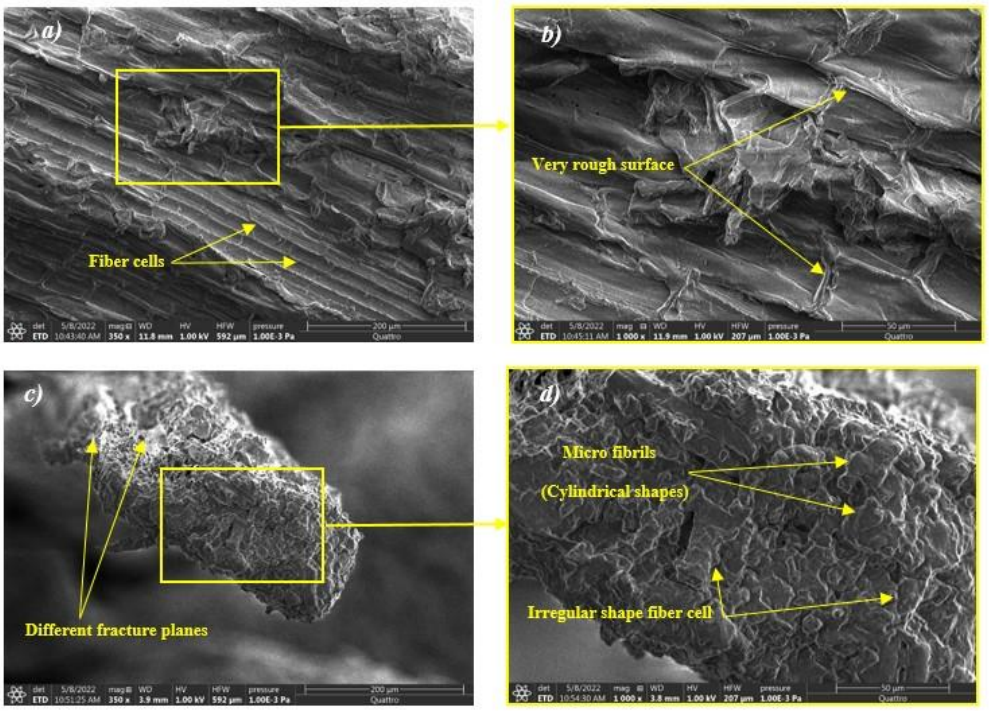

Figure IV. 3: SEM micrographs of A_{ESFs}: (a) & (b) longitudinal section and (c) & (d) cross-section

Figure IV.3 (c) presents a cross-sectional micrograph of the A_{ESF}, highlighting various fracture planes. Figure IV.3 (d) offers a magnified view of Figure IV.3 (c), clearly showing changes in the shape of the fiber bundles, resulting from the filling of lumens (pores and voids) following the treatment [35]. When chemical treatment with 3% alkali affects the ratios of the components of these fiber cell parts (cellulose, hemicellulose and lignin) [36].

As previously noted through density measurements and FTIR and XRD analyses, the cellulose content has increased. It is well established that the cylindrical structure of the fiber cells positively influences the mechanical properties of ES fibers, leading to significant improvements in performance by enhancing both Young's modulus and tensile strength. This finding aligns with earlier discussions and is consistent with observations reported in other studies, particularly those on Strelitzia reginae [1, 37].

IV. 3. 3. 3. Scanning electron microscopy analysis of P_{ESFs}

The SEM micrographs in Figure IV.4 (a–d) depict the morphology of permanganate-treated ESF. Figure IV.4 (a) presents an overall longitudinal view of the P_{ESF}, showing well-aligned fiber cells. The magnified image in Figure IV.4 (b) clearly reveals a highly roughened surface, which is favorable for enhanced adhesion with the polymer matrix compared to the untreated fibers [38]. It can also be observed that there appear to be no impurities, such as wax or grease, present. This is primarily attributed to the two processes: pretreatment with 3% alkali and treatment with 0.033% permanganate [39].

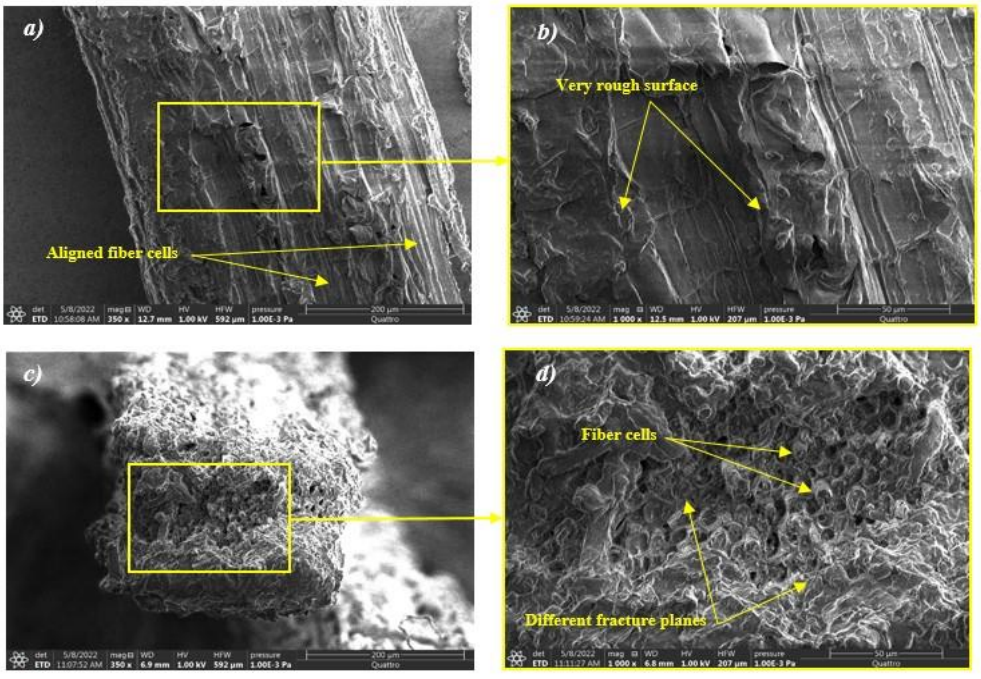

Figure IV. 4: SEM micrographs of P_{ESFs}: (a) & (b) longitudinal section and (c) & (d) cross-section

Figure IV.4 (c) presents a cross-sectional micrograph of the P_{ESF}, while Figure IV.4 (d) provides a magnified view of Figure IV.4 (c), clearly revealing a transformation in the shape of the fiber bundles into cylindrical structures, referred to as microfibrils. This modification results from the filling of lumens (pores and voids) on the surface of the R_{ESF} following the treatment, and also highlights various fracture planes within nearly all of the fiber cells.

The effect of the 0.033% permanganate chemical treatment on the proportions of fiber components (cellulose, hemicellulose, and lignin) appears to be similar to that of the 3% alkaline treatment. In both cases, the cellulose content increased [34], as confirmed by density measurements and FTIR and XRD analyses, the cylindrical shape of the fiber cells also enhances the mechanical properties, leading to improved performance [40] by increasing tensile strength and Young's modulus. This result is consistent with other published work.

IV. 3. 4. Energy-dispersive X-ray (EDX) spectroscopy analysis of ESFs

Figures IV. 5 (a–c) show the distribution of various elements in R_{ESF}, A_{ESF}, and P_{ESF}, respectively. Elements such as carbon (C), oxygen (O), calcium (Ca), manganese (Mn), arsenic (As), neon (Ne), sodium (Na), magnesium (Mg), and silicon (Si) are clearly detected.

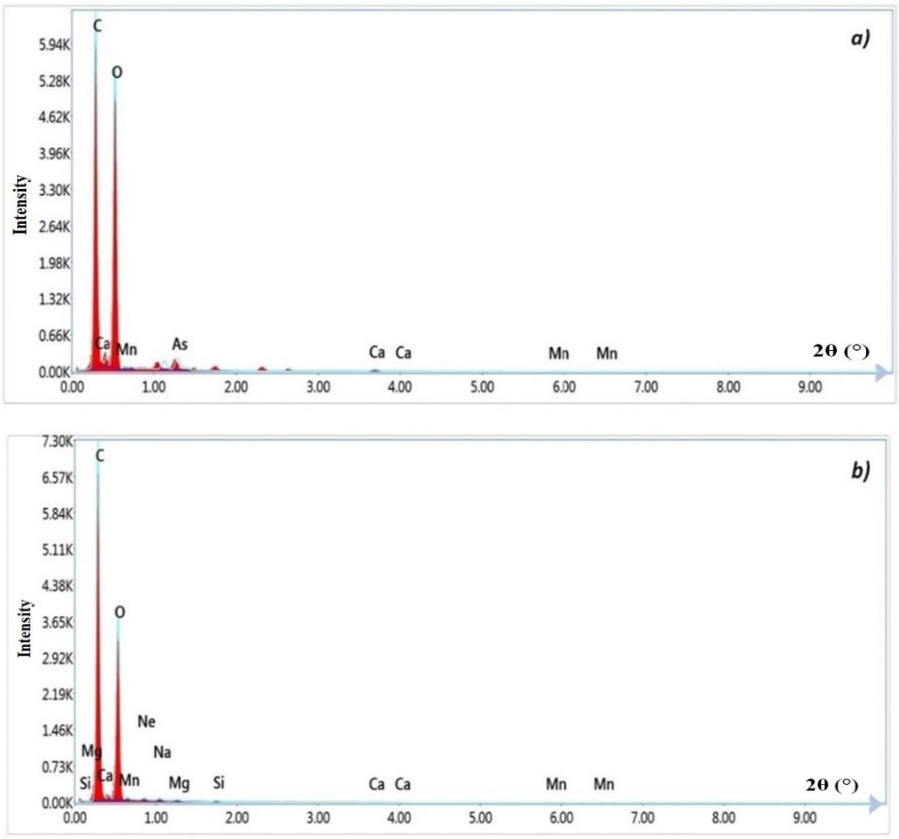

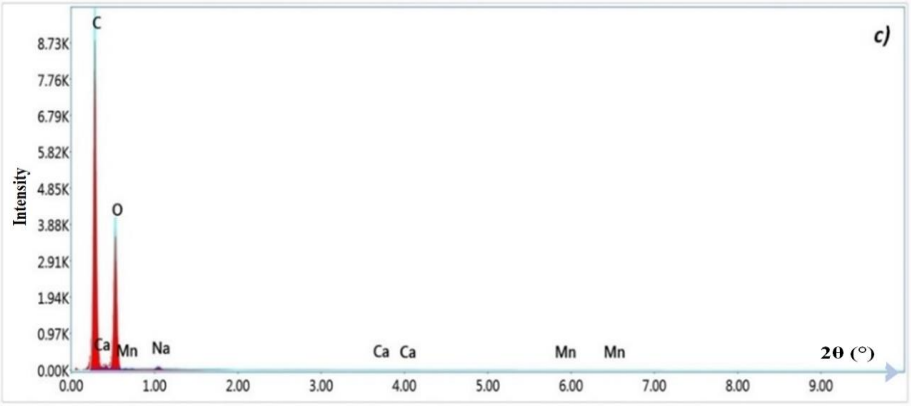

Figure IV. 5: EDX analysis of: (a) R_{ESFs}, (b) A_{ESFs} and (c) P_{ESFs}

In other words, energy-dispersive X-ray spectroscopy (EDS) analysis provides valuable insight into the composition of natural fibers considered for potential use as reinforcement elements, particularly in thermoset matrix composites. The weight and atomic percentages of each element in the ESF fibers with their three variants, and other fibers are presented in the Table IV.2 .The mass and atomic percentages of C and O are higher than those of the other elements identified in the EDX analysis. Because the presence of C and O elements tends to be the most important in the EDX continuum [41]. These elements are the critical components of natural fiber architectures, as usually seen in most cellulosic fibers.

Table IV. 2. Weight and atomic percentages of each elements found on the surface of the three type of ESFs

Fibers	R_{ESFs}		A_{ESFs}		P_{ESFs}		Ficus religiosa root [42]	
Elements	Weight %	Atomic %	Weight %	Atomic %	Weight %	Atomic %	Weight %	Atomic %
C	45.93	54.94	55.88	63.36	70.36	76.10	67.48	75.5
O	48.75	43.76	41.88	35.65	29.17	23.68	25.32	21.27
Ne	-	-	0.28	0.19	-	-	-	-
Na	-	-	0.44	0.26	0.31	0.17	2.71	1.58
Mg	-	-	0.21	0.12	-	-	-	-
Si	-	-	0.24	0.12	-	-	-	-
Ca	1.35	0.48	0.49	0.17	0.16	0.05	-	-
Mn	0.81	0.21	0.58	0.14	0.00	0.00	-	-
As	3.16	0.61	-	-	-	-	-	-
Cl	-	-	-	-	-	-	3.11	1.18
K	-	-	-	-	-	-	1.37	0.47

IV. 3. 5. Attenuated Total Reflectance-Fourier transform infrared spectrometry analysis (ATR-FTIR)

To study the changes in the composition of the ES fiber produced during the treatments carried out, FTIR (analysis by Fourier transform infrared spectroscopy) was applied. The identification of the most important peaks is taken from the literature [43-45].

In this section, various functional groups present in the three types of ESF are identified through FTIR analysis. The FTIR spectra of R_{ESF}, A_{ESF}, and P_{ESF} are presented in Figure IV.6. A broad absorption band observed around 3340 cm^{-1} is assigned to the hydroxyl (-OH) group [2]. The two peaks at 2921 cm^{-1} and 2862 cm^{-1} are associated with the (CH_2) groups present in cellulose and hemicellulose [46]. The bands peaking at 1732 cm^{-1} are attributed to the stretching vibration of the C=O bond in the carbonyl ester group of hemicellulose. The wavenumber at 1592 cm^{-1} corresponds to the carbonyl (C=O) groups present in both lignin and hemicellulose [47, 48], while the band at 1512 cm^{-1} is indicative of the (C=C) groups found in lignin [29]. The peak around 1457 cm^{-1} corresponds to the (CH_2) groups in cellulose, while the presence of a peak near 1371 cm^{-1} is associated with the (C–H) groups of cellulose [49]. The peak around 1325 cm^{-1} is attributed to the (C–H) groups present in lignin [3]. The peak observed at 1237 cm^{-1} indicates the presence of (-COO) groups from hemicellulose. Additionally, at 1158 cm^{-1}, the (C–O–C) groups associated with both cellulose and hemicellulose are identified [50, 51]. The wavenumber around 1024 cm^{-1} corresponds to the (C–O) groups in cellulose. Moreover, the presence of a peak near 898 cm^{-1} is associated with (C–O) groups linked to β-glycosidic bonds [29].

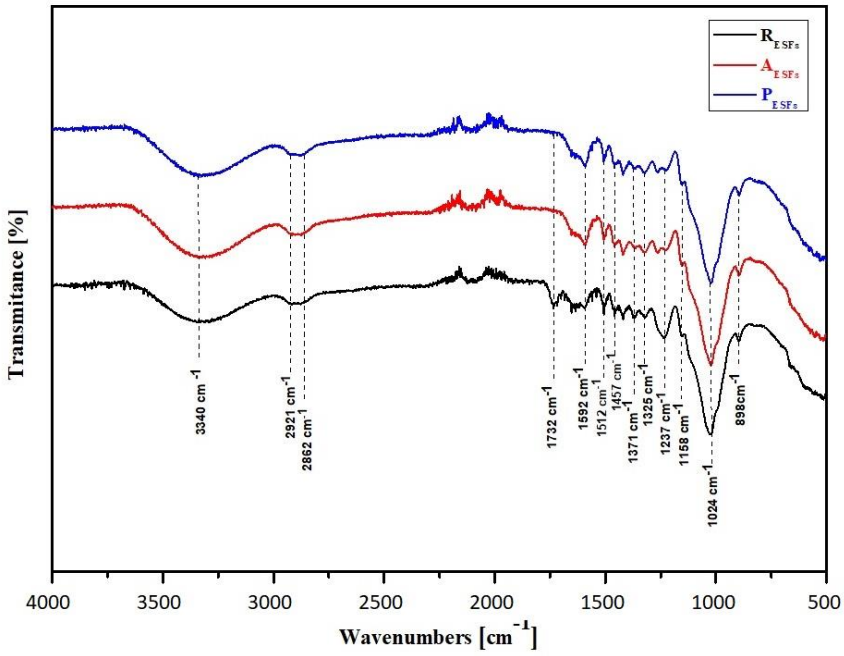

Figure IV. 6. FTIR spectra of R_{ESFs}, A_{ESFs} and P_{ESFs}

Based on the above analysis, the ATR-FTIR results confirmed the presence of the main components (cellulose, hemicellulose, and lignin) in ES fibers. The FTIR spectra of the fibers reveal compositional changes in the ES fibers following treatment. The peak at 1732 cm^{-1}, associated with hemicelluloses and observed in the spectrum of untreated ES fibers, disappeared after treatment. This observation suggests the removal of residual hemicellulosic components following alkali and permanganate treatments. Furthermore, a significant portion of hemicellulose and other non-cellulosic substances was eliminated after treatment with sodium hydroxide and $KMnO_4$, a phenomenon previously reported for sugar palm fiber [52, 53]. The peak at 1237 cm^{-1} indicates a significant reduction in the transmittance ratio of hemicelluloses, while the peak at 1024 cm^{-1} reflects an increase in the transmittance ratio of cellulose.

This demonstrates that the increase in cellulose content and the removal of hemicellulose and lignin from the two types of treated ESF support the findings from the chemical analysis [18, 54]. Therefore, the positions of the bands differ depending on the surveys [37, 49]. The peak wavenumbers in the FTIR spectrum and the assignment of the stretching vibrations to the chemical composition of ESF are summarized in Table IV.3.

Table IV. 3. Identification of peaks ATR-FTIR spectra of ESFs

Wave numbers (cm^{-1})	Vibrations mode(s)	Source(s)	References
3340	O–H stretching	Cellulose, Hemicelluloses	[55]
2862-2921	C–H stretching	Cellulose, Hemicelluloses	[37]
1732	C=O stretching	Hemicelluloses, lignin and extractives	[48]
1592	H–O–H bending of absorbed water	Water	[37]
1457–1512	H–C–H bending of absorbed water	Cellulose	[56]
1325–1371	C–H stretching	Lignin compounds	[55]
1237	-COO stretching	Hemicelluloses	[53]
1158	C–O bridge stretching	Cellulose	[54]
1024	C–O–C bridge stretching	Cellulose, Hemicelluloses	[51]
898	ß-glycosidic linkage	Cellulose, hemicelluloses	[51]

IV. 3. 6. X-ray diffraction analysis

To further investigate the effect of chemical treatment on the crystalline phases of ES fibers, X-ray diffraction (XRD) analysis was conducted. This analysis revealed the crystallinity and structural characteristics of the ES fibers both before and after chemical treatment. Figure IV.7 illustrates the XRD pattern of the three types of ES fibers and the corresponding planes involved. Each sample displayed two peaks and one amorphous plane (I_{am}) [57]. For the R_{ESF}, the first peak

observed at 2θ = 16.55° corresponds to the overlapping (110) peak, which is attributed to hemicellulose [58], In contrast, the second high-intensity peak observed at 2θ = 22.04° corresponds to the primary (200) peak of cellulose [58], this is the crystalline peak. For the A_{ESF}, the first peak observed at 2θ = 16.32° corresponds to the overlapping (110) peak, while the second high-intensity peak at 2θ = 22.19° represents the primary (200) cellulose peak, which is the crystalline peak. Similarly, for the P_{ESF}, the first peak observed at 2θ = 16.84° represents the overlapping (110) peak, while the second high-intensity peak at 2θ = 22.17° corresponds to the primary (200) cellulose peak, which is the crystalline peak. The Iam values for R_{ESF}, A_{ESF}, and P_{ESF} are observed at the intensity minimum around 17.67°, 18.11°, and 17.69°, respectively [59-61].

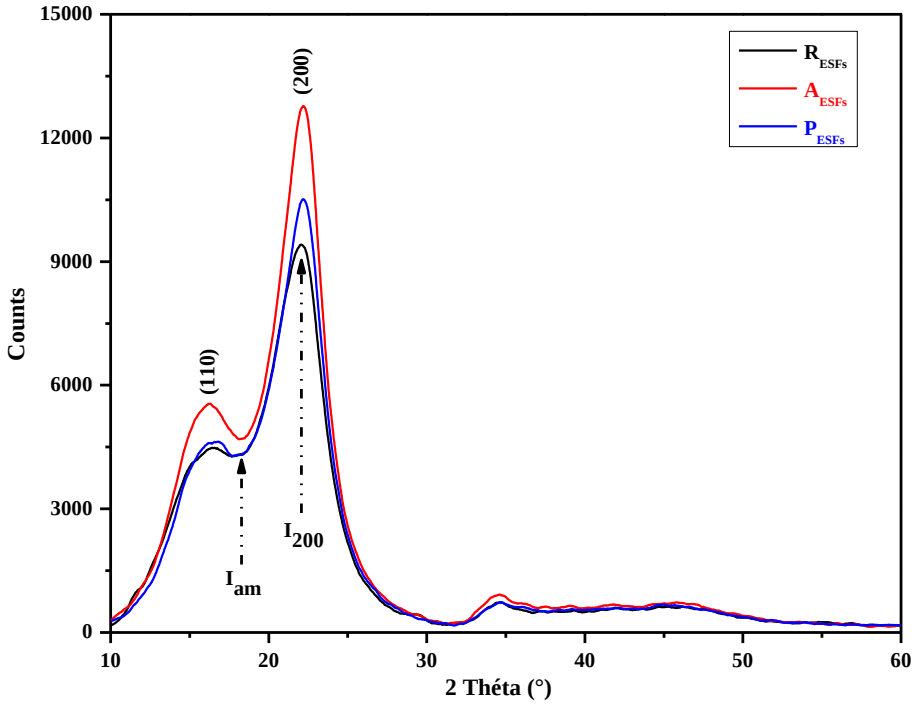

Figure IV. 7. XRD pattern of R_{ESFs}, A_{ESFs} and P_{ESFs}

The crystallinity index (CI) was highest for A_{ESF} fibers (63.28%), followed by P_{ESF} fibers (59.29%) and R_{ESF} fibers (54.64%). It was demonstrated that chemically treated fibers, with alkali and permanganate, exhibited superior performance compared to the untreated fibers [62-64]. The higher index is attributed to the elimination of amorphous components and non-cellulosic materials [55], enhanced hydrogen bonding network, better packing of cellulose chains, rearrangement of crystalline regions, and loss of hydrophilic character [65-67].

This result aligns with the morphology observed in SEM, where impurities from the fibers were removed through chemical treatment. The crystallinity index (CI) of the ESF from all three types is higher than that of Juncus effusus L, Grewia tilifolia, Pongamia Pinnata, and Sahara Aloe

vera fibers, respectively 33,4 %[68], 41.70% [69], 45.31% [70] and 52.6% [71]. A comparison of the crystallinity properties of ES fibers with other natural fibers is given in Table IV.4.

Table IV. 4. Comparison of ES fibers with other cellulosic fibers for crystallinity properties and thermal stability

Fibers	Crystallinity index %	Thermal stability (C°)	References
R_{ESFs}	54.64	190	
A_{ESFs}	63.28	203	Current study
P_{ESFs}	59.29	208	
InV	54.25	200	Moussaoui et al. [3]
Chrysanthemum morifolium	65.18	267.5	Dalmis et al. [72]
Pongamia Pinnata	45.31	210	Umashankaran et al. [70]
Albizia Lebbeck	52.99	-	Manimaran et al. [19]
Epipremnum aureum	49.33	-	Maheshwaran et al. [73]
Vachellia farnesiana	13	165	Vijay et al. [29]
Elettaria Cardamomum	36.84	230	Javeed et al. [74]
Centaurea Melitensis	47.69	210	Khaldoune et al. [7]
Areca catechu L	57.35	240	Binoj et al. [75]
Silybum marianum	45	225	Laifa et al. [76]

IV. 3. 7. Thermogravimetric analysis (TGA)

Thermogravimetric analysis are carried out to be able to study the influence of treatments on the thermal stability of the reinforcements (Table IV.4) which is an essential characteristic in biocomposites [46]. To simplify reading, it is convenient to represent the derived curve DTG of the ATG. This curve makes it easier to recognize mass loss phenomena since they appear in the form of peaks.

Figure IV. 8 (a) shows the TG/DTG curves of the R_{ESF}, with two stages of weight loss observed. The initial weight loss (6.07%) occurred between 29°C and 166°C, which is attributed to the evaporation of water [42, 72, 77]. The second weight loss (89.97%) was observed between 190°C and 403°C, with a maximum decomposition rate at 310°C. This weight loss corresponds to the decomposition of cellulose I and α-cellulose [46]. The weight loss continued up to 700°C, reaching a loss rate of approximately 97.60%. Figure IV. 8 (b) presents the TG/DTG curves of the A_{ESF}, showing two stages of weight loss. The initial weight loss (6.52%) was similar to that of the R_{ESF}, occurring between 30°C and 173°C, and corresponds to the evaporation of water [77]. The second weight loss (81%) was observed between 203°C and 365°C, with a maximum decomposition rate at 295°C. This weight loss corresponds to the degradation of the cellulosic components [78]. The weight loss continued up to 700°C, reaching a loss rate of approximately 96.37%. Figure IV.8 (c) then presents the TG/DTG curves of the P_{ESF}, showing two stages of

weight loss. The initial weight loss (4.72%) occurred between 39°C and 183°C, also corresponding to the evaporation of water [41, 77]. The second weight loss (81%) was observed between 208°C and 380°C, with a maximum decomposition rate at 287°C.

This loss rate corresponds to the degradation of the cellulosic components [78]. Subsequently, the weight loss continued up to 700°C, reaching a loss rate of approximately 94.30%.

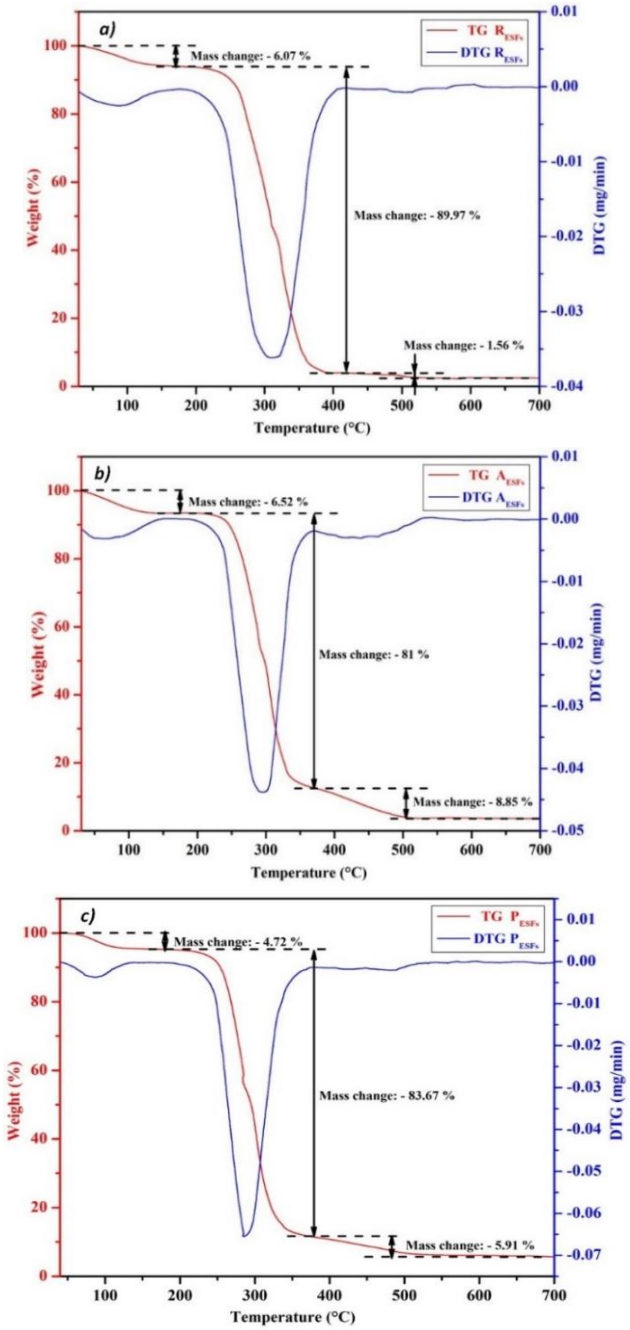

Figure IV. 8**.** Thermogravimetric curves (TG and DTG) of: a) R_{ESFs}, b) A_{ESFs} and c) P_{ESFs}

According to the thermal analysis, it was shown that the maximum decomposition temperature of the chemically treated fibers were higher than the maximum decomposition temperature of the raw fibers. Onset degradation temperature of R_{ESFs}, A_{ESFs} and P_{ESFs} were obtained to be 190°C, 203°C and 208°C, respectively. It was clearly showed that chemical treatment led to increase the onset degradation temperature of fibers by decreasing the relative content of hemicellulose [2, 79, 80].

Our results are consistent with other work. [81, 82]. From room temperature to higher temperatures up to 700°C, the degradation of lignin, which has a complex structure consisting of aromatic rings with various branches, may occur with a very minimal weight loss .The thermal stability of ES fibers is compared with that of other natural cellulosic fibers in Table (IV.4). It is deduced that the thermal characteristics of ESFs ensure its potential as a viable substitute material for the development of eco-friendly composites in both the manufacturing and automobile sectors.

IV. 3. 8. Tensile test on monofilament fibers

The study of the mechanical properties of polymer composites reinforced with natural fibers or textiles is crucial for understanding their potential for various structural applications and plays a key role in the decision to use natural fibers. Where mechanical tensile tests carried out on the treated and untreated ES fibers made it possible to obtain information on the force as a function of the fiber elongation [84]. This aims to illustrate the impact of chemical treatment on the mechanical behavior of the fibers [76].

Figure IV. 9 (a–c) Illustrates how stress changes with deformation for the successful samples with length of 40 mm of each fiber type. There were a number of samples broken during placing it on the tensile machine, highlighting variations in the behavior of individual fibers. These differences can be attributed to factors such as i) growth conditions, ii) climatic variables (harvest season, temperature, etc.) and iii) extraction methods and stages (retting, scutching, drying, treatments) [1]. Additionally, the characteristics of the tested fibers are influenced by their geometry [37].

Al of the curves of the three types of treated and untreated ES fibers have a quasi-linear behavior and are composed of two parts. The first is linear elastic, corresponding to the loading of the fiber. The alignment of twisted fibrils and the elongation of amorphous regions [85] affect it. Then the stress-strain curve enters a non-linear part during which the stress continues until the fiber breaks. According to the authors, this is due to the rearrangement of microfibrils [9, 86, 87].

We also observe the presence of small peaks for some fibers before total rupture, which are possibly due to the appearance of cracks in their structure [50, 88]. These cracks are due to the breakage of the microfibers constituting the Echinops spinosissimus fiber [89]. Indeed, the fibers are composed of tight cellulosic cells placed end to end and linked together by lignin and hemicellulose [16], and the breakage of the fibers begins with the breakage of the microfibers which make up their structure [90, 91].

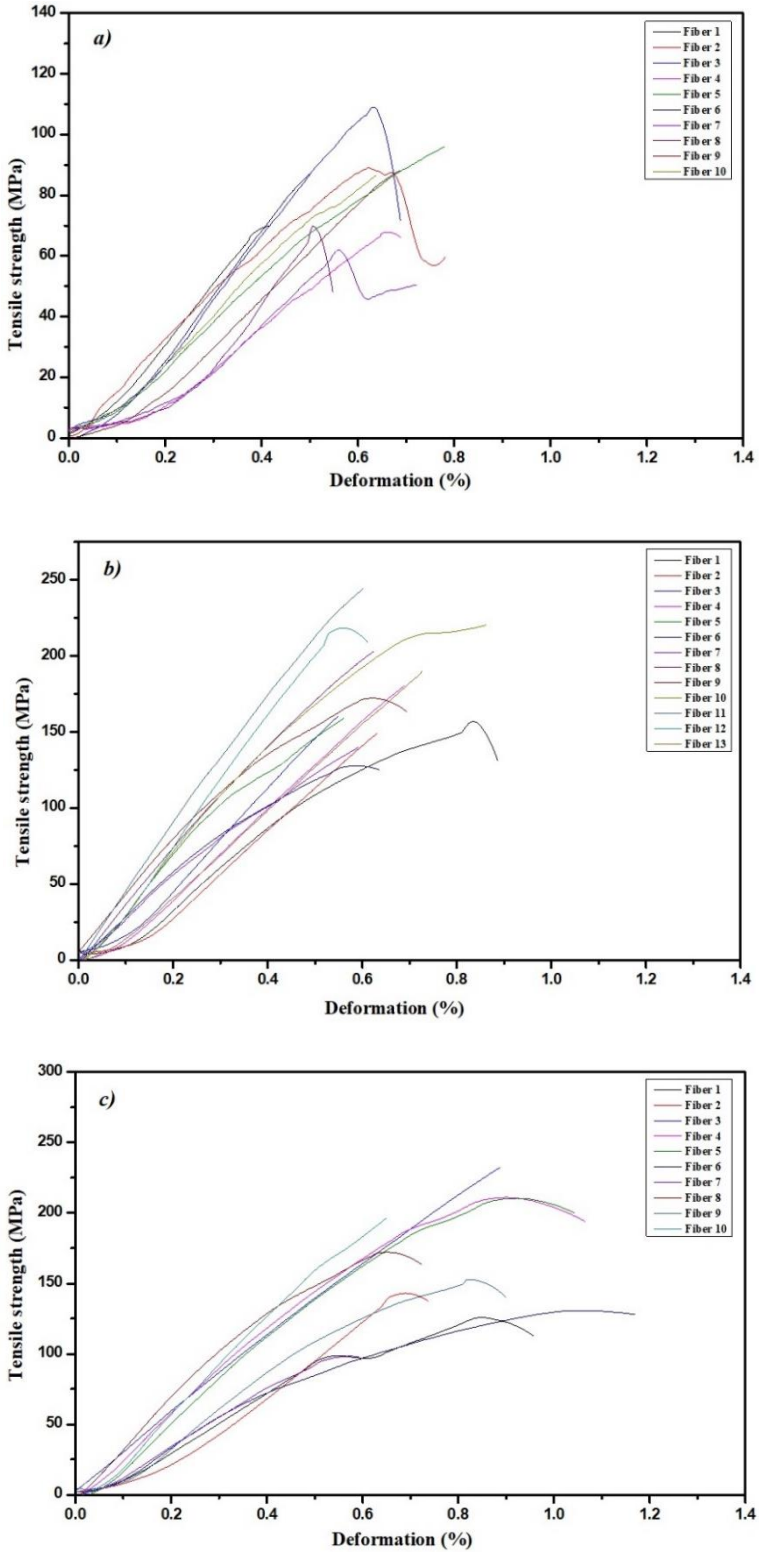

Figure IV. 9**.** Stress-strain curves: a) R_{ESFs}, b) A_{ESFs} and c) P_{ESFs}

In addition, Figure IV. 10. (a–c) represents histograms, which illustrate the variations in tensile strength, Young's modulus and strains at break of ES fibers, treated and untreated.

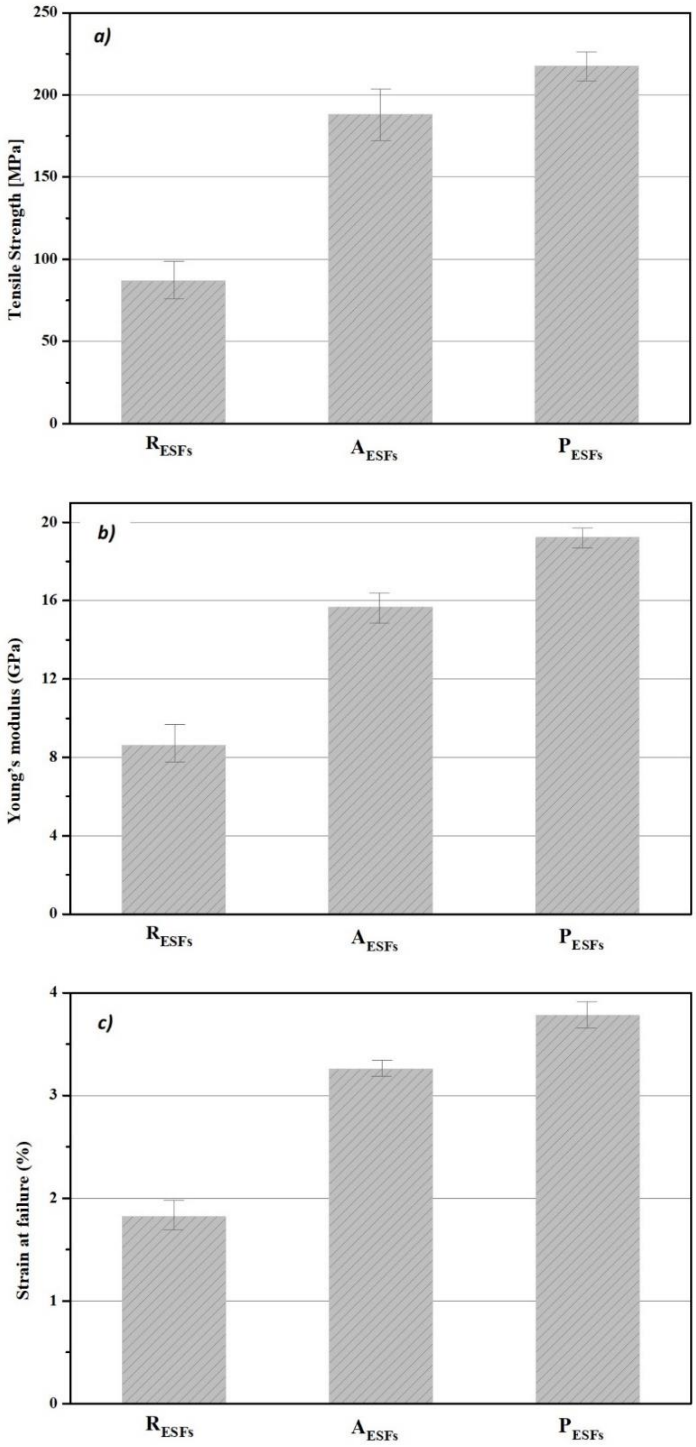

Figure IV. 10**.** Mechanical properties of R_{ESFs}, A_{ESFs} and P_{ESFs}: a) Tensile strength, b) Young's modulus and c) strain at failure

Figure IV. 10. (a) show a comparison of the tensile strength of the three types of 40 mm long ESF samples was conducted. As shown in the figure, the tensile strength increased for the A_{ESF} and P_{ESF} compared to the R_{ESF}, with respective values of 188.16 ± 36.28 MPa, 217.54 ± 54.16 MPa, and 87.09 ± 9.41 MPa. The increase in tensile strength for the chemically treated ESF is attributed to the removal of impurities from their surface and the enhancement of cellulose content [20]. Previous research indicates that the tensile strength values of plant fibers were comparable to those of ESFs, such as Stipa tenacissima (134 - 264 MPa) [25], Inula viscosa (196.99 MPa) [3], Atriplex halimus (64.31 - 229.26 MPa) [55], Date palm (170 - 275 MPa) [92] and Banana (222.3 MPa) [93]. Note that the tensile strength of ES is lower than that of Vakka (549 Mpa) [94] and Centaurea Melitensis (336.87 MPa) [7], and is superior to that of Kigelia africana (50 - 73 Mpa) [95] and Arundo donax (60 - 80 Mpa) [46].

Figure IV. 10. (b) presents the main values of Young's modulus of R_{ESF}, A_{ESF} and P_{ESF} fibers, which were respectively 8.63 ± 1,12 GPa, 15,68 ± 0,87 GPa et 19,23 ± 0,76 GPa. The tensile modulus of A_{ESF} and P_{ESF} was higher than that of R_{ESF} fibers. These values were quite similar to those of other plant fibers, such as banana fiber (8 to 20 GPa) [93] and sisal (6.7 - 21.7 GPa) [96]. The brittle nature of the material causes rapid collapse of the fibers due to the main components such as lignin, wax and hemicellulose [7]. However, after the chemical treatment of the ESF (alkaline and permanganate treatment), the mechanical properties were significantly improved, and the Young's modulus increased. This enhancement is attributed to the performance of the fibers, mainly resulting from the removal of stress-induced deformations of the non-cellulosic components [8].

Figure IV. 10. (c) presents the strain rates of the three types of ESFs. The deformation rates for R_{ESFs}, A_{ESFs}, and P_{ESFs} were 1.82 ± 0.28%, 3.26 ± 0.17%, and 3.78 ± 0.36%, respectively, which directly influenced the microfibril angle in the electrospun fibers. These findings are consistent with previous analyses, indicating that alkaline and permanganate treatments enhance both Young’s modulus and tensile strength [97, 98]. The results of mechanical tests confirmed that ESFs could be used as polymer reinforcement.

It can be said that the fiber treated with KMnO4 offers the best mechanical properties. It is followed by the fiber treated with NaOH, then lastly the untreated fiber. It can be concluded that the chemical treatment increases the mechanical properties of the ES fibers for a length of 40 mm tested as a result of impurities being eliminated from their surface.

Table IV.5. presents a comparison of physical and mechanical properties resulting from the tests of treated and untreated Echinops spinosissimus fibers with similar works in this area, namely: Density, Diameter, Résistance à la traction, module de Young et déformations à la rupture.

Table IV. 5. Comparison of physical and mechanical properties of ESFs with other cellulosic fibers.

Plant species	Density (g/cm^3)	Diameter (µm)	Tensile strength (MPa)	Young's modulus (GPa)	Strain at Failure (%)	References
Raw ESFs	0.8	336.52	87.09	8.63	1.82	Currentwork
Alkaline ESFs	0.93	305.34	188.16	15.68	3.26	
Permanganate ESFs	0.97	280.76	217.54	19.23	3.78	
Stippa tenacissima	0.89- 2.10	6 - 22	134 - 264	11 - 22	1.5 - 5.8	[25]
Hyphaene thebaica	1.36	165.81	215.98-593.35	12.79-24.29	1.51 - 2.92	[99]
Inula viscosa	78.60	1.154	196.99	12.98	1.57	[3]
Atriplex halimus	1.466	214 - 531	64.31 - 229.26	6.60 - 19.38	0.97 - 2.61	[55]
Lygeum spartum	-	180 - 433	64.63 - 280.03	4.47 - 13.27	1.49 - 3.74	[2]
Chrysanthemum m	1.336	-	65.12	1.55	4.51	[72]
Ficus religiosa tree	1.27	22.54	530.3	8.02	6.60	[42]
Arundo donax	1.168	-	60 - 80	3.6 - 4.0	2.5 - 3.5	[46]
Phaseolus vulgaris	0.96	345	523	10.64	1.63	[100]
Vakka	-	-	549	15.85	3.46	[94]
Date palm	-	-	170 - 275	5 - 12	5 - 10	[92]
Albizia lebbeck	0.90	-	270	67.45	2.57	[19]
Centaurea Melitensis	1.269	187.11	336.87	23.87	1.27	[7]
Strelitzia reginae	1.075	170	269.45	12.30	3.43	[37]
Kigelia africana	1.31	0.50 - 0.62	50.31 - 73.12	2.17 - 39.84	0.15 - 2.98	[95]
Sansevieria cylindrica	0.915	-	673.12	6.72	10.04	[20]
Vachellia farnesiana	1.270	231	33.075	-	-	[101]
Thespesia lampas	-	-	573	61.2	0.79	[47]
Prosopis juliflor	0.58	20	558	-	1.77	[77]
Furcraea foetida	0.77	12.8	612.43	6.44	10.45	[97]
Banana	-	0.17 - 0.21	222.3	6.6	3.27	[93]

A fairly large and significant dispersion of the diameters of the ES fibers tested as shown in (Figure IV. 11. a and b), as well as the values of the mechanical properties obtained. These dispersions whose values obtained can be due according to the previous researches: (i) to the measurement of its section [91]. (ii) to the experimental conditions (precision of the instrumentation, speed of deformation and type machine jaws) [70, 72] and (iii) the characteristics of the fiber (Age, orientation angle of the fibrils, difference in crystallization of cellulose in locations in the plant and ……) [73].

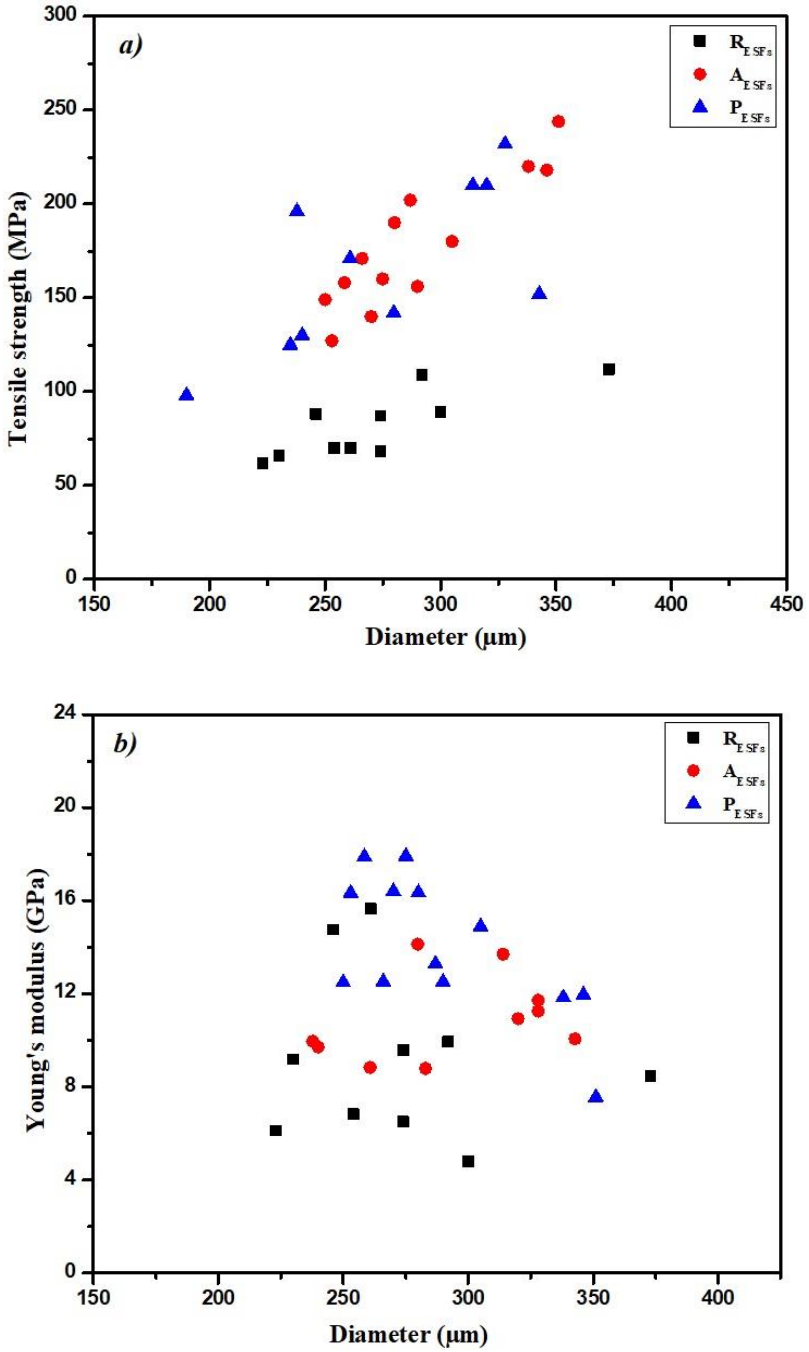

Figure IV. 11**.** Curves of: a) Tensile strength- diameter and b) Young's modulus- diameter

IV. 3. 9. Micromechanical analysis by Micro-droplet (Pull-out test)

This work evaluated the decohesion strength between ES fiber and epoxy resin by microdroplet test. The data of these tests is presented in the curves of Figure IV. 12 and in the form of a histogram in Figure IV. 13

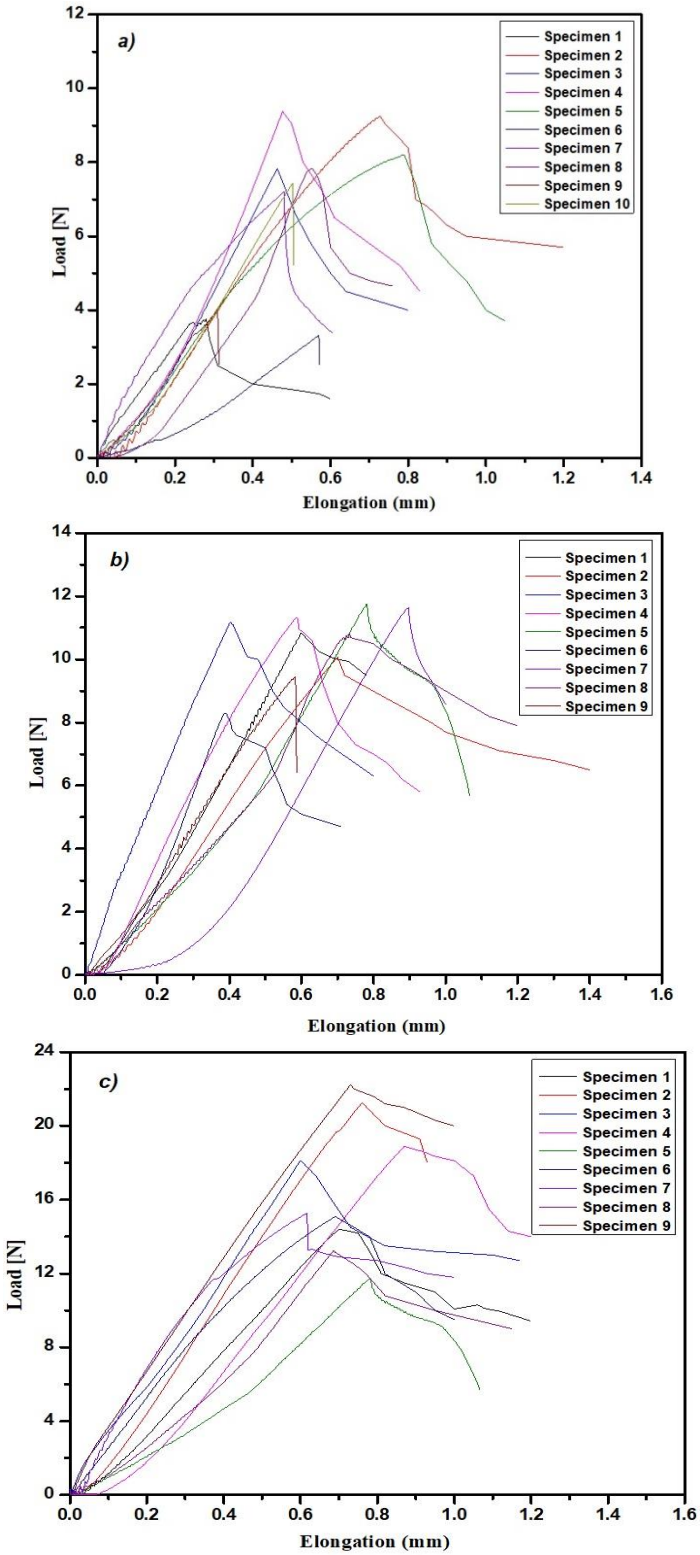

Figure IV. 12**.** Stress-strain curves of the epoxy micro-droplet on the fibers: a) R_{ESFs}, b) A_{ESFs} c) and P_{ESFs}

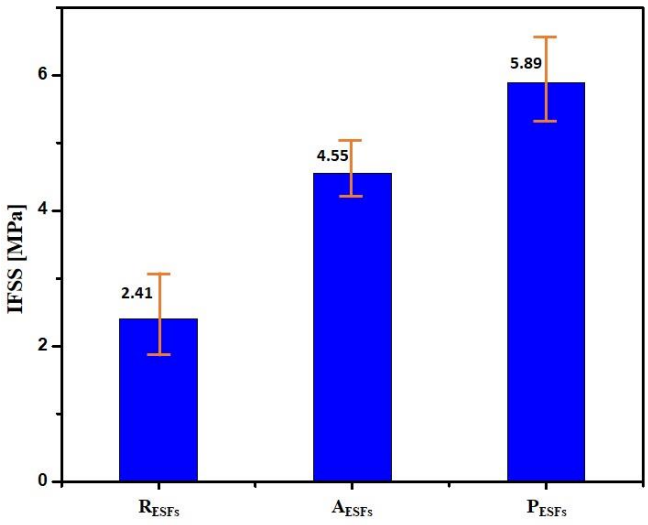

Figure IV. 13. Histogram of IFSS properties of Epoxy micro-droplet on R_{ESFs}, A_{ESFs} and P_{ESFs}

All samples have shown similar behavior when extraction of the fiber. A Type load-landing curve is given in Figure IV. 12. We see from this curve that the force increases almost linearly until a maximum value, and then decreases to the lower level of the friction load. After reaching the maximum load, the interfacial rupture occurs between the fiber and the droplet.

Between the matrix and the fiber, a certain load of friction is maintained (sliding) during the test of the drop-off (dropout) along the fiber [102]. Unlike other fiber pull -ups, this technique makes it possible to determine the tangential constraint (IFSS) once the fiber is offset by force (Fd).

IFSS is calculated from the results of the tests by equation III.9. The diameter of the fibers, the size of the droplets, the Young module of the matrix and the residual constraints affect the level of membership and therefore the value of IFSS. The residual constraints have a great effect in the initiation of the rupture, which is one of the reasons why so many fibers are broken. It should be noted that apparent grip strength measured with micro-drop tests varies considerably. The dimension of ES fibers that have different diameters causes this variability. The micro-drop test mechanism showed that when the force required for pulling is too high, the fiber breaks easily.

From the results obtained, the highest IFSS (Interfacial Shear Strength) value is that of permanganate treated fiber with 5.89 ± 0.68 MPa, followed by that of alkali treated fiber, and at the end the untreated ES fiber with 4.55 ± 0.43 MPa and 2.41 ± 0.72 MPa, respectively.

Table IV.6. Summarizes the values of apparent interfacial shear strengths (IFSS) evaluated from relation IV.9 for the three types of fibers of Echinops spinosissimus.

Table IV. 6. Comparison of the physical and mechanical properties of ESFs with other cellulosic fibers.

Specimens	Number of specimens ±	τ (MPa)
R_{ESF} - Epoxy	10	2.41 ± 0.72
A_{ESF} - Epoxy	10	4.55 ± 0.43
P_{ESF} - Epoxy	10	5.89 ± 0.68

The enhanced bonding between treated fibers and the matrix, in comparison to untreated fibers, can likely be attributed to improved wetting. This is associated with the removal of waxes that coat the outer surface of the fiber cell wall, thereby reinforcing it and improving stress transfer from the matrix to the fiber. Nevertheless, the main factor behind the increase in interfacial shear strength (IFSS) is the modification of the surface morphology.

As previously noted, chemical treatments caused the formation of surface cracks in a random pattern [103]. Therefore, the enhanced mechanical interaction resulting from surface irregularities is likely the primary factor contributing to the improvement in IFSS [104]. This effect was further enhanced by residual compressive stresses in the radial direction of the fiber, which are associated with matrix shrinkage around the fibers. The data obtained are comparable to the IFSS of Inula Viscosa, hemp and sisal [3, 105, 106]. In summary, we will say that the force required to detach treated Echinops Spinosissimus fibers/epoxy is greater than the force required to detach untreated Echinops Spinosissimus fibers /epoxy.

IV. 3. 10. Analysis of tensile test on a single fiber fragmentation

To study the contribution of chemical treatments of ES fibers, the influence of reinforcement in composites and to judge whether the implementation method brings us back to homogeneous materials, we carried out the traction test on monofilament specimens developed according to the ASTM standard (D 638-03 type V). These composites, the method of preparation of which was described in Chapter III, use the three types of ES fibers (R_{ESFs}, A_{ESFs} and P_{ESFs}) as reinforcement with the Epoxy matrix.

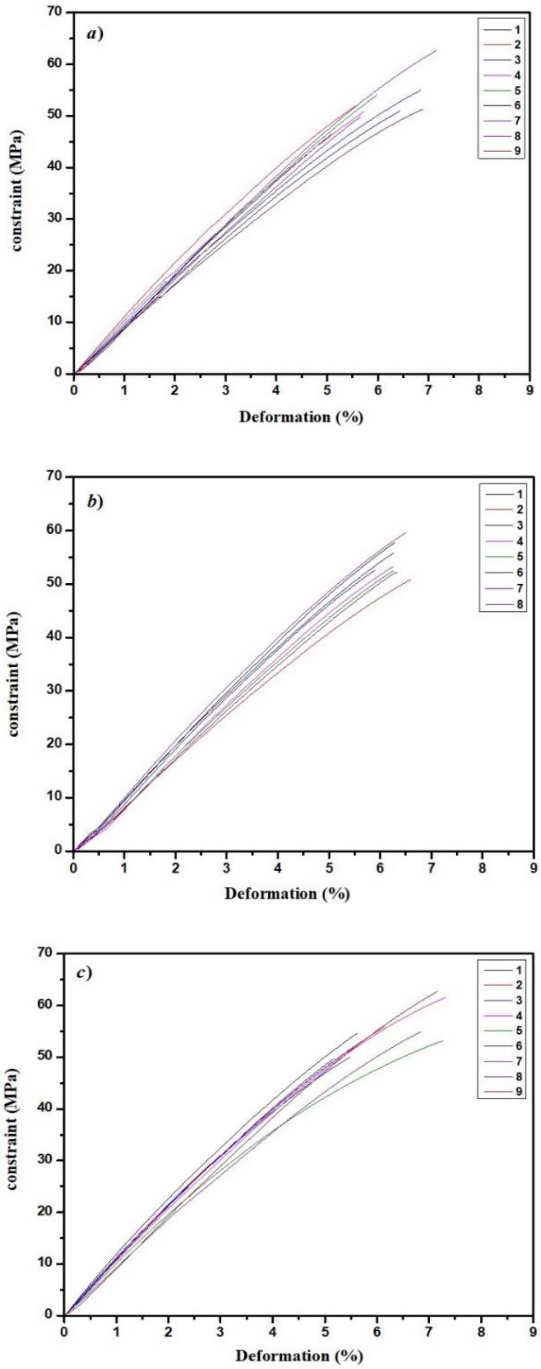

Figure IV. 14**.** Stress-strain curve of composites model: a) R_{ESF}/Epoxy, b) A_{ESF}/Epoxy and c) P_{ESF}/Epoxy.

Figure IV. 14 a), b) and c) respectively represent the curves of the evolution of the stress as a function of the deformation of the composites model with Epoxy resin tested in monotonic traction (fragmentation) in the direction of the fibers. The general appearance of the stress-strain curves for the specimens of each type of composite model shows that the latter gives an almost

non-linear behavior independently of the behavior of the fiber alone (treated or not). This is not the case of plastic deformation of ductile materials, but this curvature is due to microscopic damage such as matrix cracking, fiber breakage and fiber/matrix interfacial decohesion, which can occur at relatively high stresses [107].

This damage increases at different points of the monofilament composite, as the stress increases. They do not cause a direct break of the composite, but its strength gradually decreases. A similar aspect was presented by King, Julia A., et al.[108]. The attribution of this microscopic damage is probably influenced by the chemical treatments and this is surely due to the change in the affinity between the fiber and the matrix. Table Ⅳ.7, presents a comparison of mechanical properties resulting from fragmentation test where we see there is no big difference in values between the three types of model composites.

Table IV. 7. Comparison of single fiber fragmentation properties of three types of model composites ESF.

Composite Specimens (Average values)	R_{ESF}/ Epoxy	A_{ESF}/ Epoxy	P_{ESF}/ Epoxy
Deformation (%)	6.15 ± 0.67	6.30 ± 0.18	6.29 ± 0.81
Constraint (Mpa)	52.60 ± 4.24	54.38 ± 2.84	54.99 ± 4.32

The most representative images (photos) of the results obtained for the different tested specimens are presented below in Figure IV. 15

Figure IV. 15**.** Photographs of fracture facies of model composites: a) R_{ESF}, b) A_{ESF} and c) P_{ESF} with Epoxy matrix after the tensile test

Concerning the monofilament specimens without treatment in Figure IV. 15. a, ES fiber inside the specimen sometimes breaks towards the middle, this means that it divides into two length segments almost analogous, and no gradual fragmentation phenomenon is noticed for this series

of test specimens. From the photographic image in this Figure, we clearly see that no decohesion is visible at the fiber/matrix interface. The same observation for the case of monofilament composites Figure IV. 15. b and c treated with NaOH and $KMnO_4$. However, it appears that the resistance at the fiber/Epoxy interface is greater than the resistance of the fiber.

The breaking stress of the sample with an untreated fiber is almost the same value compared to that of samples, which contains a chemically treated fiber ($A_{ESF\ and}\ P_{ESF}$), such as mentions Table IV.7. The average stress values are close to each other for the ESF model composites. It was noted that the reinforcement of the matrix by monofibers (monofilament composite), whether treated or untreated, does not change the values of the mechanical characteristics.

IV. 3. 11. Analysis of tensile test on a composite reinforced by ES fibers (NFCs)

Investigating the mechanical characteristics of composites, particularly those strengthened with natural fibers (Figure IV. 16), is crucial for comprehending their suitability in various industries, especially diverse structural applications [109, 110]. The outcomes of mechanical tensile tests conducted on NFCs, reinforced with both treated and untreated ES fibers, provide valuable insights into the force dynamics relative to the elongation [111]. This investigation seeks to elucidate the influence of fiber chemical treatment on the mechanical behavior of NFCs [112].

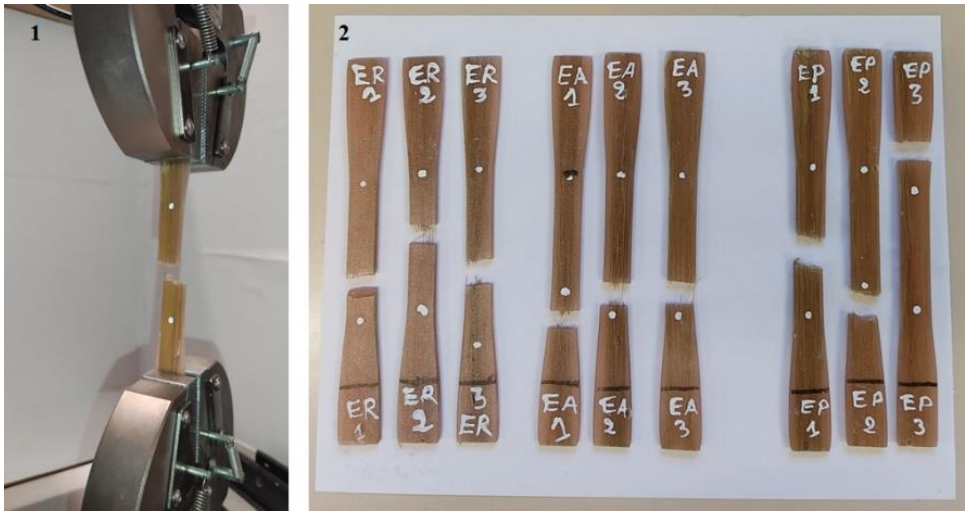

Figure IV. 16. Photographs of model composites **R_{ESF}**, **A_{ESF}** and **P_{ESF}** with Epoxy matrix after tensile test

Figure IV. 17. a), b) and c), illustrates how tensile load changes with elongation for the samples of each composite type. Al of the curves of the three types of NFCs have a quasi-linear behavior and are composed of two parts. The initial stage is linear elastic, corresponding to the loading of the composite. The mechanical properties of the composite are influenced by the position, orientation, and distribution of the fibers within the matrix, according to the authors, this is due to the rearrangement of reinforcement fibers [113-115]. Then the tensile load curve enters

a non-linear part during which the stress continues until the NFC samples breaks, the orange curve represents the average of the three sample curves for the three types of sample. Additionally, we note the presence of minor peaks in certain NFCs prior to complete rupture, likely attributable to the initiation of cracks in their structure.

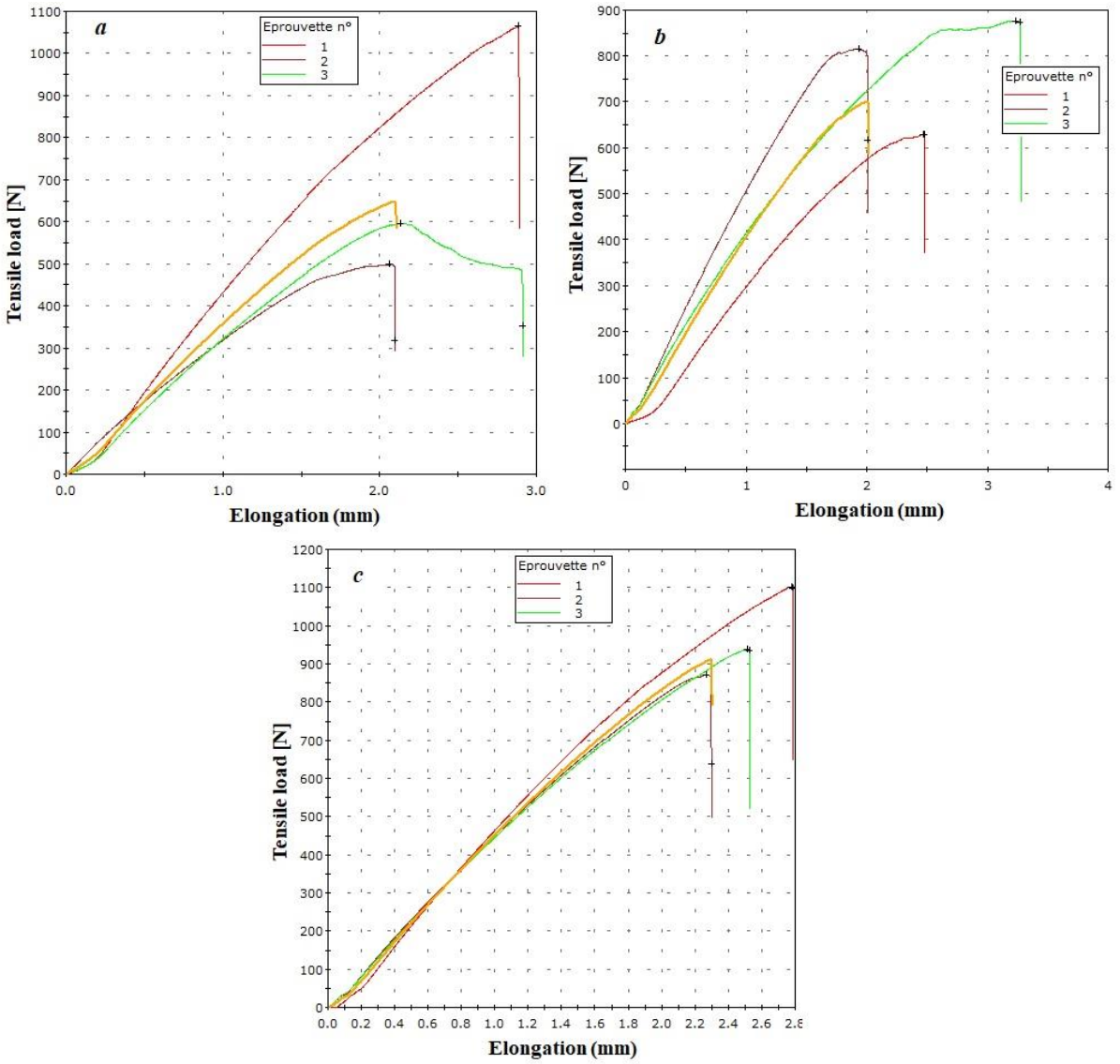

Figure IV. 17**.** Tensile load curves: a) R_{ESFs}, b) A_{ESFs} and c) P_{ESFs}

Figure IV. 18. Represents histogram, which illustrate the variations in tensile strength at break of NFCs reinforced by ES fibers, treated and untreated. This figure compares the tensile strength of the three types of NFC samples. As illustrated, the tensile strength was greater for NFC3 and NFC2 compared to NFC1 with values of 18.81 ± 1.28 MPa, 16.36 ± 1.16 MPa and

15.03 ± 1.45 MPa, respectively. The higher values of tensile strength of NFCs reinforced by chemically treated ESFs is due to the improvement of their mechanical properties.

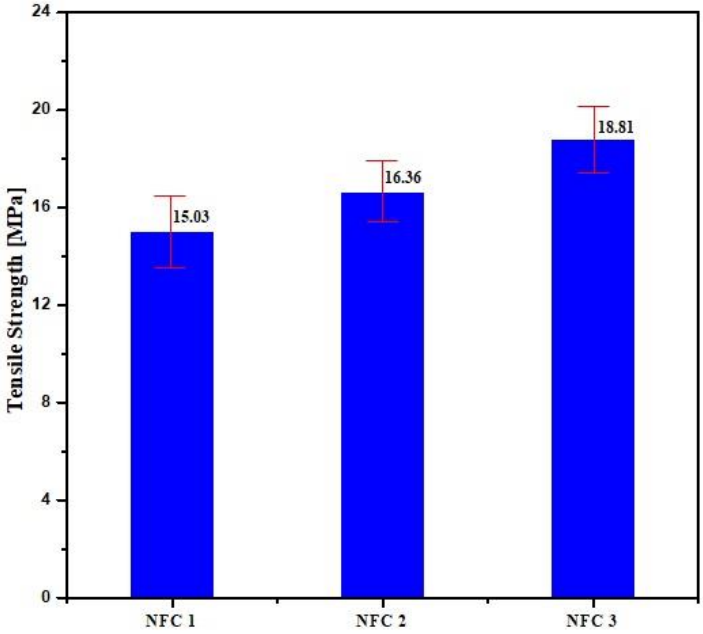

Figure IV. 18**.** Tensile strength histogram of NFCs (1, 2 and 3)

It can be said that the NFCs reinforced by ES fibers treated with KMnO4 offers the best mechanical properties. It is followed by the NFCs reinforced by ES fibers treated with NaOH, and then lastly the NFCs reinforced by untreated ES fibers. It can be concluded that chemical treatment of reinforcing fibers increases the mechanical properties of NFCs.

References

[1] S. A. Zernadji, M. Rokbi, M. Benhamida, and A. Kellai, "Extraction and characterization of novel natural cellulosic fiber from Echinops spinosissimus plant stem," *Journal of Composite Materials,* vol. 57, pp. 4503-4519, 2023.

[2] Z. Belouadah, A. Ati, and M. Rokbi, "Characterization of new natural cellulosic fiber from Lygeum spartum L," *Carbohydrate polymers,* vol. 134, pp. 429-437, 2015.

[3] N. Moussaoui, M. Rokbi, H. Osmani, M. Jawaid, A. Atiqah, M. Asim, and L. Benhamadouche, "Extraction and characterization of fiber treatment Inula viscosa fibers as potential polymer composite reinforcement," *Journal of Polymers and the Environment,* vol. 29, pp. 3779-3793, 2021.

[4] J. N. Wood, "From plant extract to molecular panacea: a commentary on Stone (1763)'An account of the success of the bark of the willow in the cure of the agues'," *Philosophical Transactions of the Royal Society B: Biological Sciences,* vol. 370, p. 20140317, 2015.

[5] P. C. Hemmer and A. Hansen, "The distribution of simultaneous fiber failures in fiber bundles," 1992.

[6] H. Li and S. Shen, "The mechanical properties of bamboo and vascular bundles," *Journal of Materials Research,* vol. 26, pp. 2749-2756, 2011.

[7] A. Raouf KHALDOUNE and M. Rokbi, "Extraction and characterization of novel natural fiber from Centaurea melitensis plant," *Journal of Composite Materials,* vol. 57, pp. 913-928, 2023.

[8] M. Meddah, M. Rokbi, and M. Zaoui, "Extraction and characterization of novel natural lignocellulosic fibers from Malva sylvestris L," *Journal of Composite Materials,* vol. 57, pp. 897-912, 2023.

[9] H. Makri, M. Rokbi, M. Meddah, N. Belayachi, and A. Khaldoune, "Extraction and characterization of novel lignocellulosic fibers from Centaurea hyalolepis plant as a potential reinforcement for composite materials," *Journal of Composite Materials,* p. 00219983231184020, 2023.

[10] S. Carlquist, "Wood, bark, and pith anatomy of Old World species of Ephedra and summary for the genus," *Aliso: A Journal of Systematic and Floristic Botany,* vol. 13, pp. 255-295, 1992.

[11] D. Zou, D. Wang, Z. Chu, Z. Lv, and X. Fan, "Fiber-shaped flexible solar cells," *Coordination Chemistry Reviews,* vol. 254, pp. 1169-1178, 2010.

[12] R. W. Mathangadeera, E. F. Hequet, B. Kelly, J. K. Dever, and C. M. Kelly, "Importance of cotton fiber elongation in fiber processing," *Industrial Crops and Products,* vol. 147, p. 112217, 2020.

[13] H. J. Kim, C. M. Lee, K. Dazen, C. D. Delhom, Y. Liu, J. E. Rodgers, A. D. French, and S. H. Kim, "Comparative physical and chemical analyses of cotton fibers from two near isogenic upland lines differing in fiber wall thickness," *Cellulose,* vol. 24, pp. 2385-2401, 2017.

[14] M. Gao, J. L. Snider, H. Bai, W. Hu, R. Wang, Y. Meng, Y. Wang, B. Chen, and Z. Zhou, "Drought effects on cotton (Gossypium hirsutum L.) fibre quality and fibre sucrose metabolism during the flowering and boll-formation period," *Journal of Agronomy and Crop Science,* vol. 206, pp. 309-321, 2020.

[15] J. Cai, L. Zhang, J. Zhou, H. Li, H. Chen, and H. Jin, "Novel fibers prepared from cellulose in NaOH/urea aqueous solution," *Macromolecular Rapid Communications,* vol. 25, pp. 1558-1562, 2004.

[16] N. Reddy and Y. Yang, "Structure and properties of high quality natural cellulose fibers from cornstalks," *Polymer,* vol. 46, pp. 5494-5500, 2005.

[17] F. Delzendehrooy, M. Ayatollahi, A. Akhavan-Safar, and L. da Silva, "Strength improvement of adhesively bonded single lap joints with date palm fibers: Effect of type, size, treatment method and density of fibers," *Composites Part B: Engineering,* vol. 188, p. 107874, 2020.

[18] M. Rokbi, H. Osmani, A. Imad, and N. Benseddiq, "Effect of chemical treatment on flexure properties of natural fiber-reinforced polyester composite," *procedia Engineering,* vol. 10, pp. 2092-2097, 2011.

[19] P. Manimaran, K. Solai Senthil Kumar, and M. Prithiviraj, "Investigation of physico chemical, mechanical and thermal properties of the albizia lebbeck bark fibers," *Journal of Natural Fibers,* vol. 18, pp. 1151-1162, 2021.

[20] V. Sreenivasan, S. Somasundaram, D. Ravindran, V. Manikandan, and R. Narayanasamy, "Microstructural, physico-chemical and mechanical characterisation of Sansevieria cylindrica fibres–An exploratory investigation," *Materials & Design,* vol. 32, pp. 453-461, 2011.

[21] A. Beakou, R. Ntenga, J. Lepetit, J. Ateba, and L. Ayina, "Physico-chemical and microstructural characterization of “Rhectophyllum camerunense” plant fiber," *Composites Part A: Applied Science and Manufacturing,* vol. 39, pp. 67-74, 2008.

[22] A. R. Marques, P. S. de Oliveira Patrício, F. S. dos Santos, M. L. Monteiro, D. de Carvalho Urashima, and C. de Souza Rodrigues, "Effects of the climatic conditions of the southeastern Brazil on degradation the fibers of coir-geotextile: Evaluation of mechanical and structural properties," *Geotextiles and Geomembranes,* vol. 42, pp. 76-82, 2014.

[23] H. A. Khalil, M. S. Hossain, E. Rosamah, N. Azli, N. Saddon, Y. Davoudpoura, M. N. Islam, and R. Dungani, "The role of soil properties and it’s interaction towards quality plant fiber: A review," *Renewable and Sustainable Energy Reviews,* vol. 43, pp. 1006-1015, 2015.

[24] M. Kathirselvam, A. Kumaravel, V. Arthanarieswaran, and S. Saravanakumar, "Assessment of cellulose in bark fibers of Thespesia populnea: influence of stem maturity on fiber characterization," *Carbohydrate Polymers,* vol. 212, pp. 439-449, 2019.

[25] Z. Belouadah, A. Ati, M. Rokbi, A. Bezazi, and A. Imad, "Optimisation Des méthodes D’extraction Et Caractérisation Mécanique De La Fibre Alfa En Vue De Son Application Comme Renfort Des Matériaux Composites," *Journal of Materials, Processes and Environment,* vol. 2, pp. 51-57, 2014.

[26] L. Huang, Q. Wu, Q. Wang, and M. Wolcott, "Mechanical activation and characterization of micronized cellulose particles from pulp fiber," *Industrial Crops and Products,* vol. 141, p. 111750, 2019.

[27] B. Abdelhak, M. Noureddine, and M. Hacen, "Improvement of the Interfacial Adhesion Between Fiber and Matrix," *Mechanics & Mechanical Engineering,* vol. 22, 2018.

[28] C. Li, W. Guo, and T. Zhang, "Fiber initiation development in Upland cotton (Gossypium hirsutum L.) cultivars varying in lint percentage," *Euphytica,* vol. 165, pp. 223-230, 2009.

[29] R. Vijay, J. D. James Dhilip, S. Gowtham, S. Harikrishnan, B. Chandru, M. Amarnath, and A. Khan, "Characterization of natural cellulose fiber from the barks of vachellia farnesiana," *Journal of Natural Fibers,* vol. 19, pp. 1343-1352, 2022.

[30] S. Yurgartis, "Measurement of small angle fiber misalignments in continuous fiber composites," *Composites Science and Technology,* vol. 30, pp. 279-293, 1987.

[31] C. Gonzalez and J. LLorca, "Multiscale modeling of fracture in fiber-reinforced composites," *Acta materialia,* vol. 54, pp. 4171-4181, 2006.

[32] Z. Wu, K. H. Khayat, and C. Shi, "How do fiber shape and matrix composition affect fiber pullout behavior and flexural properties of UHPC?," *Cement and Concrete Composites,* vol. 90, pp. 193-201, 2018.

[33] Y. Li, H. Ma, Y. Shen, Q. Li, and Z. Zheng, "Effects of resin inside fiber lumen on the mechanical properties of sisal fiber reinforced composites," *Composites Science and Technology,* vol. 108, pp. 32-40, 2015.

[34] M. Kathirselvam, A. Kumaravel, V. Arthanarieswaran, and S. Saravanakumar, "Characterization of cellulose fibers in Thespesia populnea barks: Influence of alkali treatment," *Carbohydrate polymers,* vol. 217, pp. 178-189, 2019.

[35] T. Glozman, L. Bruckert, F. Pestilli, D. W. Yecies, L. J. Guibas, and K. W. Yeom, "Framework for shape analysis of white matter fiber bundles," *NeuroImage,* vol. 167, pp. 466-477, 2018.

[36] M. Cai, H. Takagi, A. N. Nakagaito, M. Katoh, T. Ueki, G. I. Waterhouse, and Y. Li, "Influence of alkali treatment on internal microstructure and tensile properties of abaca fibers," *Industrial Crops and Products,* vol. 65, pp. 27-35, 2015.

[37] N. Lemita, S. Deghboudj, M. Rokbi, F. M. L. Rekbi, and R. Halimi, "Characterization and analysis of novel natural cellulosic fiber extracted from Strelitzia reginae plant," *Journal of Composite Materials,* vol. 56, pp. 99-114, 2022.

[38] A. Valadez-Gonzalez, J. Cervantes-Uc, R. Olayo, and P. Herrera-Franco, "Effect of fiber surface treatment on the fiber–matrix bond strength of natural fiber reinforced composites," *Composites Part B: Engineering,* vol. 30, pp. 309-320, 1999.

[39] F. A. Allafi, M. S. Hossain, M. Shaah, J. Lalung, M. O. Ab Kadir, and M. I. Ahmad, "A review on characterization of sheep wool impurities and existing techniques of cleaning: industrial and environmental challenges," *Journal of Natural Fibers,* vol. 19, pp. 8669-8687, 2022.

[40] L. Yan, N. Chouw, L. Huang, and B. Kasal, "Effect of alkali treatment on microstructure and mechanical properties of coir fibres, coir fibre reinforced-polymer composites and reinforced-cementitious composites," *Construction and Building Materials,* vol. 112, pp. 168-182, 2016.

[41] R. Siva, T. Valarmathi, K. Palanikumar, and A. V. Samrot, "Study on a Novel natural cellulosic fiber from Kigelia africana fruit: Characterization and analysis," *Carbohydrate polymers,* vol. 244, p. 116494, 2020.

[42] D. Ravindran, S. B. SR, and S. Indran, "Characterization of surface-modified natural cellulosic fiber extracted from the root of Ficus religiosa tree," *International journal of biological macromolecules,* vol. 156, pp. 997-1006, 2020.

[43] C.-M. Popescu, P. T. Larsson, N. Olaru, and C. Vasile, "Spectroscopic study of acetylated kraft pulp fibers," *Carbohydrate polymers,* vol. 88, pp. 530-536, 2012.

[44] H. Zhang, R. Ming, G. Yang, Y. Li, Q. Li, and H. Shao, "Influence of alkali treatment on flax fiber for use as reinforcements in polylactide stereocomplex composites," *Polymer Engineering & Science,* vol. 55, pp. 2553-2558, 2015.

[45] V. Hospodarova, E. Singovszka, and N. Stevulova, "Characterization of cellulosic fibers by FTIR spectroscopy for their further implementation to building materials," *American journal of analytical chemistry,* vol. 9, pp. 303-310, 2018.

[46] V. Fiore, T. Scalici, and A. Valenza, "Characterization of a new natural fiber from Arundo donax L. as potential reinforcement of polymer composites," *Carbohydrate polymers,* vol. 106, pp. 77-83, 2014.

[47] K. O. Reddy, B. Ashok, K. R. N. Reddy, Y. Feng, J. Zhang, and A. V. Rajulu, "Extraction and characterization of novel lignocellulosic fibers from Thespesia lampas plant," *International Journal of Polymer Analysis and Characterization,* vol. 19, pp. 48-61, 2014.

[48] S. Indran, R. E. Raj, and V. Sreenivasan, "Characterization of new natural cellulosic fiber from Cissus quadrangularis root," *Carbohydrate Polymers,* vol. 110, pp. 423-429, 2014.

[49] K. Subramanian, P. S. Kumar, P. Jeyapal, and N. Venkatesh, "Characterization of ligno-cellulosic seed fibre from Wrightia Tinctoria plant for textile applications—an exploratory investigation," *European Polymer Journal,* vol. 41, pp. 853-861, 2005.

[50] I. M. De Rosa, J. M. Kenny, D. Puglia, C. Santulli, and F. Sarasini, "Morphological, thermal and mechanical characterization of okra (Abelmoschus esculentus) fibres as potential reinforcement in polymer composites," *Composites Science and Technology,* vol. 70, pp. 116-122, 2010.

[51] R. Kumar, A. Meena, A. Chopra, and A. Kumar, "Keratin gene expression differences in wool follicles and sequence diversity of high glycine-tyrosine keratin-associated proteins (Kaps) in magra sheep of India," *Journal of Natural Fibers,* vol. 17, pp. 1257-1263, 2020.

[52] Z. Leman, E. S. Zainudin, and M. R. Ishak, "Effectiveness of alkali and sodium bicarbonate treatments on sugar palm fiber: mechanical, thermal, and chemical investigations," *Journal of Natural Fibers,* 2018.

[53] Z. Kovačević, S. B. Vukušić, and M. Zimniewska, "Comparison of Spanish broom (Spartium junceum L.) and flax (Linum usitatissimum) fibre," *Textile Research Journal,* vol. 82, pp. 1786-1798, 2012.

[54] A. Jabbar, J. Militký, J. Wiener, M. U. Javaid, and S. Rwawiire, "Tensile, surface and thermal characterization of jute fibres after novel treatments," *Indian Journal of Fibre & Textile Research (IJFTR),* vol. 41, pp. 249-254, 2016.

[55] Z. Belouadah, N. Belhaneche-Bensemra, and A. Ati, "Characterization of ligno-cellulosic fiber extracted from Atriplex halimus L. plant," *International Journal of Biological Macromolecules,* vol. 168, pp. 806-815, 2021.

[56] M. K. Hossain, M. W. Dewan, M. Hosur, and S. Jeelani, "Effect of surface treatment and nanoclay on thermal and mechanical performances of jute fabric/biopol 'green'composites," *Journal of Reinforced Plastics and Composites,* vol. 30, pp. 1841-1856, 2011.

[57] O. Ellefsen, E. W. Lund, B. Tønnesen, and K. Øien, "Studies on Cellulose Characterization by Means of X-ray Methods," *Norsk Skogind,* vol. 11, p. 284, 1957.
[58] A. D. French, "Idealized powder diffraction patterns for cellulose polymorphs," *Cellulose,* vol. 21, pp. 885-896, 2014.
[59] A. Isogai and R. Atalla, "Amorphous celluloses stable in aqueous media: regeneration from SO2–amine solvent systems," *Journal of Polymer Science Part A: Polymer Chemistry,* vol. 29, pp. 113-119, 1991.
[60] X. Ju, M. Bowden, E. E. Brown, and X. Zhang, "An improved X-ray diffraction method for cellulose crystallinity measurement," *Carbohydrate polymers,* vol. 123, pp. 476-481, 2015.
[61] D. R. del Cerro, T. V. Koso, T. Kakko, A. W. King, and I. Kilpeläinen, "Crystallinity reduction and enhancement in the chemical reactivity of cellulose by non-dissolving pre-treatment with tetrabutylphosphonium acetate," *Cellulose,* vol. 27, pp. 5545-5562, 2020.
[62] U. P. Agarwal, S. A. Ralph, C. Baez, and R. S. Reiner, "Contributions of crystalline and noncrystalline cellulose can occur in the same spectral regions: evidence based on Raman and IR and its implication for crystallinity measurements," *Biomacromolecules,* vol. 22, pp. 1357-1373, 2021.
[63] W. Yao, Y. Weng, and J. M. Catchmark, "Improved cellulose X-ray diffraction analysis using Fourier series modeling," *Cellulose,* vol. 27, pp. 5563-5579, 2020.
[64] A. D. French, "Increment in evolution of cellulose crystallinity analysis," *Cellulose,* vol. 27, pp. 5445-5448, 2020.
[65] A. D. French and M. Santiago Cintrón, "Cellulose polymorphy, crystallite size, and the Segal Crystallinity Index," *Cellulose,* vol. 20, pp. 583-588, 2013.
[66] A. Thygesen, J. Oddershede, H. Lilholt, A. B. Thomsen, and K. Ståhl, "On the determination of crystallinity and cellulose content in plant fibres," *Cellulose,* vol. 12, pp. 563-576, 2005.
[67] S. Park, J. O. Baker, M. E. Himmel, P. A. Parilla, and D. K. Johnson, "Cellulose crystallinity index: measurement techniques and their impact on interpreting cellulase performance," *Biotechnology for biofuels,* vol. 3, pp. 1-10, 2010.
[68] M. Maache, A. Bezazi, S. Amroune, F. Scarpa, and A. Dufresne, "Characterization of a novel natural cellulosic fiber from Juncus effusus L," *Carbohydrate polymers,* vol. 171, pp. 163-172, 2017.
[69] J. Jayaramudu, B. Guduri, and A. V. Rajulu, "Characterization of new natural cellulosic fabric Grewia tilifolia," *Carbohydrate polymers,* vol. 79, pp. 847-851, 2010.
[70] M. Umashankaran and S. Gopalakrishnan, "Effect of sodium hydroxide treatment on physico-chemical, thermal, tensile and surface morphological properties of pongamia Pinnata L. bark fiber," *Journal of Natural Fibers,* vol. 18, pp. 2063-2076, 2021.
[71] A. Balaji and K. Nagarajan, "Characterization of alkali treated and untreated new cellulosic fiber from Saharan aloe vera cactus leaves," *Carbohydrate Polymers,* vol. 174, pp. 200-208, 2017.
[72] R. Dalmis, G. B. Kilic, Y. Seki, S. Koktas, and O. Y. Keskin, "Characterization of a novel natural cellulosic fiber extracted from the stem of Chrysanthemum morifolium," *Cellulose,* vol. 27, pp. 8621-8634, 2020.

[73] M. Maheshwaran, N. R. J. Hyness, P. Senthamaraikannan, S. Saravanakumar, and M. Sanjay, "Characterization of natural cellulosic fiber from Epipremnum aureum stem," *Journal of Natural Fibers,* vol. 15, pp. 789-798, 2018.

[74] J. Ahmed, M. Balaji, S. Saravanakumar, and P. Senthamaraikannan, "A comprehensive physical, chemical and morphological characterization of novel cellulosic fiber extracted from the stem of Elettaria cardamomum plant," *Journal of Natural Fibers,* vol. 18, pp. 1460-1471, 2021.

[75] J. Binoj, R. E. Raj, V. Sreenivasan, and G. R. Thusnavis, "Morphological, physical, mechanical, chemical and thermal characterization of sustainable Indian areca fruit husk fibers (Areca catechu L.) as potential alternate for hazardous synthetic fibers," *Journal of Bionic Engineering,* vol. 13, pp. 156-165, 2016.

[76] F. Laifa, M. Rokbi, S. Amroune, M. Zaoui, and Y. Seki, "Investigation of mechanical, physicochemical, and thermal properties of new fiber fromSilybum marianumbark fiber," *Journal of Composite Materials,* vol. 56, pp. 2227-2238, 2022.

[77] S. Saravanakumar, A. Kumaravel, T. Nagarajan, P. Sudhakar, and R. Baskaran, "Characterization of a novel natural cellulosic fiber from Prosopis juliflora bark," *Carbohydrate polymers,* vol. 92, pp. 1928-1933, 2013.

[78] A. Shebani, A. Van Reenen, and M. Meincken, "The effect of wood extractives on the thermal stability of different wood species," *Thermochimica Acta,* vol. 471, pp. 43-50, 2008.

[79] N. Mohanta and S. Acharya, "Fiber surface treatment: Its effect on structural, thermal, and mechanical properties of Luffa cylindrica fiber and its composite," *Journal of composite materials,* vol. 50, pp. 3117-3131, 2016.

[80] B. G. Babu, D. Princewinston, S. Saravanakumar, A. Khan, P. Aravind Bhaskar, S. Indran, and D. Divya, "Investigation on the physicochemical and mechanical properties of novel alkali-treated phaseolus vulgaris fibers," *Journal of Natural Fibers,* vol. 19, pp. 770-781, 2022.

[81] R. Siakeng, M. Jawaid, H. Ariffin, and M. S. Salit, "Effects of surface treatments on tensile, thermal and fibre-matrix bond strength of coir and pineapple leaf fibres with poly lactic acid," *Journal of Bionic Engineering,* vol. 15, pp. 1035-1046, 2018.

[82] M. Kabir, H. Wang, K. Lau, and F. Cardona, "Tensile properties of chemically treated hemp fibres as reinforcement for composites," *Composites Part B: Engineering,* vol. 53, pp. 362-368, 2013.

[83] A. Khan, R. Vijay, D. L. Singaravelu, M. Sanjay, S. Siengchin, F. Verpoort, K. A. Alamry, and A. M. Asiri, "Characterization of natural fibers from Cortaderia selloana grass (pampas) as reinforcement material for the production of the composites," *Journal of Natural Fibers,* vol. 18, pp. 1893-1901, 2021.

[84] S. Alix, E. Philippe, A. Bessadok, L. Lebrun, C. Morvan, and S. Marais, "Effect of chemical treatments on water sorption and mechanical properties of flax fibres," *Bioresource technology,* vol. 100, pp. 4742-4749, 2009.

[85] P. Madhu, M. Sanjay, M. Jawaid, S. Siengchin, A. Khan, and C. I. Pruncu, "A new study on effect of various chemical treatments on Agave Americana fiber for composite

reinforcement: Physico-chemical, thermal, mechanical and morphological properties," *Polymer Testing,* vol. 85, p. 106437, 2020.

[86] U. Mukhopadhyay and A. Mukherjee, "Density and X-ray diffraction studies of jute at different stages of growth," *Textile Research Journal,* vol. 47, pp. 224-227, 1977.

[87] M. Abdullahi and D. Samson, "Effect of metakaolin on the strength properties of sisal fibre reinforced concrete," *Current Journal of Applied Science and Technology,* vol. 25, pp. 1-12, 2017.

[88] M. Maalej, V. C. Li, and T. Hashida, "Effect of fiber rupture on tensile properties of short fiber composites," *Journal of engineering mechanics,* vol. 121, pp. 903-913, 1995.

[89] C. Ostertag and C. Yi, "Crack/fiber interaction and crack growth resistance behavior in microfiber reinforced mortar specimens," *Materials and structures,* vol. 40, pp. 679-691, 2007.

[90] K. C. Mouli, N. Pannirselvam, V. Anitha, D. V. Kumar, and S. V. Rao, "Strength studies on banana fibre concrete with metakaolin," *Int. J. Civ. Eng. Technol,* vol. 10, pp. 684-689, 2019.

[91] A. Arul Marcel Moshi, D. Ravindran, S. Sundara Bharathi, V. Suganthan, and G. Kennady Shaju Singh, "Characterization of new natural cellulosic fibers–a comprehensive review," in *IOP Conference Series: Materials Science and Engineering*, 2019, p. 012013.

[92] A. Al-Khanbashi, K. Al-Kaabi, and A. Hammami, "Date palm fibers as polymeric matrix reinforcement: fiber characterization," *Polymer composites,* vol. 26, pp. 486-497, 2005.

[93] J. C. Mejía Osorio, R. Rodríguez Baracaldo, and J. J. Olaya Florez, "The influence of alkali treatment on banana fibre's mechanical properties," *Ingeniería e investigación,* vol. 32, pp. 83-87, 2012.

[94] K. M. M. Rao and K. M. Rao, "Extraction and tensile properties of natural fibers: Vakka, date and bamboo," *Composite structures,* vol. 77, pp. 288-295, 2007.

[95] M. Ilangovan, V. Guna, B. Prajwal, Q. Jiang, and N. Reddy, "Extraction and characterisation of natural cellulose fibers from Kigelia africana," *Carbohydrate polymers,* vol. 236, p. 115996, 2020.

[96] A. Pappu, M. Saxena, V. K. Thakur, A. Sharma, and R. Haque, "Facile extraction, processing and characterization of biorenewable sisal fibers for multifunctional applications," *Journal of Macromolecular Science, Part A,* vol. 53, pp. 424-432, 2016.

[97] P. Manimaran, P. Senthamaraikannan, M. Sanjay, M. Marichelvam, and M. Jawaid, "Study on characterization of Furcraea foetida new natural fiber as composite reinforcement for lightweight applications," *Carbohydrate polymers,* vol. 181, pp. 650-658, 2018.

[98] M. Noureddine, "Study of composite-based natural fibers and renewable polymers, using bacteria to ameliorate the fiber/matrix interface," *Journal of Composite Materials,* vol. 53, pp. 455-461, 2018.

[99] R. Mansour, A. Abdelaziz, and A. F. Zohra, "Characterization of long lignocellulosic fibers extracted from Hyphaene thebaica L. leaves," *Research Journal of Textile and Apparel,* 2018.

[100] B. Babu, D. Princewinston, S. Saravanakumar, A. Khan, P. Aravind Bhaskar, S. Indran, and D. Divya, "Investigation on the physicochemical and mechanical properties of novel alkali-treated Phaseolus vulgaris fibers. J Nat Fibers," ed, 2020.

[101] R. Vijay, S. Manoharan, S. Arjun, A. Vinod, and D. Singaravelu, "Characterization of silane-treated and untreated natural fibers from stem of Leucas aspera. J Nat Fibers," ed, 2020.
[102] U. Gaur and B. Miller, "Microbond method for determination of the shear strength of a fiber/resin interface: Evaluation of experimental parameters," *Composites science and technology,* vol. 34, pp. 35-51, 1989.
[103] S. Bouzouita, M. Salvia, H. Ben Daly, A. Dogui, and E. Forest, "Effect of fiber treatment on fiber strength and fiber/matrix interface of hemp reinforced polypropylene composites," *Advanced Materials Research,* vol. 112, pp. 1-8, 2010.
[104] X. Liu and G. Dai, "Surface modification and micromechanical properties of jute fiber mat reinforced polypropylene composites," *Express Polymer Letters,* vol. 1, pp. 299-307, 2007.
[105] J. Andersons, J. Modniks, R. Joffe, B. Madsen, and K. Nättinen, "Apparent interfacial shear strength of short-flax-fiber/starch acetate composites," *International Journal of Adhesion and Adhesives,* vol. 64, pp. 78-85, 2016.
[106] D. Pantaloni, A. L. Rudolph, D. U. Shah, C. Baley, and A. Bourmaud, "Interfacial and mechanical characterisation of biodegradable polymer-flax fibre composites," *Composites Science and Technology,* vol. 201, p. 108529, 2021.
[107] K. Charlet, "Contribution à l'étude de composites unidirectionnels renforcés par des fibres de lin: relation entre la microstructure de la fibre et ses propriétés mécaniques," Université de Caen/Basse-Normandie, 2008.
[108] J. A. King, D. R. Klimek, I. Miskioglu, and G. M. Odegard, "Mechanical properties of graphene nanoplatelet/epoxy composites," *Journal of applied polymer science,* vol. 128, pp. 4217-4223, 2013.
[109] R. D. Campilho, *Natural fiber composites*: CRC Press, 2015.
[110] T. Yashas Gowda, M. Sanjay, K. Subrahmanya Bhat, P. Madhu, P. Senthamaraikannan, and B. Yogesha, "Polymer matrix-natural fiber composites: An overview," *Cogent Engineering,* vol. 5, p. 1446667, 2018.
[111] M. Y. Khalid, A. Al Rashid, Z. U. Arif, W. Ahmed, H. Arshad, and A. A. Zaidi, "Natural fiber reinforced composites: Sustainable materials for emerging applications," *Results in Engineering,* vol. 11, p. 100263, 2021.
[112] A. C. Milanese, M. O. H. Cioffi, and H. J. C. Voorwald, "Mechanical behavior of natural fiber composites," *Procedia Engineering,* vol. 10, pp. 2022-2027, 2011.
[113] P. Herrera-Franco and A. Valadez-Gonzalez, "A study of the mechanical properties of short natural-fiber reinforced composites," *Composites Part B: Engineering,* vol. 36, pp. 597-608, 2005.
[114] F. Zicari, E. Coutinho, R. Scotti, B. Van Meerbeek, and I. Naert, "Mechanical properties and micro-morphology of fiber posts," *Dental Materials,* vol. 29, pp. e45-e52, 2013.
[115] A. Qaiss, R. Bouhfid, and H. Essabir, "Effect of processing conditions on the mechanical and morphological properties of composites reinforced by natural fibres," *Manufacturing of natural fibre reinforced polymer composites,* pp. 177-197, 2015

GENERAL CONCLUSION

General conclusion and perspectives

The uses of cellulose fibers and polymer matrix composites are increasing due to the multiple advantages they offer. However, these composites often face the problem of adhesion between plant fibers and polymer resins, due to the incompatibility between the components, which negatively affects the durability of these materials.

The main objective of this thesis is to contribute to the search for solutions to overcome the problem of incompatibility between plant fibers and epoxy matrix. The study addresses a set of aspects related to the preparation of materials based on renewable resources, as these materials in most cases require special treatment to clarify the effect of the interface interaction between the fibers and the matrix within the composite.

The reinforcement fibers used in our work are new fibers derived and extracted from the stems of the Echinops spinosissimus plant by a biological retting technique with fresh water. This plant (ES) constitutes an abundant plant wealth in Algeria. For the reinforcement of the polymer matrix (Epoxy), the ES fibers underwent chemical treatments in order to reduce their hydrophilic character. In addition, two types of treatment are chosen: The first is an alkaline treatment by NaOH and the second is the treatment by potassium permanganate (KMnO4). The highlighting of the modification was examined by microstructural analysis FTIR, XRD and the impact of the treatments on the mechanical and micromechanical properties of the materials were also studied. The effect of the treatments applied and the implementation techniques were studied on the three levels of the composite material; the fiber, the interface and the overall composite.

Through the results obtained, it was shown that:

• ES fiber is characterized by a density of 0.97 g/cm3 and a diameter of 280.76 μm, which favors the use of this fiber as an alternative material for lightweight composite applications. It was noted that the two chemical treatments with NaOH and KMnO4 allowed increasing the density compared to that of the untreated fiber. This increase is due to the elimination of non-cellulosic materials and the fullness of pores and voids in the fibers surface during the treatment, which allow the cellulose microfibrils to come closer together. In other hand decrease the diameter compared to that of the untreated fiber

• Scanning electron microscope observations showed an improvement in the quality of ES fibers after chemical treatments were used. The fiber became cleaner, with a rougher surface, because the waxes, and oils removed from the fiber surface were eliminated by these treatments. This rough surface can improve wettability or adhesion when (ES) fibers are used as reinforcing materials.

• Infrared results showed that the chemical structure of the cell wall of ES fibers was modified by both chemical treatments. A difference in peak intensity was noted, depending on the type and time of treatment. The two peaks at 1237 cm-1 and 1732 cm-1 observed on the spectrum of untreated ES fibers, which correspond to hemicelluloses, disappeared from the spectrum of permanganate and alkali treated fibers. This result could be explained by the degradation of residual hemicellulose materials after treatments.

• X-ray analysis showed an improvement in the crystallinity index (CI) of the ES fiber after treatments. The alkali treated fibers have the highest CI of 63.28%. Followed by the permanganate treated fibers that have the CI of 59.29%. Lastly the CI of the untreated ES fibers, which are 54.64%. The increase in ES fiber CI with alkali and permanganate treatments reduce their chemical reactivity and water absorption capacity. This increase in CI is explained by a weakening of the cellulose chains causing the disappearance of excess amorphous constituents, such as lignin, hemicellulose. This result was in agreement with the results in infrared (FTIR), where the impurities of the fiber are eliminated by chemical treatment.

• The results of the tensile tests of ES fibers clearly show that the chemical treatment with KMnO4 and NaOH leads to a significant increase in mechanical properties compared to the ES fibers without treatment (breaking stress and Young's modulus with a low influence on deformations).

• To experimentally characterize the fiber/matrix interface, the droplet shedding test is chosen as a characterization method, however, an implementation can be difficult.

The permanganate-treated fibers showed the best interfacial strengths (IFSS) of 5.89 MPa, followed by the NaOH-treated fibers of 4.55 MPa. And lastly the untreated fibers with a value equal to 2.41 MPa. This benefit is attributed to the increase in adhesion at the fiber/resin interface by the chemical treatments.

• The analysis of the mechanical characteristics of the ESF/Epoxy monofilament composites using the tensile test allowed finding different trends than during the tensile test for the fibers or the micromechanical study of the interfaces by micro-drop. The three types of composite present almost the same breaking stress with a value of 54 MPa. The fracture facies of the model composites observed by photography, after tensile failure, showed a better adhesion for the three types of model composites.

• The analysis of the mechanical characteristics of composite (NFCs) reinforced with both treated and untreated ES fibers using the tensile test allowed finding same trends than during the tensile test for the fibers or the micromechanical study of the interfaces by micro-drop. NFC3 (P_{ESFs}/Epoxy) exhibited the best fracture stress with a value of 18.81±1.28 MPa. The fracture surfaces of the model composites observed by photography, after tensile failure, showed a better adhesion for the three types of NFC.

This research has shown the consequence of chemical treatments on the characteristics of the plant fibers of the ES, which are valued for the first time. We were interested in studying composites with plant and epoxy reinforcement at four scales; the fiber, the interface, the monofilament composite and then the multi-fiber composite (NFCs).

However, many study works remain to be accomplished all around this axis for a better discernment of this type of composites and the improvement of the methods of treatment and implementation.

A first perspective is to try other chemical treatments such as silane and acetylation to minimize the hydrophilic effect of the fibers in order to obtain a better compatibility between fiber and matrix. Second perspective is to analyze the interface with other micromechanical techniques

such as indentation. Finally, the third perspective is to make a comparison between thermosetting and thermoplastic matrices in ES fiber composites. This allows bettering understanding the mechanisms that manage the assembly of fibers and resins, which will contribute to a good and wide use of these materials.

This plant has several possible applications in various fields, whether in Medicine and phyto-therapy, Agriculture and agro-ecology, Landscaping and horticulture, Ecology and environmental restoration, Education and awareness of biodiversity and finally Craft and decorative products.

Cultivating Echinops spinosissimus plant means cultivating a sustainable future. It is not only an agricultural approach, but also an act in favor of environmental sustainability and biodiversity, with an emphasis on the long-term benefits of exploiting this resilient plant.

It would also be very important from an environmental point of view to combine the fibers with a resin from natural resources. This study topic is attracting more and more attention from researchers worldwide because of the maintenance of the environment and also for the richness of the biomass.

APPENDIX

SAFETY DATA SHEET
according to Regulation (EC) No. 1907/2006

HUNTSMAN
Enriching lives through innovation

ARALDITE® LY 564

Version	Revision Date:	SDS Number:	Date of last issue: 29.07.2022
1.2	01.12.2023	400001008622	Date of first issue: 11.10.2018

Print Date 03.04.2024

SECTION 1: Identification of the substance/mixture and of the company/undertaking

1.1 Product identifier

Trade name : ARALDITE® LY 564

Unique Formula Identifier (UFI) : 07XA-V0MJ-Q00M-C977

1.2 Relevant identified uses of the substance or mixture and uses advised against

Use of the Substance/Mixture : Epoxy resin solution

Recommended restrictions on use : For industrial use only.

1.3 Details of the supplier of the safety data sheet

Company : Huntsman Advanced Materials (Europe) BV
Address : Everslaan 45
3078 Everberg
Belgium
Telephone : +41 61 299 20 41
Telefax : +41 61 299 20 40

E-mail address of person responsible for the SDS : Global_Product_EHS_AdMat@huntsman.com

1.4 Emergency telephone number

Emergency telephone number : Centres Antipoison et de Toxicovigilance:
ANGERS: 02 41 48 21 21
BORDEAUX: 05 56 96 40 80
LILLE: 0 825 812 822
LYON: 04 72 11 69 11
MARSEILLE 04 91 75 25 25
NANCY: 03 83 32 36 36
PARIS: 01 40 05 48 48
RENNES: 02 99 59 22 22
STRASBOURG: 03 88 37 37 37
TOULOUSE: 05 61 77 74 47
EUROPE: +32 35 75 1234
France ORFILA: +33(0)145425959
ASIA: +65 6336-6011
China: +86 20 39377888
+86 532 83889090
India: + 91 22 42 87 5333
Australia: 1800 786 152
New Zealand: 0800 767 437
USA: +1 800-424-9300

SAFETY DATA SHEET
according to Regulation (EC) No. 1907/2006

HUNTSMAN
Enriching lives through innovation

ARALDITE® LY 564

Version	Revision Date:	SDS Number:	Date of last issue: 29.07.2022
1.2	01.12.2023	400001008622	Date of first issue: 11.10.2018

Print Date 03.04.2024

SECTION 2: Hazards identification

2.1 Classification of the substance or mixture

Classification (REGULATION (EC) No 1272/2008)

Skin irritation, Category 2	H315: Causes skin irritation.
Serious eye damage, Category 1	H318: Causes serious eye damage.
Skin sensitisation, Category 1	H317: May cause an allergic skin reaction.
Long-term (chronic) aquatic hazard, Category 2	H411: Toxic to aquatic life with long lasting effects.

2.2 Label elements

Labelling (REGULATION (EC) No 1272/2008)

Hazard pictograms :

Signal word : Danger

Hazard statements :
H315 Causes skin irritation.
H317 May cause an allergic skin reaction.
H318 Causes serious eye damage.
H411 Toxic to aquatic life with long lasting effects.

Precautionary statements :

Prevention:
P261 Avoid breathing mist or vapours.
P264 Wash skin thoroughly after handling.
P273 Avoid release to the environment.
P280 Wear protective gloves/ eye protection/ face protection.

Response:
P305 + P351 + P338 + P310 IF IN EYES: Rinse cautiously with water for several minutes. Remove contact lenses, if present and easy to do. Continue rinsing. Immediately call a POISON CENTER/ doctor.
P391 Collect spillage.

Hazardous components which must be listed on the label:
2,2'-[(1-methylethylidene)bis(4,1-phenyleneoxymethylene)]bisoxirane
1,4-bis(2,3 epoxypropoxy)butane

2.3 Other hazards

This substance/mixture contains no components considered to be either persistent, bioaccumulative and toxic (PBT), or very persistent and very bioaccumulative (vPvB) at levels of 0.1% or higher.

Ecological information: The substance/mixture does not contain components considered to have endocrine disrupting properties according to REACH Article 57(f) or Commission Delegated regulation (EU) 2017/2100 or Commission Regulation (EU) 2018/605 at levels of 0.1% or higher

Toxicological information: The substance/mixture does not contain components considered to have endocrine disrupting properties according to REACH Article 57(f) or Commission Delegated regulation (EU) 2017/2100 or Commission Regulation (EU) 2018/605 at levels of 0.1% or higher

SECTION 3: Composition/information on ingredients

3.2 Mixtures

Hazardous components

Chemical name	CAS-No. EC-No. Index-No. Registration number	Classification	Concentration (% w/w)
2,2'-[(1-methylethylidene)bis(4,1-phenyleneoxymethylene)]bisoxirane	1675-54-3 216-823-5 603-073-00-2 01-2119456619-26	Skin Irrit. 2; H315 Eye Irrit. 2; H319 Skin Sens. 1; H317 Aquatic Chronic 2; H411 specific concentration limit Skin Irrit. 2; H315 >= 5 % Eye Irrit. 2; H319 >= 5 %	>= 70 - < 90
1,4-bis(2,3 epoxypropoxy)butane	2425-79-8 219-371-7 603-072-00-7 01-2119494060-45	Acute Tox. 4; H302 Acute Tox. 4; H332 Acute Tox. 4; H312 Skin Irrit. 2; H315 Eye Dam. 1; H318 Skin Sens. 1; H317 Aquatic Chronic 3; H412 Acute toxicity estimate Acute dermal toxicity: 1 100 mg/kg	>= 10 - < 20

For explanation of abbreviations see section 16.

Both 25068-38-6 and 1675-54-3 can be used to describe the epoxy resin which is produced through the reaction of bisphenol A and epichlorohydrin

SAFETY DATA SHEET
according to Regulation (EC) No. 1907/2006

HUNTSMAN
Enriching lives through innovation

ARADUR® 3486 BD

Version	Revision Date:	SDS Number:	Date of last issue: 10.10.2018
1.2	22.05.2023	400001014180	Date of first issue: 08.09.2016

Print Date 03.04.2024

SECTION 1: Identification of the substance/mixture and of the company/undertaking

1.1 Product identifier

Trade name : ARADUR® 3486 BD

1.2 Relevant identified uses of the substance or mixture and uses advised against

Use of the Substance/Mixture : Hardener

1.3 Details of the supplier of the safety data sheet

Company : Huntsman Advanced Materials (Europe) BV
Address : Everslaan 45
3078 Everberg
Belgium
Telephone : +41 61 299 20 41
Telefax : +41 61 299 20 40

E-mail address of person responsible for the SDS : Global_Product_EHS_AdMat@huntsman.com

1.4 Emergency telephone number

Emergency telephone number : Centres Antipoison et de Toxicovigilance:
ANGERS: 02 41 48 21 21
BORDEAUX: 05 56 96 40 80
LILLE: 0 825 812 822
LYON: 04 72 11 69 11
MARSEILLE 04 91 75 25 25
NANCY: 03 83 32 36 36
PARIS: 01 40 05 48 48
RENNES: 02 99 59 22 22
STRASBOURG: 03 88 37 37 37
TOULOUSE: 05 61 77 74 47
EUROPE: +32 35 75 1234
France ORFILA: +33(0)145425959
ASIA: +65 6336-6011
China: +86 20 39377888
+86 532 83889090
India: + 91 22 42 87 5333
Australia: 1800 786 152
New Zealand: 0800 767 437
USA: +1 800-424-9300

SECTION 2: Hazards identification

2.1 Classification of the substance or mixture

Classification (REGULATION (EC) No 1272/2008)

Acute toxicity, Category 4 H332: Harmful if inhaled.

SAFETY DATA SHEET
according to Regulation (EC) No. 1907/2006

HUNTSMAN
Enriching lives through innovation

ARADUR® 3486 BD

Version	Revision Date:	SDS Number:	Date of last issue: 10.10.2018
1.2	22.05.2023	400001014180	Date of first issue: 08.09.2016

Print Date 03.04.2024

Skin corrosion, Sub-category 1A	H314: Causes severe skin burns and eye damage.
Serious eye damage, Category 1	H318: Causes serious eye damage.
Skin sensitisation, Category 1	H317: May cause an allergic skin reaction.
Long-term (chronic) aquatic hazard, Category 3	H412: Harmful to aquatic life with long lasting effects.

2.2 Label elements

Labelling (REGULATION (EC) No 1272/2008)

Hazard pictograms :

Signal word : Danger

Hazard statements :
H314 Causes severe skin burns and eye damage.
H317 May cause an allergic skin reaction.
H332 Harmful if inhaled.
H412 Harmful to aquatic life with long lasting effects.

Precautionary statements :

Prevention:

P261 Avoid breathing mist or vapours.
P273 Avoid release to the environment.
P280 Wear protective gloves/ protective clothing/ eye protection/ face protection/ hearing protection.

Response:

P303 + P361 + P353 IF ON SKIN (or hair): Take off immediately all contaminated clothing. Rinse skin with water.
P304 + P340 + P310 IF INHALED: Remove person to fresh air and keep comfortable for breathing. Immediately call a POISON CENTER/ doctor.
P305 + P351 + P338 + P310 IF IN EYES: Rinse cautiously with water for several minutes. Remove contact lenses, if present and easy to do. Continue rinsing. Immediately call a POISON CENTER/ doctor.

Hazardous components which must be listed on the label:

Reaction products of di-, tri- and tetra-propoxylated propane-1,2-diol with ammonia
3-aminomethyl-3,5,5-trimethylcyclohexylamine
2,2'-dimethyl-4,4'-methylenebis(cyclohexylamine)

2.3 Other hazards

This substance/mixture contains no components considered to be either persistent, bioaccumulative and toxic (PBT), or very persistent and very bioaccumulative (vPvB) at levels of 0.1% or higher.

Ecological information: The substance/mixture does not contain components considered to have endocrine disrupting properties according to REACH Article 57(f) or Commission Delegated regulation (EU) 2017/2100 or Commission Regulation (EU) 2018/605 at levels of 0.1% or higher

SAFETY DATA SHEET
according to Regulation (EC) No. 1907/2006

HUNTSMAN
Enriching lives through innovation

ARADUR® 3486 BD

Version	Revision Date:	SDS Number:	Date of last issue: 10.10.2018
1.2	22.05.2023	400001014180	Date of first issue: 08.09.2016

Print Date 03.04.2024

Toxicological information: The substance/mixture does not contain components considered to have endocrine disrupting properties according to REACH Article 57(f) or Commission Delegated regulation (EU) 2017/2100 or Commission Regulation (EU) 2018/605 at levels of 0.1% or higher

SECTION 3: Composition/information on ingredients

3.2 Mixtures

Hazardous components

Chemical name	CAS-No. EC-No. Index-No. Registration number	Classification	Concentration (% w/w)
Reaction products of di-, tri- and tetra-propoxylated propane-1,2-diol with ammonia	- - 01-2119557899-12	Skin Corr. 1C; H314 Eye Dam. 1; H318 Aquatic Chronic 3; H412	>= 70 - < 90
3-aminomethyl-3,5,5-trimethylcyclohexylamine	2855-13-2 220-666-8 612-067-00-9 01-2119514687-32	Acute Tox. 4; H302 Skin Corr. 1B; H314 Eye Dam. 1; H318 Skin Sens. 1A; H317 specific concentration limit Skin Sens. 1A; H317 >= 0,001 % Acute toxicity estimate Acute oral toxicity: 1 030 mg/kg	>= 10 - < 20
2,2'-dimethyl-4,4'-methylenebis(cyclohexylamine)	6864-37-5 229-962-1 612-110-00-1 01-2119497829-12	Acute Tox. 4; H302 Acute Tox. 2; H330 Acute Tox. 3; H311 Skin Corr. 1A; H314 Eye Dam. 1; H318 STOT RE 2; H373 (Liver, Kidney, Skeletal muscle, Heart) Aquatic Chronic 2; H411	>= 5 - < 10

For explanation of abbreviations see section 16.